

**CHARACTERIZATION OF AGGREGATE SHAPE PROPERTIES USING A
COMPUTER AUTOMATED SYSTEM**

A Dissertation

by

TALEB MUSTAFA AL ROUSAN

Submitted to the Office of Graduate Studies of
Texas A&M University
in partial fulfillment of the requirements for the degree of

DOCTOR OF PHILOSOPHY

December 2004

Major Subject: Civil Engineering

**CHARACTERIZATION OF AGGREGATE SHAPE PROPERTIES USING A
COMPUTER AUTOMATED SYSTEM**

A Dissertation

by

TALEB MUSTAFA AL ROUSAN

Submitted to Texas A&M University
in partial fulfillment of the requirements
for the degree of

DOCTOR OF PHILOSOPHY

Approved as to style and content by:

Eyad Masad
(Chair of Committee)

Dallas Little
(Member)

Robert Lytton
(Member)

Amy Epps Martin
(Member)

Thomas Yancey
(Member)

Paul Roschke
(Head of Department)

December 2004

Major Subject: Civil Engineering

ABSTRACT

Characterization of Aggregate Shape Properties Using a Computer Automated System.

(December 2004)

Taleb Mustafa Al Rousan, B.S., Jordan University of Science and Technology;

M.S., Jordan University of Science and Technology

Chair of Advisory Committee: Dr. Eyad Masad

Shape, texture, and angularity are among the properties of aggregates that have a significant effect on the performance of hot-mix asphalt, hydraulic cement concrete, and unbound base and subbase layers. Consequently, there is a need to develop methods that can quantify aggregate shape properties rapidly and accurately. In this study, an improved version of the Aggregate Imaging System (AIMS) was developed to measure the shape characteristics of both fine and coarse aggregates. Improvements were made in the design of the hardware and software components of AIMS to enhance its operational characteristics, reduce human errors, and enhance the automation of test procedure.

AIMS was compared against other test methods that have been used for measuring aggregate shape characteristics. The comparison was conducted based on statistical analysis of the accuracy, repeatability, reproducibility, cost, and operational characteristics (e.g. ease of use and interpretation of the results) of these tests. Aggregates that represent a wide range of geographic locations, rock type, and shape characteristics were used in this evaluation.

The comparative analysis among the different test methods was conducted using the Analytical Hierarchy Process (AHP). AHP is a process of developing a numerical score to rank test methods based on how each method meets certain criteria of desirable characteristics. The outcomes of the AHP analysis clearly demonstrated the advantages of AIMS over other test methods as a unified system for measuring the shape characteristics of both fine and coarse aggregates.

A new aggregate classification methodology based on the distribution of their shape characteristics was developed in this study. This methodology offers several advantages over current methods used in practice. It is based on the distribution of shape characteristics rather than average indices of these characteristics. The coarse aggregate form is determined based on three-dimensional analysis of particles. The fundamental gradient and wavelet methods are used to quantify angularity and surface texture, respectively. The classification methodology can be used for the development of aggregate shape specifications.

DEDICATION

This dissertation is dedicated to the soul of my father and to my mother with all my love and gratefulness. I also dedicate this dissertation to my wife “Manar” and my son “Mustafa” and daughter “Noor” for the love, help, and patience they showed during my study years. Last but not least, I dedicate this work to my brothers, Ra’ed & Tariq, sisters, Buthaina & Maisa, and brothers-in-law, Dr. Mufadi & Mr. Fawwaz, who provided me with an enormous amount of support and encouragement.

ACKNOWLEDGMENTS

Many people really deserve my appreciation and thanks. First is Dr. Eyad Masad. He, Dr. Masad, always provided me with the guidance, knowledge, encouragement and support throughout my study years while pursuing my Ph.D. He was a symbol of intelligence, creativeness, and humbleness that inspired me all the time. I learned a lot from him and I consider myself fortunate that I knew him and had him as my advisor.

I would also like to thank the Federal Highway Administration and the National Cooperative Highway Research Program for providing the necessary funds to complete this work. Thanks are due to Dr. Dallas Little, Dr. Robert Lytton, Dr. Amy Epps Martin, and Dr. Thomas Yancey for serving as committee members and for their valuable input to this work. Special thanks to Dr. Clifford Spiegelman from the Department of Statistics at Texas A&M University for his supervision and appropriate guidance on the statistical part of this dissertation.

Special thanks to people in Applied Scientific Instrumentation (ASI), Dr. Anal Mukhopadhyay, Mr. Tom Fletcher, Mr. Andrew Fawcett, Mr. Mathew Potter, Mr. Hassan Charara, Ms. Aparna Kanungo, for their help with technical and programming issues. Also, I would like to thank Ms. Manjula Bathina, Mr. Jeremy Mcgahan, Mr. Syam, and Mr. Dennis Gatchalian for their help with the testing and data collection process. Special thanks to all my friends especially my officemates, Mr. Aslam Al Omari and Mr. Shadi Saadeh, for their understanding, patience, and valuable discussions.

TABLE OF CONTENTS

	Page
ABSTRACT.....	iii
DEDICATION.....	v
ACKNOWLEDGMENTS.....	vi
TABLE OF CONTENTS.....	vii
LIST OF FIGURES.....	x
LIST OF TABLES.....	xv
 CHAPTER	
I INTRODUCTION.....	1
Problem Statement.....	1
Objectives.....	3
Dissertation Outline.....	4
II LITERATURE REVIEW.....	6
Introduction.....	6
The Influence of Aggregate Shape on Pavement Performance...	7
Hot-mix Asphalt Mixtures.....	7
Hydraulic Cement Concrete Mixtures.....	11
Unbound Layers.....	14
Identifying Aggregate Characteristics Affecting Performance...	16
Test Methods for Measuring Aggregate Characteristics.....	18
Indirect Methods.....	20
Direct Methods.....	26
Image Analysis Methods for Characterizing Aggregates.....	41
Typical Analysis of Form.....	42
Typical Analysis of Angularity.....	45
Typical Analysis of Texture.....	54
Summary.....	60
III IMPROVED AGGREGATE IMAGING SYSTEM (AIMS) FOR MEASURING SHAPE PROPERTIES.....	61

CHAPTER	Page
Introduction.....	61
Description of Aggregate Imaging System “AIMS”.....	61
Improvements Made to Hardware Components and Functions...	64
Hardware Improvements.....	64
Fine Aggregate Module Operation Procedure.....	72
Coarse Aggregate Module Operation Procedure.....	73
Development of Texture Lighting Scale.....	76
Control and Analysis Software.....	79
Control Software.....	79
Analysis Software.....	84
Summary.....	88
 IV COMPARATIVE ANALYSIS OF TEST METHODS FOR MEASURING AGGREGATE SHAPE.....	90
Introduction.....	90
Evaluation of Merits and Deficiencies of Test Methods.....	90
Laboratory Testing Procedures.....	100
Description of Aggregates.....	101
Testing Methods Procedures.....	104
Evaluation of Repeatability and Reproducibility.....	111
Evaluation of Accuracy.....	124
Accuracy of Analysis Methods.....	125
Accuracy of Test Methods.....	136
Cost and Operational Characteristics of Test Methods.....	143
Summary.....	147
 V RANKING OF TEST METHODS USING THE ANALYTICAL HIERARCHY PROCESS (AHP).....	149
Introduction.....	149
Analytical Hierarchy Process (AHP).....	149
AHP Program Description.....	150
AHP Ranking of Test Methods.....	155
Fine Aggregate Angularity.....	161
Coarse Aggregate Texture.....	167
Coarse Aggregate Form.....	170
Summary.....	172
 VI STATISTICALLY BASED METHODOLOGY FOR AGGREGATE SHAPE CLASSIFICATION.....	174

CHAPTER	Page
Introduction.....	174
Classification System Features.....	175
Classification System Development Methodology.....	176
Statistical-Based Aggregate Shape Classification.....	177
Analysis and Results.....	181
Aggregate Texture versus Angularity.....	181
Effect of Crushing and Size on Shape Properties.....	187
Identifying Flat, Elongated, or Flat and Elongated Particles.....	189
Summary.....	191
VII SUMMARY, CONCLUSIONS, IMPLEMENTATION, AND RECOMMENDATIONS.....	192
Summary and Conclusions.....	192
Implementation.....	196
Recommendations.....	197
REFERENCES.....	199
VITA.....	211

LIST OF FIGURES

FIGURE		Page
2.1	Components of Aggregate Shape Properties: Form, Angularity and Texture.....	7
2.2	Correlation between Coarse Aggregate Texture Measured Using Image Analysis and Rut Depth in the Creep Compliance of HMA.....	12
2.3	Correlation between Coarse Aggregate Texture Measured Using Image Analysis and HMA Rut Depth in the Georgia Loaded Wheel Test (GWLTT).....	12
2.4	Correlation between Coarse Aggregate Angularity and Shear Strength.....	16
2.5	Uncompacted Void Content of Fine Aggregate Apparatus.....	21
2.6	Uncompacted Void Content of Coarse Aggregate Apparatus.....	21
2.7	CAR Testing Machine.....	22
2.8	Schematic Description of Florida Bearing Ratio Apparatus.....	23
2.9	Schematic Description of the Pouring Device Used by Rugosity Test..	24
2.10	Time Index Test Apparatus.....	25
2.11	Direct Shear Testing Machine.....	26
2.12	Illustration of Counting Percent of Fractured Faces.....	27
2.13	Flat and Elongated Coarse Aggregate Caliper.....	28
2.14	Improved Digital Multiple Ratio Analysis Device (MRA) by Martin Marietta.....	29
2.15	VDG-40 Videograder.....	30
2.16	Computer Particle Analyzer System (CPA).....	31
2.17	Micromeritics OptiSizer (PSDA).....	33

FIGURE	Page
2.18 Video Imaging System (VIS).....	33
2.19 Buffalo Wire Works (PSSDA) Systems for Coarse and Fine Aggregates.....	34
2.20 Camsizer System.....	36
2.21 WipShape System.....	37
2.22 University of Illinois Aggregate Image Analyzer (UIAIA).....	38
2.23 Aggregate Imaging System (AIMS).....	40
2.24 Laser-based Aggregate Scanning System (LASS) Hardware Architecture.....	41
2.25 Illustration of the Erosion-Dilation and Fractal Behavior Method.....	48
2.26 Illustration of the Difference in Gradient between Particles.....	51
2.27 Illustration of an n -Sided Polygon Approximating the Outline of a Particle.....	53
2.28 Average Minimum Curve Radius Calculations.....	55
2.29 Curve Radius Measurements around the Profile of the Rounded Particle in Fig. 2.28; Raw and Smoothed Values.....	55
2.30 Images of Smooth, and Rough-Textured Aggregates and Their Fast Fourier Transforms and Histograms.....	57
2.31 Illustration of the Wavelet Decomposition.....	59
3.1 3-Dimensional Graphical Model of AIMS.....	62
3.2 First Prototype of Aggregate Imaging System (AIMS).....	65
3.3 Improved Aggregate Imaging System (AIMS).....	66
3.4 Lighting Table Using LEDs for Backlighting Source.....	67

FIGURE	Page
3.5 Top Lighting Used in the Improved AIMS.....	67
3.6 Top Lightings in Different Versions of AIMS.....	68
3.7 Ventilation System.....	69
3.8 Adjusting Sample Tray Level.....	70
3.9 Illustration of the Camera Path.....	72
3.10 Mean of Gray Scale Intensity Histogram for Different Aggregates with Cut and Original Sections.....	77
3.11 Relation between Surface Texture and Histogram Intensity Mean for Different Aggregates.....	78
3.12 Front Panel Interface of the Control Program Used by AIMS First Prototype Version	80
3.13 Front Panel Interface of the Control Program Used by AIMS Improved Version	81
3.14 Control Program Interface Showing Original and Process Images while Running Angularity Analysis Scan.....	82
3.15 New Features in Control Program while Running Texture Analysis Scan.....	83
3.16 Property Distribution and Statistics Shown on the Software Results Interface.....	85
3.17 Example of the Cumulative Distribution of Texture.....	86
3.18 Example of the Data Presented in Summary Sheet.....	86
3.19 Interface of AIMS Analysis Software.....	87
3.20 New Feature to Change the Class Limits of Aggregate Shape Properties.....	88
4.1 Outline of the Approach for Preliminary Evaluation, Screening, and Prioritization of Test Methods.....	97

FIGURE	Page	
4.2	Charts Used by Geologists in the Past for Visual Evaluation of Granular Materials.....	127
4.3	Correlations of Test Methods with the Digital Caliper Results for Coarse Aggregates Form.....	137
4.4	Comparison between Sphericity Measurements of AIMS and the Digital Caliper.....	138
4.5	Correlations of Test Methods with Visual Rankings for Coarse Aggregates Texture.....	141
4.6	Correlations of Test Methods with Visual Rankings for Coarse Aggregates Surface Irregularity.....	142
4.7	Correlations of Test Methods with Visual Rankings of Fine Aggregates Angularity.....	142
5.1	Program Graphical Interface to Enter Numbers and Names of Characteristics and Test Methods.....	152
5.2	Program Graphical Interface to Enter Weights Comparing Test Methods to Characteristics, and Characteristics with Respect to Overall Satisfaction with Method.....	153
5.3	Resulting Priority Vectors and Overall Ranking of Test Methods.....	154
5.4	Basic Hierarchy for Analytical Hierarchy Process (AHP) Used in Presented Example.....	156
6.1	Shape Properties Groups for Individual and Combined Aggregates....	178
6.2	Aggregate Shape Classification Chart.....	182
6.3	Distributions of Shape Characteristics in Coarse Aggregates.....	183
6.4	Distributions of Shape Characteristics in Fine Aggregates.....	184
6.5	Variations in Texture and Angularity Properties in Coarse Aggregates.....	186
6.6	Texture Index for Different Coarse Aggregate Types.....	187

FIGURE		Page
6.7	Examples of the Effect of Coarse Aggregate Size on Texture.....	188
6.8	Example of the Effect of Fine Aggregate Size on Angularity.....	189
6.9	Chart for Identifying Flat, Elongated, or Flat and Elongated Aggregates.....	190

LIST OF TABLES

TABLE		Page
2.1	Summary of Methods for Measuring Aggregate Characteristics.....	19
3.1	Optical System Performance Specifications.....	71
3.2	Resolution and Field of View Used in Angularity Analysis for Different Fine Sieve Sizes Using 0.5X Lens.....	73
3.3	Resolution and Field of View Used in Angularity Analysis of Different Coarse Sieve Sizes Using 0.25X Lens.....	74
3.4	Resolution and Field of View Used in Texture Analysis for Coarse Sieve Sizes Using 0.25X Lens.....	75
4.1	Merits and Deficiencies of the Testing Methods Used to Measure Aggregate Shape Properties.....	91
4.2	Criteria for Selecting Test Methods for Intensive Evaluation.....	98
4.3	Aggregate Sources and Sizes.....	101
4.4	Mineralogical Content of Aggregate Using X-Ray Diffraction.....	103
4.5	Aggregate Size and Shape Parameters Measured Using the Test Methods.....	105
4.6	Fine Aggregate Blend Used in CAR Test.....	107
4.7	Arrangement of Variation in Measurements within and between Operators.....	113
4.8	Repeatability and Reproducibility of Test Methods Measuring Coarse Aggregate Shape Properties.....	115
4.9	Repeatability and Reproducibility of Test Methods Measuring Fine Aggregate Shape Properties.....	118
4.10	Classification of Coarse Aggregate Test Methods Based on Repeatability and Reproducibility.....	120

TABLE	Page
4.11 Classification of Fine Aggregate Test Methods Based on Repeatability and Reproducibility.....	122
4.12 Analysis Methods Used in Analyzing Aggregate Images	126
4.13 Pearson and Spearman Correlation Coefficients of Rittenhouse Sphericity	128
4.14 Pearson and Spearman Correlation Coefficients of Krumbein Roundness	129
4.15 Clustering of Analysis Methods (4 Clusters) Based on Pearson Correlation	132
4.16 Percentage of Clustered Aggregates for Each Analysis Method.....	132
4.17 Coarse Aggregates in Texture Classes Estimated Using Ward's Linkage	133
4.18 Coarse Aggregates in Angularity Classes Estimated Using Ward's Linkage.....	133
4.19 Analysis Methods Used in Analyzing Aggregate Images	134
4.20 Digital Caliper Results	137
4.21 Coefficient of Multiple Determination (R^2) between the Rankings of Experienced Individuals for Angularity, Texture, and Surface Irregularities	139
4.22 Average Visual Rankings of Coarse Aggregates by Experienced Individuals	140
4.23 Visual Ranking of Fine Aggregate Angularity by Experienced Individuals	140
4.24 Cost and Readiness for Implementation of Test Methods	144
4.25 Ease of Use and Data Interpretation of Test Methods	145
4.26 Portability of Test Methods	146

TABLE	Page	
4.27	Applicability of Test Methods to Measure Different Aggregate Types and Sizes.....	147
5.1	Example of the Relative Importance of the Characteristic Based on Overall Satisfaction with Method.....	157
5.2	AHP Comparison Scale.....	157
5.3	Weights that Compare Test Methods Based on Each of the Characteristics.....	158
5.4	Accuracy Categories Based on R^2 Values.....	160
5.5	Comparison of the Characteristic Based on Overall Satisfaction with Method Assuming Characteristics Are Equally Important.....	162
5.6	Comparison of Test Methods Measuring Fine Aggregate Angularity with Respect to the 9 Characteristics.....	163
5.7	Resulting Priority Vectors and Overall Ranking of Test Methods Measuring Fine Aggregate Angularity Assuming Characteristics Are Equally Important.....	166
5.8	Comparison of Characteristics with Respect to Overall Satisfaction with Method (Accuracy is Moderately More Important than Other Characteristics).....	167
5.9	Overall Ranking of Test Methods Measuring Fine Aggregate Angularity Using Different Accuracy Levels of Preference.....	167
5.10	Comparison of Characteristics with Respect to Overall Satisfaction with Method (Accuracy is Moderately More Important than Applicability and Absolutely More Important than Other Characteristics).....	168
5.11	Resulting Priority Vectors of Test Methods Measuring Coarse Aggregate Texture with Respect to Characteristics.....	169
5.12	Overall Ranking of Test Methods Measuring Coarse Aggregate Texture.....	170

TABLE		Page
5.13	Resulting Priority Vectors of Test Methods Measuring Coarse Aggregate Form with Respect to Characteristics.....	171
5.14	Overall Ranking of Test Methods Measuring Coarse Aggregate Form.....	172

CHAPTER I

INTRODUCTION

PROBLEM STATEMENT

The properties of coarse and fine aggregates used in hot-mix asphalt (HMA), hydraulic cement concrete, and unbound base and subbase layers have a significant influence on the engineering properties of the pavement structure in which they are used (Kandhal and Parker 1998; Saeed et al. 2001; Meininger 1998). The form, angularity, and texture of fine and coarse aggregate particles influence their mutual interactions and interactions with any stabilizing agents (e.g., asphalt, cement, and lime) and are related to durability, workability, shear resistance, tensile strength, stiffness, fatigue response, optimum stabilizer content, and, ultimately, performance of the pavement layer. Therefore, fundamental measurements of aggregate shape characteristics are essential for good quality control of aggregates and for understanding the influence of these characteristics on the behavior of pavement structural layers.

There are currently no standard test methods for directly and objectively measuring aggregate angularity and surface texture. The current methods used in practice have several limitations: They are laborious, subjective in nature, and/or lack a direct relationship with the fundamental parameters governing performance such as shear strength and stiffness (Fletcher et al. 2003). In addition, some of these methods are limited in their ability to differentiate among aggregate characteristics (form, angularity, and texture). These limitations have various impacts on the quality of highway pavements, as they impede the development of design methodologies and construction practices that require accurate, repeatable, and rapid measurements of aggregate properties. Moreover, these limitations can lead to the development of specifications that in some cases overemphasize the need for superior aggregate properties or allow the use of marginal aggregates without a clear relationship to performance.

This dissertation follows the style and format of the *Journal of Computing in Civil Engineering* (ASCE).

Current test limitations have directed researchers toward seeking new technologies to accurately and rapidly measure aggregate shape. Motivated by advancements in digital vision and the availability of low-cost, powerful, and fast image processing software, new techniques for directly measuring aggregate shape properties have been developed. These systems operate based on different concepts such as image analysis techniques, laser scanning, and physical measurements of aggregate dimensions (Jahn 2000; Tutumluer et al. 2000; Masad 2001; Kim et al. 2001). These newly developed direct measurement methods have the potential to objectively quantify aggregate characteristics. However, some of these methods differ significantly in their experimental setups, analysis procedures, and the shape properties they measure. Some of these systems were developed to measure only one aggregate shape property, while some were developed to measure two shape properties. Very few were developed with the intention of measuring all three aggregate shape properties (form, angularity, and texture).

One of the unique and most promising systems developed to characterize aggregate shape properties is the Aggregate Imaging System (AIMS). AIMS was developed to have the ability to capture images and analyze the shape of a wide range of aggregate sizes and types, covering those used in HMA, hydraulic cement concrete, and unbound aggregate layers of pavements. AIMS measures all three aggregate shape properties (form, angularity, and texture) for all aggregate types and for different aggregate sizes using a simple instrumental setup. AIMS uses one camera and two different lighting schemes to capture images of aggregates at different resolutions. These images are analyzed using image analysis techniques based on sound scientific concepts. AIMS represents each shape characteristic as a cumulative distribution function rather than an average value. Therefore, the system is able to better represent the influence of blending of different sources on aggregate characteristics.

A complete evaluation of most of these new methods, including AIMS, has not yet been performed. Thus, a comprehensive evaluation of these systems with respect to their accuracy, repeatability, reproducibility, cost, and operational characteristics is

necessary to discriminate between these methods. This evaluation is crucial, and without such information a rational recommendation for incorporating such test methods in aggregate specifications cannot be made. This research provides insight and much of the needed information to will help improve specifications for aggregates used in highway pavements. Also, a methodology for classification of aggregates based on their shape properties is developed as part of the research.

OBJECTIVES

In this research the following objectives are set to be achieved:

1. Develop an improved version of the Aggregate Imaging System (AIMS) for measuring shape properties. The development of the improved system addresses operational characteristics, lighting scale, and automation. These improvements include modifications to the hardware, and both the control and analysis softwares.
2. Evaluate the improved version of AIMS along with other available methods used to measure aggregate shape properties for repeatability, reproducibility, accuracy, cost, and operational characteristics. In this evaluation, different aggregate types from different sources were analyzed by three operators. In order to compare test methods based on the measured characteristics, the Analytical Hierarchy Process (AHP) was used.
3. Develop a comprehensive methodology for classification of aggregates based on the distribution of their shape characteristics measured using the improved version of AIMS. The new methodology was developed using a statistical approach. The new methodology exhibits the features of representing the three characteristics of aggregate shape, unifies the methods used to measure shape characteristics of fine and coarse aggregates, and represents characteristics by a cumulative distribution function rather than an average value to better represent the effects of blending and crushing on aggregate shape.

DISSERTATION OUTLINE

This dissertation consists of six chapters organized as follows:

Chapter I is an introduction. The problem statement is presented, followed by the objectives and the outline of the dissertation.

Chapter II presents a literature review relevant to the influence of aggregate shape on performance of different types of pavements including HMA, hydraulic cement concrete, and unbound aggregate layers. Literature on identifying aggregate characteristics affecting performance is also presented in this chapter. In addition, Chapter II includes a list of direct and indirect test methods used for measuring aggregate shape characteristics along with a brief description of each test method.

Chapter III describes the Aggregate Imaging System (AIMS) and the improvements made as part of this study. The hardware and software modifications made to the system to improve its operational characteristics and automation capabilities, and the development of a lighting scale are documented in this chapter. (Parts of Chapter III were presented in the Transportation Research Board 83rd Annual Meeting, 2004).

The experimental evaluation of the characteristics of the available methods to measure aggregate shape characteristics is presented in Chapter IV. This chapter documents the procedure followed to select the candidate tests. Repeatability, reproducibility, and accuracy of the selected methods were evaluated using different types of aggregates from different sources with various shape properties. Information about cost and operational characteristics of the test methods are also reported in Chapter IV.

Chapter V describes the procedure followed to rank the test methods based on the measured characteristics estimated in Chapter IV. This procedure is known as the Analytical Hierarchy Process (AHP), and provides a ranking, or a priority list of all the methods included in the evaluation. The main objective of this chapter is to highlight the flexibility and advantages of using AHP as a useful tool in this evaluation. This chapter includes numerical examples for using AHP to rank test methods and a description of the

program developed for AHP analysis.

The third objective of this study is accomplished in Chapter VI. A new comprehensive methodology for classification of aggregate shape based on the distribution of their shape characteristics is developed. The chapter includes a description of the statistical approach where cluster analysis was used to set new limits for aggregate shape classes. (This chapter was submitted as a paper for publication through the Transportation Research Board 84th Annual Meeting, 2005. The authors of this paper are Taleb Al-Rousan, Eyad Masad, Cliff Speigelman, and Leslie Myers).

Chapter VII presents an overall summary and conclusions of the dissertation, discussion of future implementation of the newly developed computer automated system, and recommendations for future related studies.

CHAPTER II

LITERATURE REVIEW

INTRODUCTION

Researchers have distinguished between different aspects that constitute aggregate geometry and have found that the particle geometry can be fully expressed in terms of three independent properties: form, angularity (or roundness), and surface texture (Barrett 1980). A schematic diagram that illustrates the differences between these properties is shown in Fig. 2.1. Form, the first-order property, reflects variations in the proportions of a particle. Angularity, the second-order property, reflects variations at the corners, that is, variations superimposed on shape. Surface texture is used to describe the surface irregularity at a scale that is too small to affect the overall shape (Fig. 2.1). These three properties can be distinguished because of their different scales with respect to particle size, and this feature can also be used to order them. Any of these properties can vary widely without necessarily affecting the other two properties.

Previous studies have used different terminology to refer to these aggregate properties (form, angularity, and texture). In this study, the best judgment was made in relating the description of different properties discussed in the literature to the definitions of aggregate shape properties discussed above and shown in Fig. 2.1. Form will be used interchangeably throughout the study to refer to the relative proportions of a particle's dimensions. Using a unified terminology facilitates comparing the findings of different studies and analyzing the results of different test methods.

This chapter focuses on presenting the findings of previous studies that are relevant to the influence of aggregate shape on performance of different types of pavements and on identifying aggregate characteristics affecting performance. This chapter also includes a brief description of the available test methods (direct and indirect) used for measuring aggregate shape characteristics. Image analysis techniques, that some of the imaging systems uses are also discussed in this chapter.

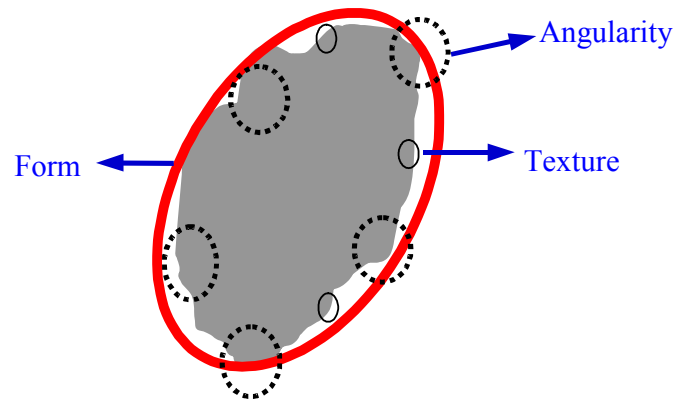


Fig. 2.1. Components of Aggregate Shape Properties: Form, Angularity and Texture (after Masad 2001)

THE INFLUENCE OF AGGREGATE CHARACTERISTICS ON PAVEMENT PERFORMANCE

This section documents the collected and reviewed information relative to the effect of aggregate shape properties on performance of different types of pavements.

Hot-mix Asphalt Mixtures

Many studies emphasized the role of aggregate shape in controlling the performance of asphalt mixtures, especially resistance to fatigue cracking and rutting (e.g., Kalcheff 1968; Monismith 1970; Benson 1970; Brown et al. 1989; Barksdale et al. 1992; Yeggoni et al. 1996; Chowdhury et al. 2001; Park et al. 2001; Button et al. 1990; Kandhal and Parker 1998). These studies conducted experiments that focused on the influence of fine aggregate, coarse aggregate, or the combined effect of fine and coarse aggregate on HMA mixture's mechanical properties and performance.

Campen and Smith (1948) found that when crushed fine aggregates were used instead of natural rounded aggregates the stability of dense-graded HMA mixtures

increased from 30 to 190%. The stability was measured using the bearing-index test (Campen and Smith 1948). Ishai and Gellber (1982) used the packing volume concept developed by Tons and Goetz (1968) to quantify the geometric irregularities of a wide range of aggregate sizes. The HMA mixtures containing different aggregates types were evaluated by Ishai and Gellber (1982) for Marshall stability and flow, resilient modulus, and split tension strength. The results showed that there was a significant increase in stability with an increase in the geometric irregularities of the aggregates. There was no correlation between geometric irregularities and resilient modulus or split tension strength of the HMA mixtures.

Kalcheff and Tunnicliff (1982) evaluated the effect of fine aggregate shape on HMA properties. HMA mixtures were tested using Marshall stability test, repeated load triaxial compression, static indirect tensile splitting strength, and repeated load indirect tensile splitting resistance tests. They found that the use of manufactured sand instead of natural sand improved the mix behavior in terms of resistance to permanent deformation from repeated traffic loadings, tensile strength, and tensile fatigue resistance. Winford (1991) reached the same conclusion by relating mechanical properties of HMA such as those obtained from the static confined creep test to the type of fine aggregate in the mix.

Herrin and Goetz (1954) reported that when the amount of crushed gravel in the coarse aggregate increased, the strength of the dense-graded HMA measured using the triaxial compression test was not significantly influenced. However, the strength of the open-graded HMA mixture increased significantly when the percentage of angular coarse aggregates was increased. Field (1958) found a considerable increase in HMA Marshall stability due to an increase in the percentage of crushed coarse particles. The influence of crushed gravel coarse aggregate on the properties of dense-graded HMA mixtures was also investigated by Kandhal and Wenger (1973). They found that the Marshall stability of the dense-graded mix decreased with increased use of uncrushed gravel particles. However, the differences among the mixes were not significant. They noted also that there was no significant difference in the tensile strength of HMA mixtures containing crushed and uncrushed coarse aggregates.

Sanders and Dukatz (1992) reported on the influence of coarse aggregate angularity on permanent deformation of four interstate sections of HMA pavements in Indiana. One of the four sections developed permanent rutting within two years of service. They found that HMA mixtures used in the binder course and the surface course of the rutted section had lower amounts of angular coarse aggregate compared to the other three sections.

Kandhal and Parker (1998) pointed out that only a few studies have been conducted to examine the influence of flat and elongated coarse aggregate particles on HMA strength compared with studies that addressed coarse aggregate angularity. The presence of excessive flat and elongated aggregate particles is undesirable in HMA mixtures because such particles tend to break down (especially in open-graded mixtures) during production and construction, thus affecting the durability of HMA mixtures (Kandhal and Parker 1998).

A study by Li and Kett (1967) found that the dimension ratio (width to thickness or length to width) had no effect on Marshall or Hveem stability as long as the dimension ratios were less than 3:1. The permissible percentage of flat and/or elongated particles (dimension ratio exceeding 3:1), that did not adversely affect the mix stability was determined to be 30% or as much as 40%. Stephens and Sinha (1978) reported that HMA mixes containing 30% or more flat particles (longest axis to shortest axis is more than or equal to three) maintained higher void contents compared to some other blends with lower percentages of flat particles. These mixes were compacted using a kneading compactor.

Some studies focused on comparing the influence of fine aggregate shape on HMA mechanical properties to the influence of coarse aggregate shape properties. Lefebure (1957) utilized the Marshall test to measure the stability of HMA mixtures with a crushed cubical coarse aggregate or crushed aggregates with flat and long particles combined with natural sand or crushed sand. His study concluded that fine aggregate was the most critical component of the HMA mixture. Its quantity and characteristics control, to a large extent, the Marshall stability. Wedding and Gaynor (1961) evaluated

the influence crushed coarse and fine aggregate on the Marshall stability of dense-graded HMA mixtures. Using crushed coarse aggregates caused a significant increase in stability compared with uncrushed coarse aggregates. The use of crushed fine aggregates caused an increase in stability of mixes with uncrushed coarse aggregates. However, the use of crushed fine aggregates had a minimal effect on HMA stability when crushed coarse aggregates were included.

Foster (1970) measured the resistance of dense-graded HMA mixtures to traffic by using test sections. He concluded that HMA mixtures with crushed coarse aggregate showed no better performance than that of the mix containing uncrushed aggregates. The study attributed this finding to the crushed fine aggregate, which controlled the capacity of the mix to resist stresses induced by traffic.

The influence of shape, size, and surface texture of aggregate on stiffness and fatigue response of HMA mixture was investigated and summarized by Monismith (1970). He indicated that aggregate characteristics affect both stiffness and fatigue response of HMA mixtures. Monismith (1970) recommended utilizing rough-textured materials with dense gradation for thick pavements in order to increase mix stiffness and fatigue life, whereas it might be acceptable to utilize smooth-textured aggregates in thin pavements since they produce less stiff mixtures resulting in increased fatigue life.

Barksdale et al. (1992) evaluated the effect of aggregate on rutting and fatigue of HMA mixtures. Aggregate shape was measured using image analysis techniques and the packing test developed by Ishai and Gellber (1982). They found that aggregate shape properties obtained from the packing test were statistically related to the rutting behavior of selected HMA mixtures. A comprehensive study by Kandhal et al. (1991) evaluated the factors that contribute to asphalt pavement performance. They found that mixtures with less than 20% natural sand in the fine aggregate had better performance than mixtures with more than 20% natural sand. They also recommended using coarse aggregate having at least 85% of particles with two or more fractured faces for heavy-duty wearing and binder courses.

A study conducted at the Texas Transportation Institute related an imaging index of aggregate texture (fractal dimension) to the creep behavior of asphalt mixes (Yeggoni et al. 1996). In this study, seven different aggregate blends of the same gradation but with varying amounts of crushed coarse aggregate particles were prepared. An example of the relationship between the fractal dimension and static creep compliance is shown in Fig. 2.2.

Fig. 2.3 shows the correlation between the texture of the coarse aggregates used in National Cooperative Highway Research Program (NCHRP) study 4-19 (Kandhal and Parker 1998) and rutting depths of HMA measured using the Georgia Loaded Wheel Test (GLWT) (a laboratory wheel tracing device). Texture measurements were conducted using the AIMS (Fletcher et al. 2002). It can be seen that an excellent relationship exists between the texture of coarse aggregates measured using image analysis techniques and the resistance to permanent deformation.

Hydraulic Cement Concrete Mixtures

Performance of Portland cement concrete pavements (PCCP) is influenced by aggregate properties. The properties of fine and coarse aggregates used in the mix can significantly increase or decrease the pavement service life. Selection of the appropriate aggregate type and properties is the key to enhancing pavement life; otherwise, poor selection can lead to premature failure in the pavement structure.

Concrete is expected to perform well during construction and service life, so PCCP will have good performance and serviceability and will last longer. The properties of the aggregate used in the concrete are expected to affect the performance parameters of both fresh and hardened Portland cement concrete (PCC). Aggregate shape characteristics affect the proportioning of PCC mixtures, the rheological properties of the mixtures, the aggregate-mortar bond, and the interlocking strength of the concrete joint/crack.

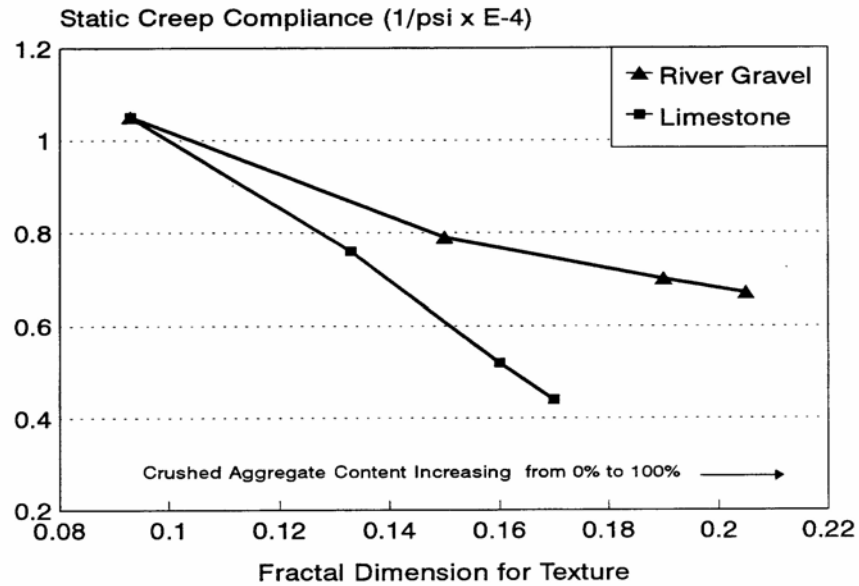


Fig. 2.2. Correlation between Coarse Aggregate Texture Measured Using Image Analysis and Rut Depth in the Creep Compliance of HMA (after Yeggoni et al. 1996)

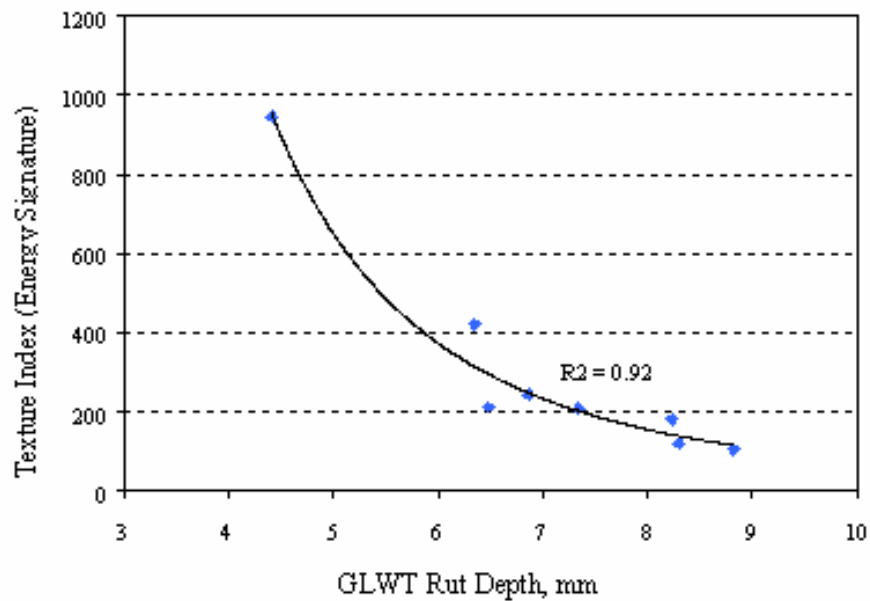


Fig. 2.3. Correlation between Coarse Aggregate Texture Measured Using Image Analysis and HMA Rut Depth in the Georgia Loaded Wheel Test (GLWT) (after Fletcher 2002)

Meininger (1998) conducted an extensive literature review and included a detailed discussion about the performance parameters of PCC used in various types of highway construction that may be affected by aggregate properties. He also presented a discussion about aggregate properties related to performance parameters. Meininger (1998) indicated that fine aggregate content and properties mostly affect the water content needed in the concrete mix. Thus, selecting or knowing the fine aggregate proper content and proper shape and texture will help in ensuring a workable, easy handling mix. Using an all crushed fine aggregate reduces the concrete workability significantly and makes it more difficult to place concrete. Workable concrete is important for proper consolidation, which in turn assures proper density, minimizes voids, and minimizes segregation at the joint areas, thus preventing spalling. An increase in the mixing water is associated with higher cement content, thus resulting in more drying shrinkage, which in turn leads to more transverse cracking. As drying shrinkage increases, the cracks and joints open leading to reduced aggregate interlock and increased tendency toward faulting and punchouts.

Coarse aggregate particle form and angularity are related to critical performance parameters such as transverse cracking, faulting of joints and cracks, punchouts, and spalling at joints and cracks. Using a high percentage of flat elongated particles might cause problems when placing the concrete, which will result in voids and incomplete consolidation of the mix, and thus contribute to spalling. If poor workability exists, then high mortar content is expected, which will lead to high rate of drying shrinkage and transverse cracking. Although flat and elongated particles may grant good interlocking at joints or cracks, the thin particles will be easier to break, causing faulting in jointed concrete pavements and punchouts in continuously reinforced concrete pavements (Meininger 1998).

Coarse aggregate form, angularity, and surface texture are believed to have a remarkable effect on the bond strength between aggregate particles and the cement paste (Mindness and Young 1981). Weak bonding between aggregates and mortar leads to distresses in concrete pavements including longitudinal and transverse cracking, joint

cracks, spalling, and punchouts (Fowler et al. 1996; Meininger 1998; Folliard 1999).

Kosmatka et al. (2002) indicated that the bond strength between the cement paste and a given coarse aggregate generally increases as particles change from smooth and rounded to rough and angular. The increase in bond strength is a consideration in selecting aggregate for concrete where flexural strength is important or where high compressive strength is needed.

Kosmatka et al. (2002) indicated that aggregate properties (particle form and surface texture) affect freshly mixed concrete more than hardened concrete. Rough-textured, angular, and elongated particles require more water to produce workable concrete than do smooth, rounded, compacted aggregates. Angular particles require more cement to maintain the same water to cement ratio. However, with satisfactory gradation, both crushed and non-crushed aggregate (of the same rock type) generally give essentially the same strength for the same cement factor. Angular and poorly graded aggregates can be difficult to pump (Kosmatka et al. 2002).

Unbound Layers

As with any other type of pavement layers, performance of unbound granular pavement base and subbase layers is greatly affected by the properties of the aggregate used. Poor performance of unbound granular base layers will result in upper pavement layer failures whether asphalt or concrete. Failure in the asphalt pavement due to poor performance of an unbound granular base layer can result in different forms of distresses in pavement, such as rutting, fatigue cracking, longitudinal cracking, depressions, corrugations, and frost heave, while poor performance of a granular base layer will result in pumping, faulting, cracking, and corner breaks in concrete pavements (Saeed et al. 2001).

A study by Barksdale and Itani (1994) showed significant correlation between aggregate shape properties and the resilient modulus and shear strength properties of unbound aggregates used in base layers. Saeed et al. (2001) showed a linkage between aggregate properties and unbound layer performance. Their study showed that the aggregate particle angularity and surface textures mostly affect shear strength and stiffness.

Shear strength is the most important property and has a great influence on unbound pavement layer performance.

The study by Saeed et al. (2001) revealed that lack of adequate particle angularity and surface texture is one of the contributing factors to fatigue cracking and rutting in asphalt pavements, while lack of adequate particle angularity and surface texture is a contributing factor to cracking in concrete pavement.

Rao et al. (2002) studied the effect of aggregate shape on strength and performance of pavement layers. They indicated that critical coarse aggregate physical properties are aspect ratio (cubical vs. flat or elongated), surface texture (smooth vs. rough surface), and angularity (sharp vs. smooth edges). While cubical particles have fewer breakdowns than flat or elongated ones, angular and rough-textured coarse aggregate particles provide higher shear strength than do rounded and smooth-textured aggregate. Coarse aggregate angularity provides a great deal of rutting resistance in asphalt pavements as a result of improved shear strength of unbound aggregate base and hot-mix asphalt. The interlocking of angular particles results in a strong aggregate skeleton under applied loads, whereas round particles tend to slide by or roll over each other, resulting in an unsuitable and weaker structure.

Rao et al. (2002) also conducted a series of experiments that demonstrated the influence of aggregate shape on the shear strength of several unbound materials as measured in triaxial tests. Fig. 2.4 shows the correlation between the shear strength of unbound aggregates and the angularity index (AI) measured using the University of Illinois imaging system (Rao 2001; Rao et al. 2002). The trend in the data presented suggests that as the AI values increase, the angle of internal friction, ϕ , increases exponentially. The correlation between the failure deviator stress and the AI value is also graphed in Fig. 2.4 for the three confining pressures. As the AI value of the unbound aggregate material increases, the deviator stress needed for failure also increases for each of the three confining pressures.

Based on reviewing several studies, Janoo (1998) concluded that form, angularity, and roughness have significant effect on base performance. He stated that

several studies have shown that there can be as much as 50% change in resilient modulus of base materials due to geometric irregularities.

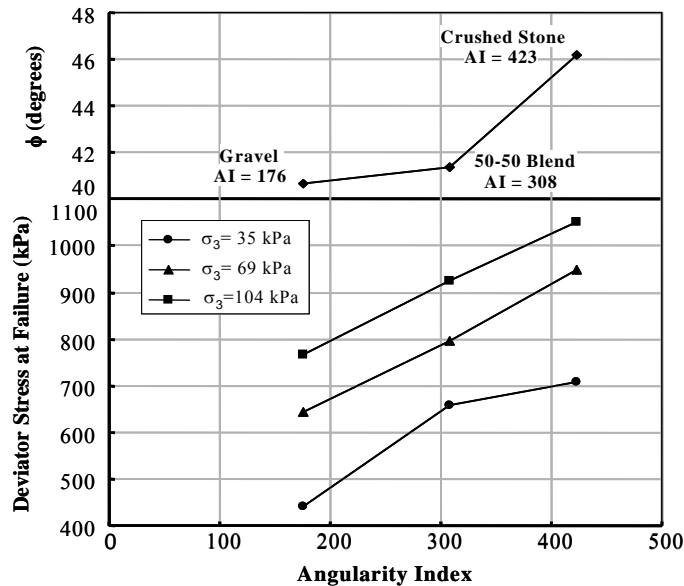


Fig. 2.4. Correlation between Coarse Aggregate Angularity and Shear Strength (after Rao 2001; Rao et al. 2002).

IDENTIFYING AGGREGATE CHARACTERISTICS AFFECTING PERFORMANCE

Most of the available information on the influence of aggregate characteristics on performance emphasizes that form, angularity, and texture play important roles in controlling performance of HMA mixtures, hydraulic cement concrete mixtures, and unbound layers. However, different shape properties influence the performance of these layers to different extents.

Most of the test methods used in the literature did not separate the influence of angularity from that of texture. Therefore, the term surface irregularity is used in this study to reflect the combined effect of angularity and texture. Previous research confirms

that aggregate geometric irregularity improves the resistance of HMA to rutting. Also, aggregate surface irregularity influences the resistance of asphalt mixtures to fatigue cracking. In general, angular aggregates that increase mix stiffness are needed for thick pavements, while smooth aggregates that reduce mixture stiffness are needed for thin pavements to provide resistance to fatigue cracking (Monismith 1970; Kandhal and Parker 1998). Surface irregularity also improves bonding between the aggregate surface and asphalt binder, and thus generally minimizes stripping problems.

The literature review also showed that the presence of excessive flat and elongated aggregate particles is undesirable in HMA mixtures because such particles tend to break down (especially in open-graded mixtures) during production and construction, thus affecting the durability of HMA mixtures. However, a limited number of studies were conducted to examine the influence of flat and elongated aggregate particles on performance of HMA mixture.

Although most available tests could not separate texture from angularity, recent studies using image analysis techniques have emphasized the significant influence that texture has on performance (Fletcher et al. 2002; Masad 2003).

The literature reviewed on the effect of aggregate properties on the performance of PCCP indicates that aggregate characteristics affect the proportioning of PCC, the rheological properties of the mixtures, the aggregate-mortar bond, and the interlocking strength of the concrete joint/crack (Meininger 1998; Kosmatka et al. 2002).

Aggregate surface irregularities have significant influence on workability and bonding between mortar and aggregates. Consequently, surface irregularities influence pavement distresses in concrete pavements including longitudinal and transverse cracking, joint cracks, spalling, and punchouts (Fowler et al. 1996; Meininger 1998; Folliard 1999).

Flat and elongated particles mainly affect the workability of fresh concrete in such a way that they might cause problems when placing the concrete, which will result in voids and incomplete consolidation of the mix, and thus contribute to spalling.

Surface characteristics of aggregates used in unbound layers of pavements is a

contributing factor to fatigue cracking and rutting in asphalt pavement, while lack of adequate particle angularity and surface texture is contributing factor to cracking in concrete pavement (Saeed et al. 2001; Rao et al. 2002).

Flat and elongated particles influence the unbound layers by increasing the anisotropic behavior of these layers. Intuitively speaking, these flat elongated particles form weak shear planes in the direction of traffic on pavements. There is no experimental evidence that this anisotropy compromises the performance significantly. However, the stiffness anisotropy should be considered in the design of asphalt pavements (Tutumluer and Thompson 1997).

Finally, Masad (2001) emphasized, based on a literature review of methods used to analyze aggregate characteristics, that most analysis methods do not differentiate between angularity and texture. This creates large discrepancies in relating aggregate characteristics to performance, as aggregates that have high texture do not necessarily exhibit high angularity, especially in coarse aggregates. It is important to develop methods that are able to quantify each of the aggregate characteristics rather than a manifestation of their interaction.

TEST METHODS FOR MEASURING AGGREGATE CHARACTERISTICS

Kandhal et al. (1991), Janoo (1998), and Chowdhury et al. (2001) classified methods that are used to describe aggregate shape characteristics into two broad categories, namely, direct and indirect. Direct methods are defined as those wherein particle characteristics (form, angularity, and texture) are measured, described qualitatively, and possibly quantified through direct measurement of individual particles. In indirect methods, particle shape characteristics are lumped together as geometric irregularities and determined based on measurements of bulk properties. Table 2.1 shows a summary of direct and indirect test methods that have been used by highway state agencies and research projects for measuring some aspects of aggregate shape properties.

Table 2.1. Summary of Methods for Measuring Aggregate Characteristics (after Masad 2001)

Test	References for the Test Method	Direct (D) or Indirect (I) Method	Field (F) or Central (C) Laboratory Application	Applicability to Fine (F) or Coarse (C) Aggregate
Uncompacted Void Content of Fine Aggregates	AASHTO T304	I	F, C	F
Uncompacted Void Content of Coarse Aggregates	AASHTO TP56, NCHRP Report 405, Ahlrich (1996)	I	F, C	C
Index for Particle Shape and Texture	ASTM D3398	I	F, C	F, C
Compacted Aggregate Resistance	Report FHWA/IN/JTRP-98/20, Mr. David Jahn (Martin Marietta, Inc.)	I	F, C	F
Florida Bearing Ratio	Report FHWA/IN/JTRP-98/20, Indiana Test Method No. 201-89	I	F, C	F
Rugosity	Tons and Goetz (1968), Ishai and Tons (1977)	I	F, C	F
Time Index	Quebec Ministry of Transportation, Janoo (1998)	I	F, C	F
Angle of Internal Friction from Direct Shear Test	Chowdhury et al. (2001)	I	C	F, C
Percentage of Fractured Particles in Coarse Aggregate	ASTM D5821	D	F, C	C
Flat and Elongated Coarse Aggregates	ASTM D4791	D	F, C	C
Multiple Ratio Shape Analysis	Mr. David Jahn (Martin Marietta, Inc.)	D	F, C	C
VDG-40 Videograder	Emaco, Ltd. (Canada), Weingart and Prowell (1999)	D	F, C	F, C
Computer Particle Analyzer	Mr. Reckart (W.S. Tyler Mentor Inc.), Tyler (2001)	D	C	F, C
Micromeritics OptiSizer (PSDA)	Mr. M. Strickland (Micromeritics OptiSizer)	D	C	F, C
Video Imaging System (VIS)	John B. Long Company	D	C	F, C
Buffalo Wire Works (PSSDA)	Dr. Penumadu, University of Tennessee	D	C	F, C
Camsizer	Jenoptik Laser Optik System and Research Technology	D	C	F, C
WipShape	Maerz and Zhou (2001)	D	C	C
University of Illinois Aggregate Image Analyzer (UIAIA)	Tutumluer et al. (2000), Rao (2001)	D	C	C
Aggregate Imaging System (AIMS)	Masad (2003)	D	C	F, C
Laser-Based Aggregate Analysis System	Kim et al., (2001)	D	C	C

Note: AASHTO = American Association of State Highway and Transportation Officials; FHWA= Federal Highway Administration; JTRP= Joint Transportation Research Program; ASTM= American Society of Testing and Materials.

Indirect Methods

As defined earlier, indirect test methods are those methods in which particle shape characteristics are lumped together as geometric irregularities and determined based on measurements of bulk properties. In indirect methods, the form, angularity, and texture are usually combined together, as it is fairly difficult to separate the effect of the individual components. A brief discussion is provided below about the commonly used indirect methods.

AASHTO 3304 (ASTM C1252) Uncompacted Void Content of Fine Aggregate

This method was originally developed by the National Aggregate Association (NAA) and was later adopted by the American Society for Testing and Material (ASTM) as method C1252 and by the American Association of State Highway and Transportation Officials (AASHTO) as method T304. This method is often referred to as the Fine Aggregate Angularity (FAA) test. It measures the loose uncompacted void content of a sample of fine aggregate that falls from a fixed distance through a given-sized orifice. A decrease in the void content is associated with more rounded, spherical, smooth-surface, fine aggregate, or a combination of these factors. Method A of this procedure is used by Superpave to determine aggregate angularity to ensure that fine aggregate has adequate internal friction to provide rut resistance to an HMA. This method has been extensively evaluated in a number of studies (Chowdhury and Button 2001; Janoo 1998; Janoo and Korhonen 1999; Kandhal and Parker 1998; Lee et al. 1999a; Meininger 1998; Saeed et al. 2001). The apparatus used in this test method is shown in Fig. 2.5.

AASHTO TP56 Uncompacted Void Content of Coarse Aggregate (as Influenced by Particle Shape, Surface Texture, and Grading)

This method was originally developed by the NAA and was later adopted by AASHTO as method TP56. It measures the loose uncompacted void content of a sample of coarse aggregate that falls from a fixed distance through a given-sized orifice. A decrease in the void content is associated with more rounded, spherical, smooth-surface coarse

aggregate, or a combination of these factors. Method A of this procedure is used to determine aggregate angularity. This method was evaluated in a number of studies (Ahlrich 1996; Kandhal and Parker 1998; Meininger 1998). The apparatus used in this method is shown in Fig. 2.6.



Fig. 2.5. Uncompacted Void Content of Fine Aggregate Apparatus



Fig. 2.6. Uncompacted Void Content of Coarse Aggregate Apparatus

ASTM D3398 Standard Test Method for Index of Aggregate Particle Shape and Texture

This test provides an index of an aggregate sample as an overall measure of its shape and texture. The test is based on the concept that not only shape, angularity, and texture of uniformly sized aggregate affects void ratio, but also the rate at which the voids change when compacted in a standard mold (ASTM D3398; Fowler et al. 1996; Lee et al. 1999b; Janoo and Korhonen 1999).

Compacted Aggregate Resistance (CAR) Test

The CAR test was developed by Mr. David Jahn for evaluating shear resistance of compacted fine aggregate in its as-received condition. The test works by applying a compressive load on the aggregate specimen using the Marshall testing machine. The compressive load versus displacement is plotted. The maximum compressive load that the specimen can carry is reported as CAR stability value. This value is assumed to be a function of the material shear strength and angularity. The CAR test method has many similarities with California Bearing Ratio test (Meininger 1998; Lee et al. 1999b; Chowdhury and Button 2001). Fig. 2.7 shows the CAR testing setup.

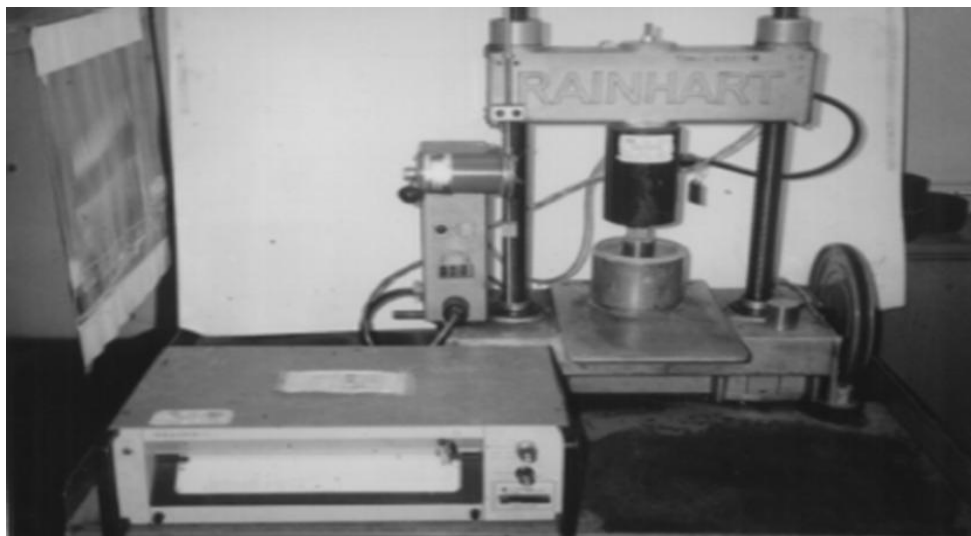


Fig. 2.7. CAR Testing Machine

Florida Bearing Value of Fine Aggregate (Indiana State Highway Commission Method 201)

This test method is used to determine the Florida Bearing value for fine aggregates used in HMA. The basic concept for this method is to determine the deformation rate of a fine aggregate subjected to a constant rate of loading. This deformation rate is taken as an indirect measure of angularity (Indiana Department of Transportation/Material and testing division/ITM No. 201-01T; Lee et al. 1999b). Fig. 2.8 shows a schematic description of Florida Bearing ratio apparatus.

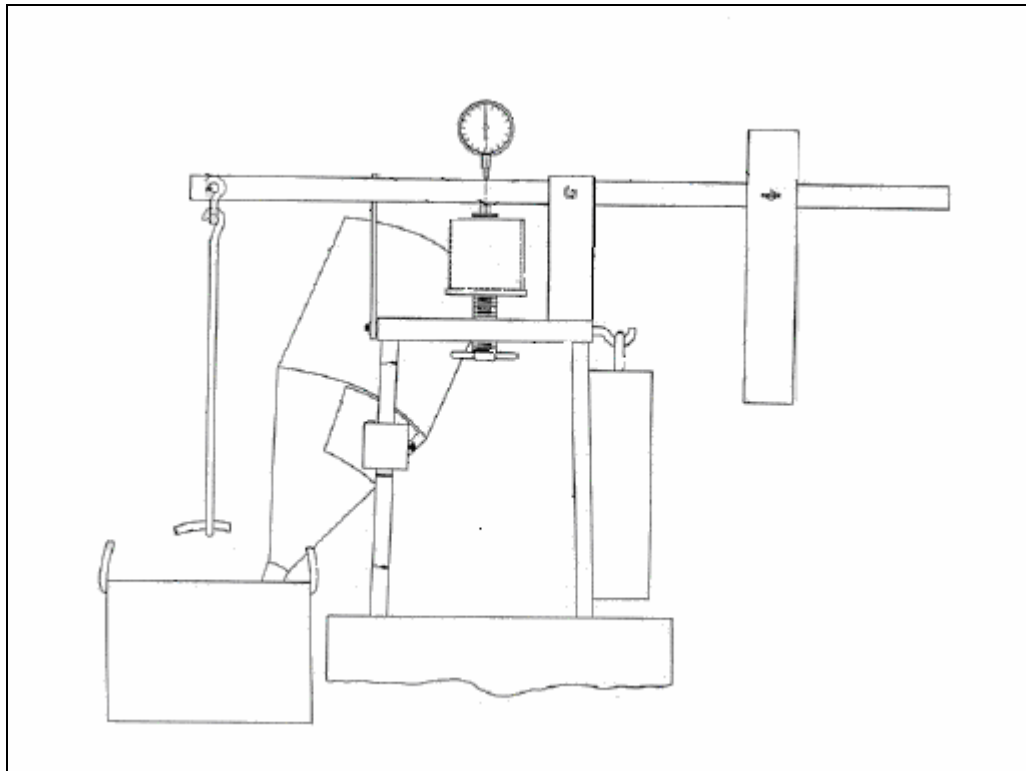


Fig. 2.8. Schematic Description of Florida Bearing Ratio Apparatus

Rugosity

This method was first developed by Tons and Goetz (1968) for coarse and fine aggregates. The method is based on relating the flow rate of aggregates through a given-sized orifice to their shape properties (Ishai and Tons 1977; Janoo 1998; Janoo and Korhonen 1999; Tons and Goetz 1968). Schematic description of the Pouring Device as presented by Janoo (1998) is shown in Fig. 2.9.

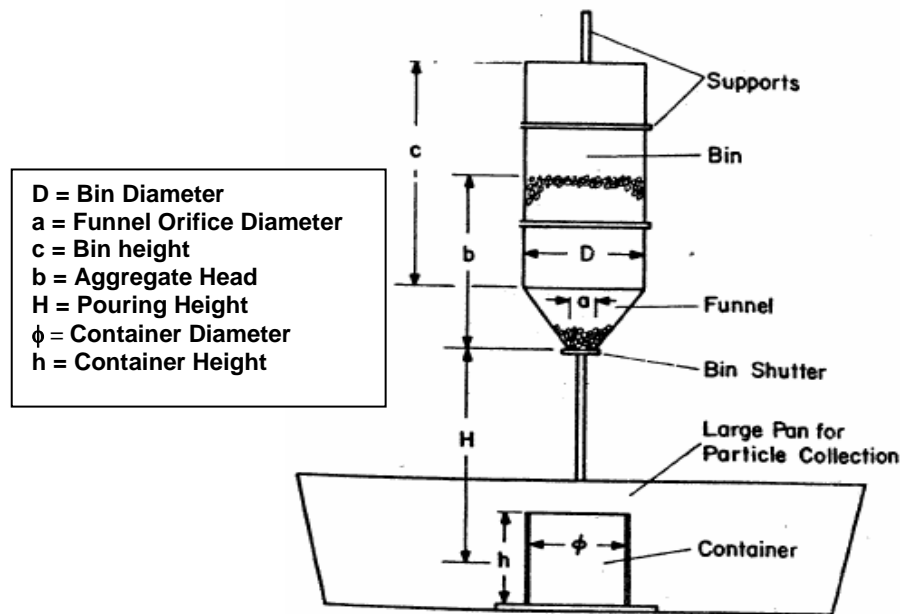


Fig. 2.9. Schematic Description of the Pouring Device Used by Rugosity Test

Time Index

This test method was developed in France in 1981, and Quebec Ministry of Transportation Aggregate Laboratory in Quebec City uses this test. It was used for fine aggregates only, but it can be modified to measure the properties of coarse aggregates. Similar to the rugosity test, the basis for this method is that the flow rate of an aggregate mass through a known orifice is affected by angularity, surface texture, and bulk specific

gravity of the aggregate (Janoo 1998; Janoo and Korhonen 1999). Time Index test apparatus is shown in Fig. 2.10.



Fig. 2.10. Time Index Test Apparatus

AASHTO T 236 (ASTM D3080) Direct Shear Test

This test is normally conducted in accordance with the AASHTO T 236 or ASTM D3080 procedure. This test is used to measure the internal friction angle of a fine aggregate under different normal stress conditions. A prepared sample of the aggregate is consolidated in a shear mold. The sample is then placed in a shear device and sheared by a horizontal force while a normal stress is applied (Chowdhury and Button 2001; Lee et al. 1999b). Fig. 2.11 shows the direct shear testing machine.

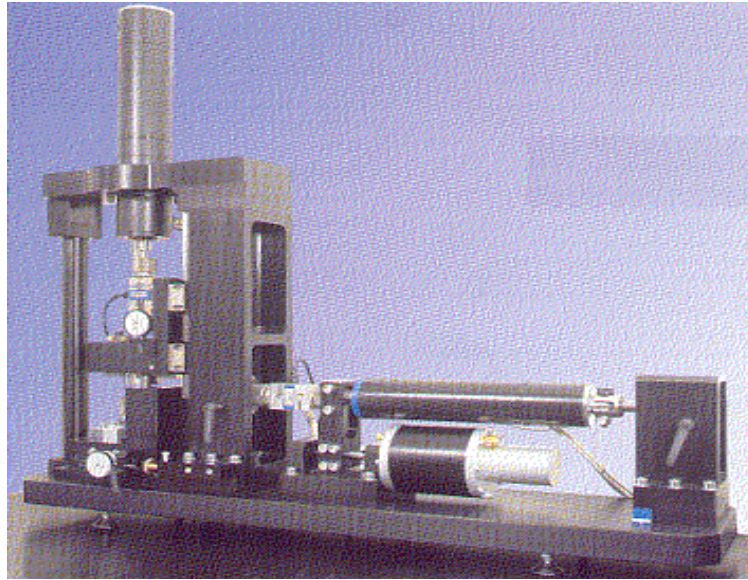


Fig. 2.11. Direct Shear Testing Machine

Direct Methods

These methods vary in the level of sophistication used to obtain direct information on aggregate shape. For example, the ASTM D5821 procedure simply relies on visual inspection of aggregates, and ASTM D4791 uses a mechanical device to classify aggregates according to the proportions of aggregate dimensions. The method developed by Jahn (2000) uses a digital caliper to provide the distribution of the proportions of aggregate dimensions, and the rest of the direct methods use imaging systems and analysis procedures to measure aggregate dimensions. An imaging system consists of a mechanism for capturing images of aggregates and methods for analyzing aggregate characteristics. Table 2.1 summarizes the majority of the imaging systems available commercially or in research institutions.

In addition to the systems in Table 2.1, several studies have presented experimental setups to facilitate capturing aggregate images (Kuo et al. 1996; Masad et al. 2001; Brzezicki and Kasperkiewicz 1999). Imaging systems and analysis procedures

focus on quantifying form (Barksdale et al. 1991; Kuo et al. 1996; Masad et al. 1999a, 1999b; Brzezicki and Kasperkiewicz 1999; Weingart and Prowell 1999; Maertz and Zhou 2001; Tutumluer et al. 2000), angularity (Li et al. 1993; Wilson and Klotz 1996; Yeggoni et al. 1994; Masad et al. 2000, 2001; Kuo and Freeman 2000; Rao et al. 2002), and texture (Hryciw and Raschke 1996; Wang and Lai 1998; Masad and Button 2000; Masad et al. 2001).

ASTM D5821 Determining the Percentages of Fractured Particles in Coarse Aggregate

This test method is considered to be a direct method for measuring coarse aggregate angularity. The method is based on evaluating the angularity of an aggregate sample (mostly used for gravel) by visually examining each particle and counting the number of crushed faces, as illustrated in Fig. 2.12. It is also the method currently used in the Superpave system for evaluating the angularity of coarse aggregate used in HMA (Lee et al. 1999a; Meininger 1998; Saeed et al. 2001).



Fig. 2.12. Illustration of Counting Percent of Fractured Faces

ASTM D4791 Flat and Elongated Coarse Aggregates

This method provides the percentage by number or weight of flat, elongated, or both flat and elongated particles in a given sample of coarse aggregate. The procedure uses a proportional caliper device, as shown in Fig. 2.13, to measure the dimensional ratio of aggregates. The aggregates are classified according to the undesirable ratios of width to thickness or length to width, respectively. Superpave specifications characterize an aggregate particle by comparing its length to its thickness or the maximum dimension to the minimum one (Yeggoni et al. 1996; Rao and Tutumluer 2000; Saeed et al. 2001; Fowler et al. 1996; Meininger 1998).



Fig. 2.13. Flat and Elongated Coarse Aggregate Caliper

Multiple Ratio Shape Analysis (MRA)

This method was developed by David Jahn (2000) from Martin Marietta, Inc. The method is used for categorizing various particle forms found in a coarse aggregate sample. It is based on classifying aggregates according to their dimensional ratios into five different categories instead of one ($<2:1$, $2:1$ to $3:1$, $3:1$ to $4:1$, $4:1$ to $5:1$, $>5:1$). The device consists mainly of a digital caliper connected to a data acquisition system and a computer. A particle is placed on a press table, and the press is lowered until it touches the aggregate particle and stops. The device records the gap between the press

and the table, which is equal to the particle dimension. The particle is then rotated in another direction and the procedure is repeated to obtain other dimensions. These readings are recorded in a custom designed spreadsheet that displays the distribution of dimensional ratio in the aggregate sample (Jahn 2000). Fig. 2.14 shows the digital MRA device.



Fig. 2.14. Improved Digital Multiple Ratio Analysis Device (MRA) by Martin Marietta

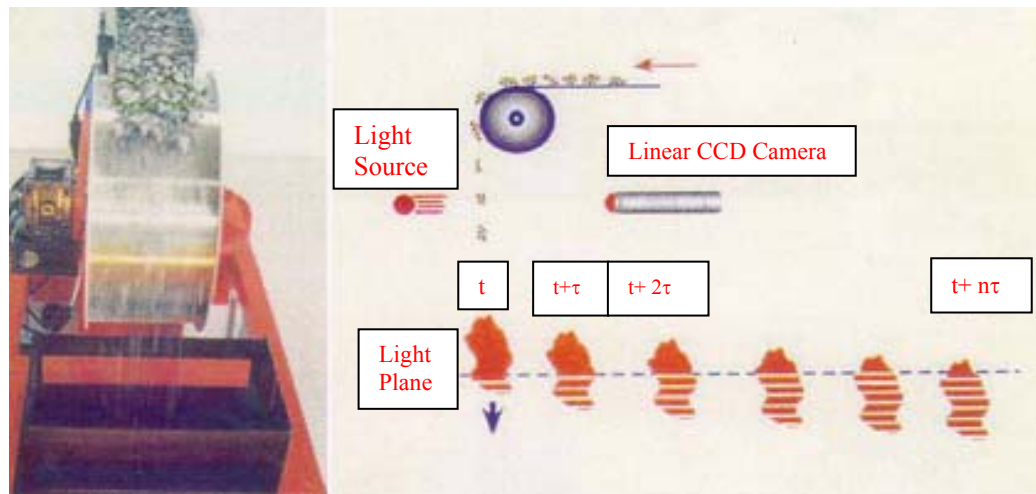
VDG-40 Videograder

This system was developed by the French public works laboratory (LCPC). The system consists mainly of a device to feed the aggregates that fall in front of a backlight and a camera to capture images. The system uses a line-scan charge-coupled device (CCD) camera to image and evaluate every particle in the sample as it falls in front of the backlight. A mathematical procedure based on assuming elliptical particles is used to calculate each particle's third dimension from the two-dimensional (2-D) projection images captured. All analysis and data reporting are performed in a custom software package. This system is used in the laboratory to obtain automated aggregate gradation measurements and also particle flatness and elongation (Emaco Ltd Canada; Browne et

al. 2001). Fig. 2.15(a) and 2.15(b) show, respectively, the VGD-40 Videograder and a schematic of image acquisition of falling aggregates.



(a)



(b)

Fig. 2.15. VDG-40 Videograder. (a) Components of VDG-40 Videograder and (b) Image Acquisition of Falling Aggregates in VDG 40 Videograder

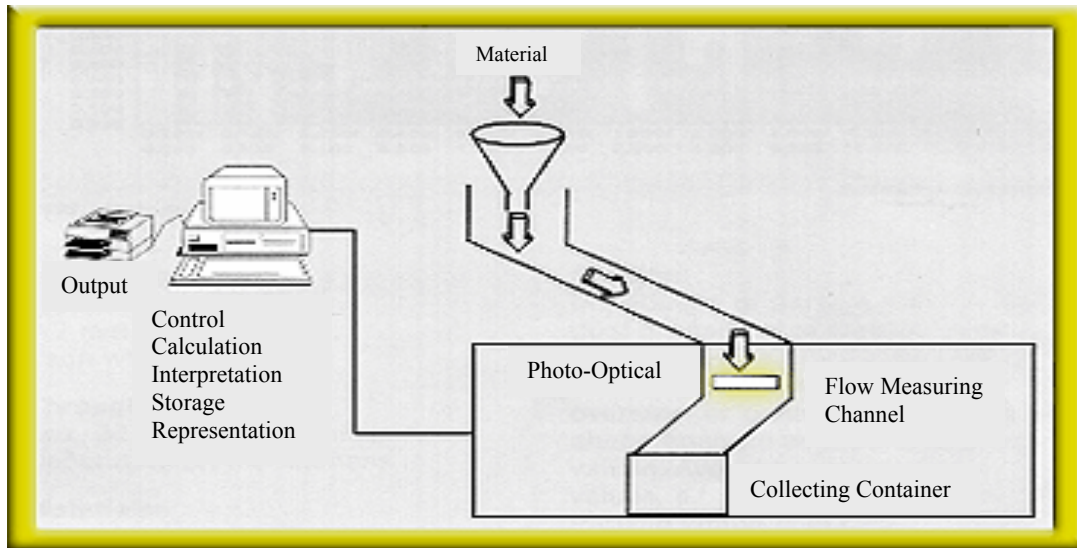
Computer Particle Analyzer CPA

The Computer Particle Analyzer (CPA) is similar to the VDG-40 Videograder, as it uses a line-scan CCD camera to image and evaluate every particle in the sample as it falls in front of the backlight. However, it can be used in the laboratory as well as on-line (continuous scanning of a product stream). The current analysis of this system focuses on gradation and form by assuming an idealized shape for aggregate particles to obtain the third dimension from images of 2-D projection. All analysis and data reporting are performed in a custom software package (Terry Reckart-W.S. Tyler mentor Inc.; Browne et al. 2001). CPA system and a schematic description of the CPA are shown in Figs. 2.16(a) and 2.16(b), respectively.



(a)

Fig. 2.16. Computer Particle Analyzer System (CPA). (a) Components of Computer Particle Analyzer System (CPA) and (b) Schematic Description of How CPA Works



(b)

Fig. 2.16. Continued*Micromeritics OptiSizer (PSDA)*

This device was initially developed for online applications. The system uses a line-scan CCD camera to image and evaluate particles in a sample as it falls in front of the backlight. Similar to the image analysis system discussed above, an idealized shape of particles is used to provide information about gradation and shape. All analysis and data reporting are performed in a custom software package (Strickland-Micromeritics OptiSizer; Browne et al. 2001). Fig. 2.17 shows the Micromeritics OptiSizer PSDA system.

Video Imaging System (VIS)

This system uses a line-scan CCD camera to image and evaluate particles in the sample as it falls in front of the backlight. Similar to the VDG-40 Videograder system, VIS assumes an idealized shape of a particle to provide information on gradation and form.

All analysis and data reporting are performed in a custom software package (John B. Lond Co.; Browne et al. 2001). The VIS is shown in Fig. 2.18



Fig. 2.17. Micromeritics OptiSizer (PSDA)



Fig. 2.18 Video Imaging System (VIS)

Buffalo Wire Works (PSSDA)

This system was developed by Dr. Dayakar Penumadu, currently with the University of Tennessee. The system uses a line-scan CCD camera to image and evaluate particles as they fall in front of the backlight. The system, mainly developed for a laboratory environment, provides information about gradation and shape. All analysis and data reporting are performed in a custom software package (Dr Penumadu-University of Tennessee; Browne et al. 2001). There are two systems available for measuring the characteristics of coarse and fine aggregates. Fig. 2.19 shows pictures of both systems used for analysis of coarse aggregates (PSSDA-Large) and fine aggregates (PSSDA-Small).



(a)

Fig. 2.19. Buffalo Wire Works (PSSDA) Systems for Coarse and Fine Aggregates. (a) PSSDA-Large and (b) PSSDA-Small

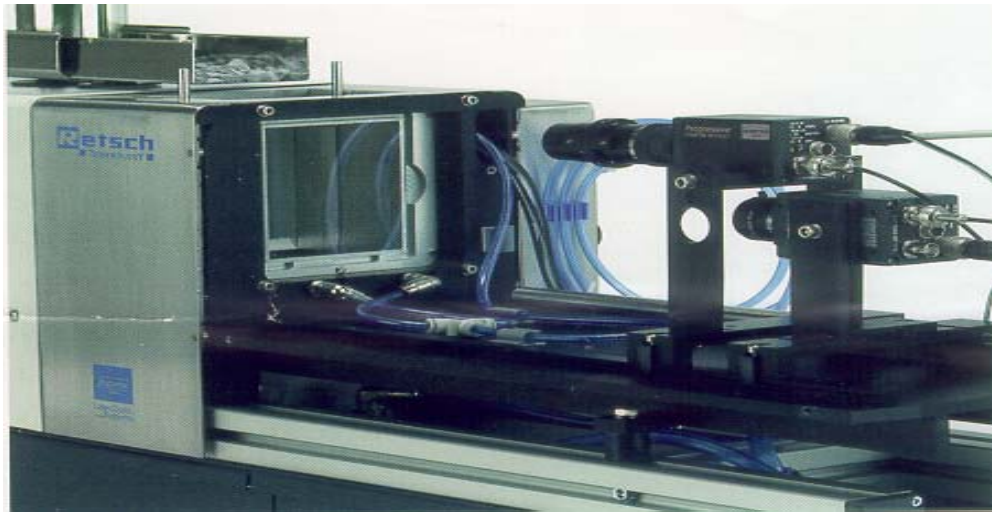


(b)

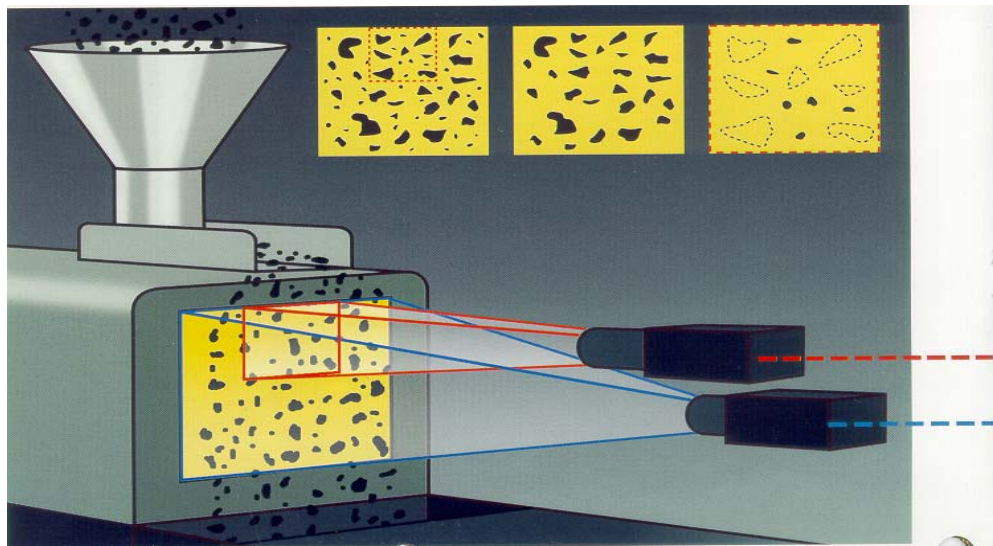
Fig. 2.19. Continued

Camsizer

Two optically matched digital cameras comprise the heart of the Camsizer system as seen in Fig. 2.20(a). These two cameras are used to capture images of fine and coarse aggregates at different resolutions. Individual particles exit the hopper and fall between the light source and the camera. Particles are detected as projected surfaces and digitized in the computer. This commercially available system automatically produces particle size distributions and some aspects of particle shape characteristics (Christison Scientific Equipment Ltd). Fig. 2.20(b) shows an illustration of the Camsizer.



(a)



(b)

Fig. 2.20. Camsizer System. (a) Overall View of the Camsizer and (b) Illustration of the Two Cameras Used in the Camsizer

WipShape

The system was developed by Dr. Maerz with the University of Missouri for coarse aggregate analysis. In the first version of the system, the aggregate particles were fed from a hopper into a mini-conveyor system. In a more recent version, the aggregate particles are placed in front of two orthogonal oriented synchronized cameras, which capture images of each particle from two views. These images are used to determine the three dimensions of particles. The system provides information on aggregate shape and gradation (Maerz et al. 1996; Maerz and Lusher 2001; Maerz and Zhou 2001). Fig. 2.21 below shows the most recent version of WipShape System.



Fig. 2.21. WipShape System

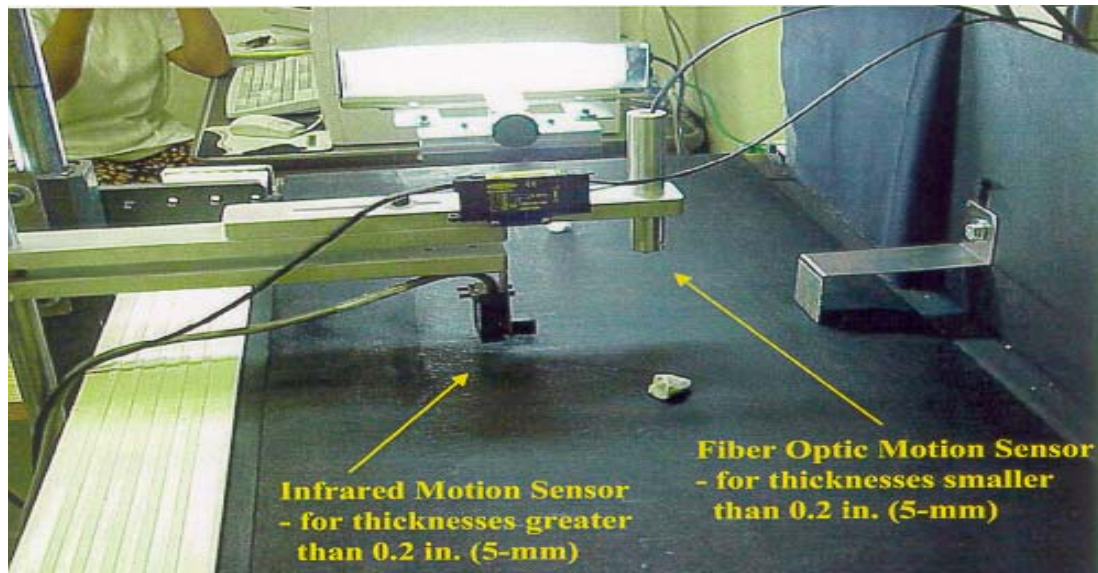
University of Illinois Aggregate Image Analyzer (UIAIA)

This method was developed by Dr. Tutumluer with the University of Illinois. It uses three cameras to capture projections of coarse particles as they move on a conveyor belt. These projections are used to reconstruct three-dimensional representations of particles. The shape is determined from the measured dimensions directly without the need to assume idealized shape of particles. The system provides information on gradation, form, angularity, and texture (Rao et al. 2002). The UIAIA and the aggregate detection system are shown in Figs. 2.22(a) and 2.22(b), respectively.



(a)

Fig. 2.22. University of Illinois Aggregate Image Analyzer (UIAIA). (a) Components of the UIAIA system and (b) Details of the Aggregate Detection System



(b)

Fig. 2.22. Continued*Aggregate Imaging System (AIMS)*

This system was developed by Dr. Eyad Masad. The system operates based on two modules. The first module is for the analysis of fine aggregates; black and white images are captured using a video camera and a microscope. The second module is devoted to the analysis of coarse aggregate; gray images as well as black and white images are captured. The fine aggregates are analyzed for form and angularity, while the coarse aggregates are analyzed for form, angularity, and texture. The video microscope is used to determine the depth of particles, while the images of 2-D projections provide the other two dimensions. These three dimensions quantify form. Angularity is determined by analyzing the black and white images, while texture is determined by analyzing the gray images (Fletcher et al. 2002; Masad 2003). A picture of AIMS is shown in Fig. 2.23.

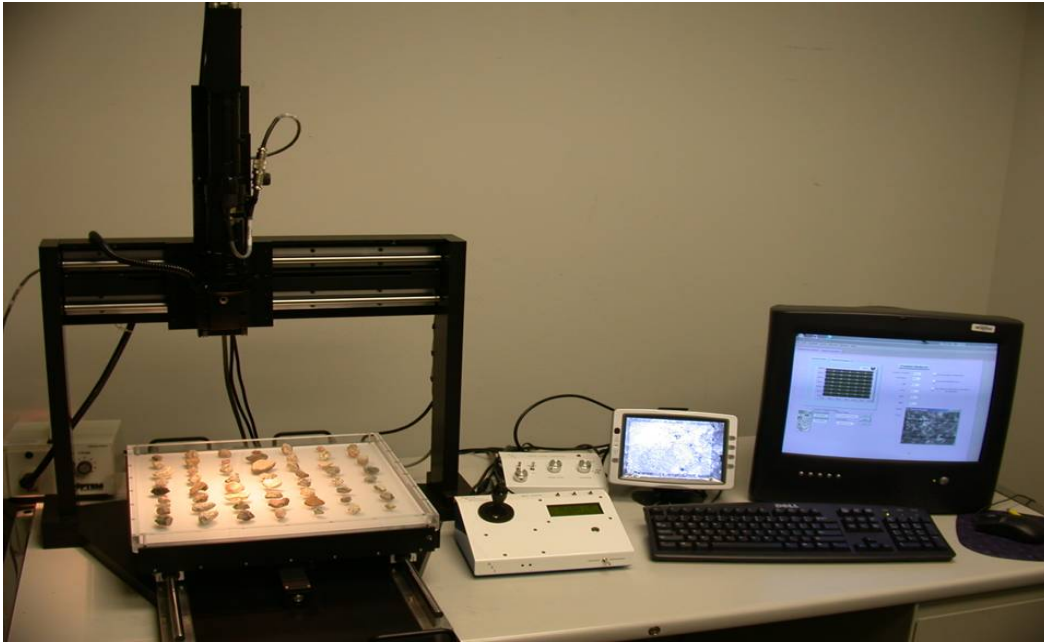


Fig. 2.23. Aggregate Imaging System (AIMS)

Laser-Based Aggregate Analysis System (LASS)

This system was developed by Dr. Carl Hass and Dr. Alan Rauch at the University of Texas-Austin to characterize size and shape parameters of coarse aggregates. A laser scanner is mounted on a linear motion slide that passes over an aggregate scattered on a flat platform, scanning the particles with a vertical laser plane. The three-dimensional (3-D) scanner data are transformed into gray-scale digital images, where the gray scale pixel values present the height of each datum point. These heights are used to calculate aggregate characteristics. These images are used to determine parameters of form, angularity, and texture (Kim et al. 2001, 2002). Fig. 2.24 shows a schematic description of LASS.

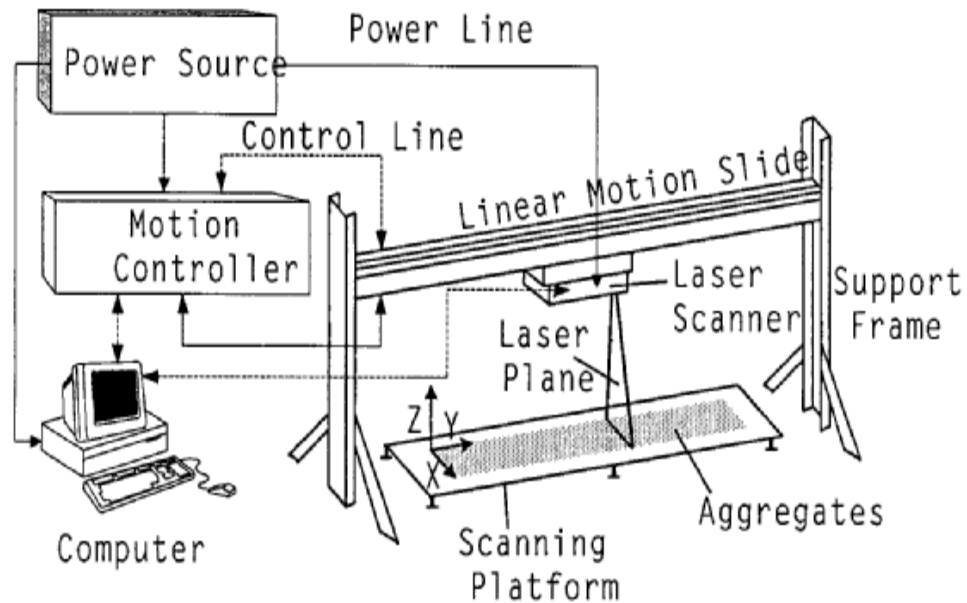


Fig. 2.24. Laser-based Aggregate Scanning System (LASS) Hardware Architecture

IMAGE ANALYSIS METHODS FOR CHARACTERIZING AGGREGATES

The imaging systems mentioned above utilize different mathematical procedures for the analysis of aggregate shape characteristics. The validity of the mathematical procedures is essential for the results to be useful in quantifying aggregate shape. However, the validity of these mathematical procedures should be evaluated separate from the capabilities of the image acquisition hardware.

Several investigation studies have been conducted on the use of imaging technology to quantify aggregate shape properties and relate them to the performance of pavement layers. Some of these studies focused on developing procedures to describe form (Barksdale et al. 1991; Kuo et al. 1996; Masad et al. 1999a,1999b; Brzezicki and Kasperkiewicz 1999; Weingart and Prowell 1999; Maertz and Zhou 2001; Tutumluer et al. 2000), angularity (Li et al. 1993; Wilson and Klotz 1996; Yeggoni et al. 1994; Masad et al. 2000; Kuo and Freeman 2000; Masad 2001; Rao et al. 2002), and surface texture (Hryciw

and Raschke 1996; Wang and Lai 1998; Masad and Button 2000; Masad 2001; Fletcher et al. 2002, 2003; Chandan et al. 2004).

This section describes, in general terms, most of the image analysis methods used to characterize particle form, angularity, or texture. *It is crucial to emphasize that the discussion provided in this section on the analysis methods is largely taken from Masad (2001), Fletcher (2002) master thesis, and Chandan et al. (2004).*

Typical Analysis of Form

In order to properly characterize the form of an aggregate particle, information about three dimensions of the particle is necessary {longest dimension, [d_l], intermediate dimension, [d_i], and shortest dimension, [d_s]}. A number of indices have been proposed for measuring form that relate the ratio of two dimensions, such as elongation and flatness. Sphericity (Krumbein 1941) and shape factor are indices that are expressed in terms of three dimensions.

$$\text{Sphericity} = \sqrt[3]{\frac{d_s * d_i}{d_l^2}} \quad (2.1)$$

$$\text{Shape Factor} = \frac{d_s}{\sqrt{d_l * d_i}} \quad (2.2)$$

Form factor is a widely used measure of form in two dimensions and is expressed by the following equation:

$$\text{Form Factor} = \frac{4\pi A}{P^2} \quad (2.3)$$

where P and A are the perimeter and area of a particle, respectively. Form factor is equal to unity for a circular-shape particle. The inverse of the form factor, which is known as roundness (ROUND) can also be used. Some analysis systems use other terms to describe form factor, the Camsizer system, for example, uses the term sphericity (SPHT) to describe this same term. As in shape factor, a circular object will have a roundness value of 1.0 and other shapes will have roundness values greater than 1.0.

The form index was proposed by Masad et al. (2001) to describe form in 2-D. It uses incremental changes in the particle radius. The length of a line that connects the center of the particle to the boundary of the particle is termed radius. The form index is expressed by the following equation:

$$\text{Form Index} = \sum_{\theta=0}^{\theta=360-\Delta\theta} \frac{|R_{\theta+\Delta\theta} - R_{\theta}|}{R_{\theta}} \quad (2.4)$$

where θ is the directional angle and R is the radius in different directions. By examining Eq. (2.4) we can see that if a particle was a perfect circle the form index would be zero. Although the form index is based on 2-D measurements, it can easily be extended to analyze the 3-D images of aggregates.

Fourier series can be used to analyze the form, angularity, and texture of aggregate shape. Each aggregate profile, defined by the function $R(\theta)$, can be analyzed using Fourier series coefficients as follows:

$$R(\theta) = a_0 + \sum_{n=1}^{\infty} [a_n \cos(n\theta) + b_n \sin(n\theta)] \quad (2.5)$$

where a_n and b_n are the Fourier coefficients. The function $R(\theta)$ traces out the distance to the boundary from a central point as a function of the angle θ , $0^\circ < \theta < 360^\circ$. Obviously, $R(\theta)$ is a periodic function. These coefficients can be evaluated using the following integrals:

$$a_0 = \frac{1}{2\pi} \int_0^{2\pi} R(\theta) d\theta \quad (2.6)$$

$$a_n = \frac{1}{\pi} \int_0^{2\pi} R(\theta) \cos(n\theta) d\theta \quad n = 1, 2, 3, \dots \quad (2.7)$$

$$b_n = \frac{1}{\pi} \int_0^{2\pi} R(\theta) \sin(n\theta) d\theta \quad n = 1, 2, 3, \dots \quad (2.8)$$

If $R(\theta)$ is only known numerically, at a discrete number of angles, the above integrals can be written using summations as follows:

$$a_0 = \frac{1}{2\pi} \sum_{\theta=0}^{2\pi-\Delta\theta} \left(\frac{R(\theta + \Delta\theta) + R(\theta)}{2} \right) \quad (2.9)$$

$$a_n = \frac{1}{\pi} \sum_{\theta=0}^{2\pi-\Delta\theta} \left(\frac{R(\theta + \Delta\theta) + R(\theta)}{2} \right) (\sin n(\theta + \Delta\theta) - \sin n\theta) \quad (2.10)$$

$$b_n = \frac{1}{\pi} \sum_{\theta=0}^{2\pi-\Delta\theta} \left(\frac{R(\theta + \Delta\theta) + R(\theta)}{2} \right) (-\cos(\theta + \Delta\theta) + \cos n\theta) \quad (2.11)$$

where $R(\theta)$ is measured only at predefined increments, and θ takes on values from 0 to $(2\pi - \Delta\theta)$ with an increment $\Delta\theta$ of about 4° . The higher the value of n used in Eq. (2.5), the better the actual particle profile is reproduced. Wang et al. (2003) formulated shape signatures using the a_n and b_n coefficients as follows:

Form Signature: $n \leq 4$

$$\alpha_s = \sum_{j=1}^4 \left[\left(\frac{a_n}{a_0} \right)^2 + \left(\frac{b_n}{a_0} \right)^2 \right] \quad (2.12)$$

The shape parameters (form, angularity, and texture) can all be represented by the same function and at the same time can be differentiated by the frequency magnitudes of the harmonics used to capture a particle boundary. Form is captured using harmonics with lower frequency than texture and angularity.

Another way of presenting the form of a particle is by using Flat and Elongated Ratio (FER). FER represents the ratio between the longest dimension and the shortest dimension of a particle. Aspect ratio (ASPCT), which is similar to FER ratio but usually used for 2-D projections, is also used to describe the form of particles. It is the ratio of the major axis to minor axis of the ellipse equivalent to the object, which is a particle image in this case. The equivalent ellipse is supposed to have the same area as the particle image and first and second degree moment. Aspect ratio is always equal or greater than 1.0 since it is defined as (major axis/minor axis).

Breadth to width ratio can also be used to describe the form of aggregate particles. The Camziser system uses the following equation to calculate this ratio:

$$\text{Ratio of Breadth to Width} = b/l = \frac{\min(x_c)}{\max(x_{Fe})} \quad (2.13)$$

Where, x_c is the maximum chord, and x_{Fe} is the Feret diameter, both determined from up to 32 directions for each particle. Feret diameter is the distance between two tangents placed 90° to the measuring direction and touching the particle.

Symmetry is another term that some imaging systems use to describe aggregate form. Symmetry of an aggregate particle can be given by:

$$\text{Symmetry} = S_{\text{symm}} = \frac{1}{2} \left[1 + \min \left(\frac{r_1}{r_2} \right) \right] \quad (2.14)$$

where r_1 and r_2 are the distances of the center of gravity to the edge in a given direction, i.e., maximum diameter = $r_1 + r_2$

2-D analysis of form may be influenced when the particle is placed on a flat plate to capture the image. A particle will tend to come to rest on a flat side rather than in a random position. Therefore, as will be evident in the discussion given later in this section, current research efforts are focusing on developing of methods for capturing the three dimensions of aggregates that can be used in Eqs. (2.1) and (2.2) to quantify form.

Typical Analysis of Angularity

Analysis methods for angularity have used mainly black and white images of 2-D projections of aggregates. The assumption here is that the angularity elements in 2-D are a good measure of the 3-D angularity. It should be noted that the image resolution required for angularity analysis can easily be achieved using automated systems for capturing images. Masad et al. (2001) specified that an image resolution with a pixel size less than or equal to 1% of the particle diameter is required for angularity analysis.

Fourier Series Analysis of Angularity

As mentioned earlier in the previous section, Fourier series analysis can be used to analyze angularity of aggregates. The shape signature for angularity as formulated by Wang et al. (2003) is given by:

Angularity Signature: $5 \leq n \leq 25$

$$\alpha_r = \sum_{j=5}^{25} \left[\left(\frac{a_n}{a_0} \right)^2 + \left(\frac{b_n}{a_0} \right)^2 \right] \quad (2.15)$$

where a_0 , a_n , and b_n are found using Eqs. (2.9 - 2.11). Angularity is captured using harmonics with frequencies that are higher than form and lower than texture.

Surface Erosion-Dilation Technique

The erosion-dilation technique has been used to capture fine aggregate angularity and even surface texture (Masad and Button 2000). Erosion-dilation is well known in image processing, where it is used both as a smoothing technique (Rosenfeld and Kak 1976) and a shape classifier (Blum 1967). Erosion is a morphological operation in which pixels are removed from the image according to the number of pixels surrounding it with different color (Masad et al. 2000). Erosion can be visualized as a fire burning inward from the periphery of an object, in order to shrink the object to a skeleton or a point (Calabi and Hartnett 1968). Layer-by-layer erosion tends to smooth a particle surface.

Dilation is the opposite of the erosion. A layer of pixels is added around the periphery of the eroded image to form a simplified version of the original object. An image does not necessarily need to be restored to its original state after a number of erosion and dilation cycles (Young et al. 1981). There may be surface angularities that are lost under erosion and will not be restored during dilation since there is no seed pixel from which the dilation can build (Ehrlich et al. 1984). Following this logic, one can state that the area of the object lost after erosion and dilation is “proportional” to the angularity of the particle, assuming that no particles are lost during the procedure. Aggregate particle angularity is measured by the area lost during the erosion-dilation process and is expressed as a percentage of the total area of the original particle, which is described by the following expression:

$$\text{Surface Parameter} = \frac{A_1 - A_2}{A_1} * 100\% \quad (2.16)$$

where A_1 and A_2 are the area of the object before and after applying the erosion-dilation operations, respectively (Fig. 2.25). A particle with more angularity would lose more area than that of a smooth one; therefore, the surface parameter would be higher. Masad and Button (2000) found that this parameter correlated to angularity of a particle at low resolutions and to surface texture of a particle at higher resolutions.

Fractal Behavior Technique

In its simplest form, fractal behavior is defined as the self-similarity exhibited by an irregular boundary when captured at different magnifications. Fractal behavior has many applications in science (Mandelbrot 1984), particularly for describing the shape of natural objects (e.g., clouds, body organs, rocks, etc.). Smooth boundaries erode (or dilate) at a constant rate. However, irregular or fractal boundaries have more pixels touching opposite-color neighbors, and, hence, they do not erode (or dilate) uniformly. This effect has been used to estimate fractal dimensions, and, consequently, angularity along the object boundary. The basic idea for measuring a fractal dimension by image analysis came from the Minkowski definition of a fractal boundary dimension (Russ 1998). This procedure was used by Masad et al. (2000) to characterize the angularity of a wide range of aggregates used in asphalt mixes. The procedure is depicted in Fig. 2.25. The first step is to apply a number of erosion and dilation operations on the original image as shown in Fig. 2.25(a), (b), and (d). Then, the eroded and dilated images are combined using the logical operator (Ex-OR). Using this operator, the two images (b and d) are compared and pixels that have black color representing aggregate and are at the same location on both images are removed, as shown in Fig. 2.25(e). By doing so, the pixels retained on the final image (Fig. 2.25(e)) are only those removed during erosion and added during dilation. These pixels form a boundary, which has a width proportional to the number of erosion-dilation cycles and surface angularity (Fig. 2.25e).

The procedure continues by varying the number of erosion-dilation cycles and measuring the increase in the effective width of the boundary (total number of pixels divided by boundary length and number of cycles). Then, the effective width is plotted

versus the number of erosion-dilation cycles on a log-log scale. For a smooth boundary, the effective width to number-of-cycles relationship shows no trend; that is, the effective width remains constant at different numbers of cycles. However, for a boundary with angularity, the graph would show a linear variation, where the slope gives the fractal length of the boundary.

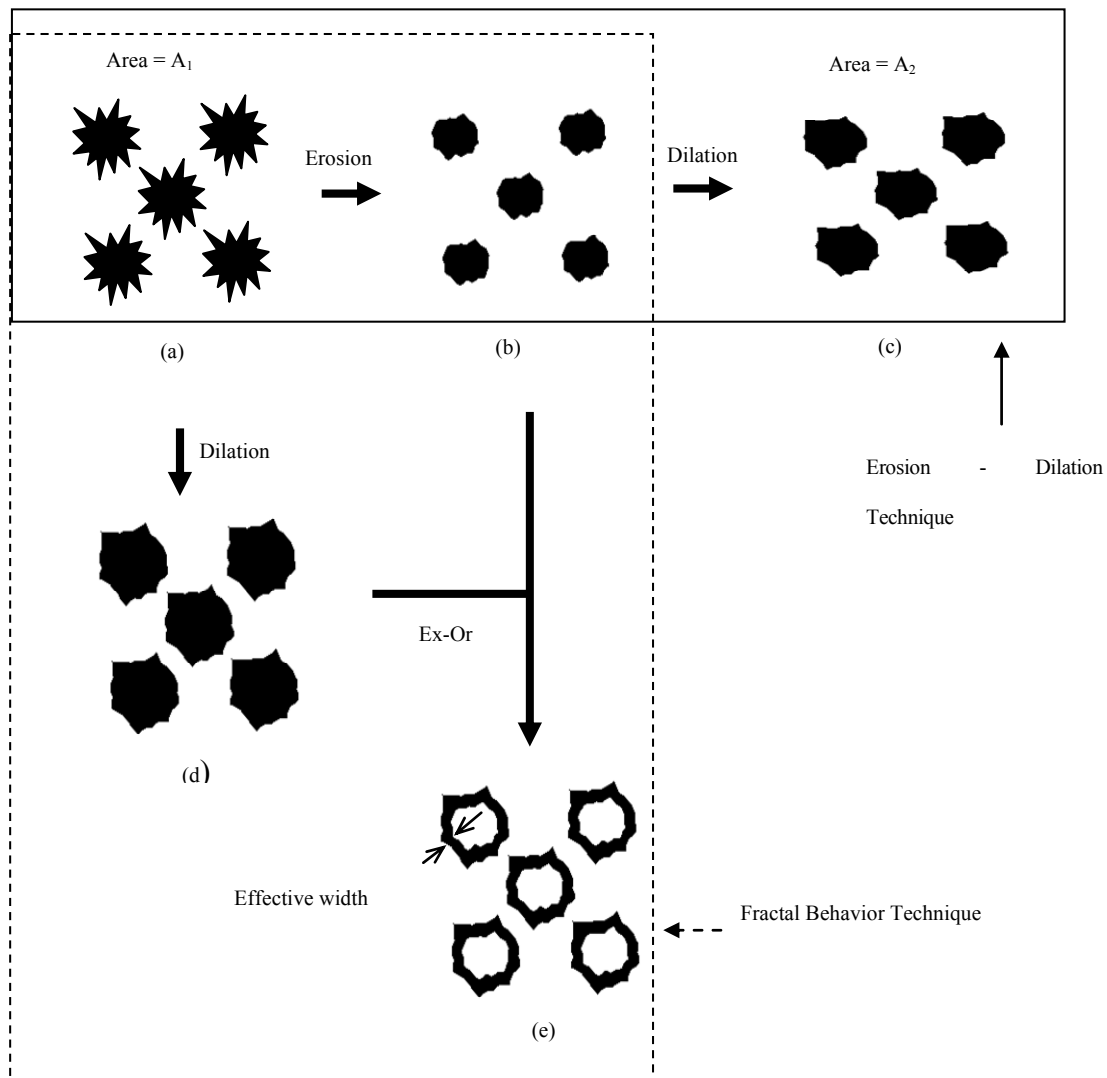


Fig. 2.25. Illustration of the Erosion-Dilation and Fractal Behavior Method (after Masad et al. 2001)

Hough Transform

Hough Transform is another technique used to recognize co-linearity in pixels that form the particle outline (Hough 1962). This technique has been successfully implemented in the medical field and in the analysis of aerial images. By detecting and measuring the length of any straight lines in a 2-D image and the angle between them, angularity of a particle can easily be determined.

Wilson et al. (1997) used the Hough Transform to develop an index for quantifying aggregate angularity. This transform was used to determine the longest line on the outline of particle images at each possible direction $A(\theta)$. Then, the length of the longest line, A_{Max} , in all directions and the average length of the line, A , which also corresponds to the longest line on the edge of the particle are computed. Angularity is then quantified by the index:

$$\text{Hough Transform Shape Index} = 1 - \frac{A}{A_{Max}} \quad (2.17)$$

Wilson and Klotz (1996) noted that if only one or two lines dominated the particle the value approached 1.0. However, if the particle was rounded or irregular, then the all of the straight lines are short and close to the average and the index approached 0.0. Therefore, the index approaches 0.0 for rounded particles and is typically greater than 0.6 for angular particles.

Gradient Method

The main idea behind this method is that at sharp corners of the surface of a particle image, the direction of the gradient vector for adjacent points on the surface changes rapidly. On the other hand, the direction of the gradient vector for rounded particles change slowly for adjacent points on the surface.

The gradient-based method for measuring angularity consists of the following steps. The acquired image is first thresholded to get a binary image. This is followed by the boundary-detection step. Next, the gradient vectors at each surface point are

calculated, using a Sobel mask that operates at each point on the surface and its eight nearest neighbors (Chandan et al. 2004).

The Sobel operator performs a 2-D spatial gradient measurement on an image and emphasizes regions of high spatial gradient that are located at the surface. The Sobel operator picks up the horizontal (G_x) and vertical (G_y) running edges in an image. These can then be combined to find the absolute magnitude of the gradient at each point and the orientation of the gradient. The angle of orientation of the edge (relative to the pixel grid) that results in the spatial gradient is given by:

$$\theta(x, y) = \tan^{-1} \left(\frac{G_x}{G_y} \right) \quad (2.18)$$

For the angularity analysis, the angle of orientation values of the edge points (θ) and the magnitude of the difference in these values ($\Delta\theta$) for adjacent points on the edge are calculated to describe how sharp or how rounded the corner is. Fig. 2.26 illustrates the method of assigning angularity values to a corner point on the edge. The angularity values for all the boundary points are calculated and their sum accumulated around the edge to finally form a measure of angularity, which is denoted the gradient index (GI) (Chandan et al. 2004):

$$GI = \sum_{i=1}^{N-3} |\theta_i - \theta_{i+3}| \quad (2.19)$$

where i denotes the i^{th} point on the edge of the particle and N is the total number of points on the edge of the particle.

Direct Measurements of Particle Dimensions

Kuo and Freeman (2000) proposed an angularity parameter, which is expressed by the following equation:

$$\text{Angularity Parameter} = \left(\frac{P_{convex}}{P_{ellipse}} \right)^2 \quad (2.20)$$

where $P_{ellipse}$ is the perimeter of an equivalent ellipse (i.e., an ellipse with the same longest and shortest axes of a particle), and P_{convex} is the perimeter of the bounding polygon.

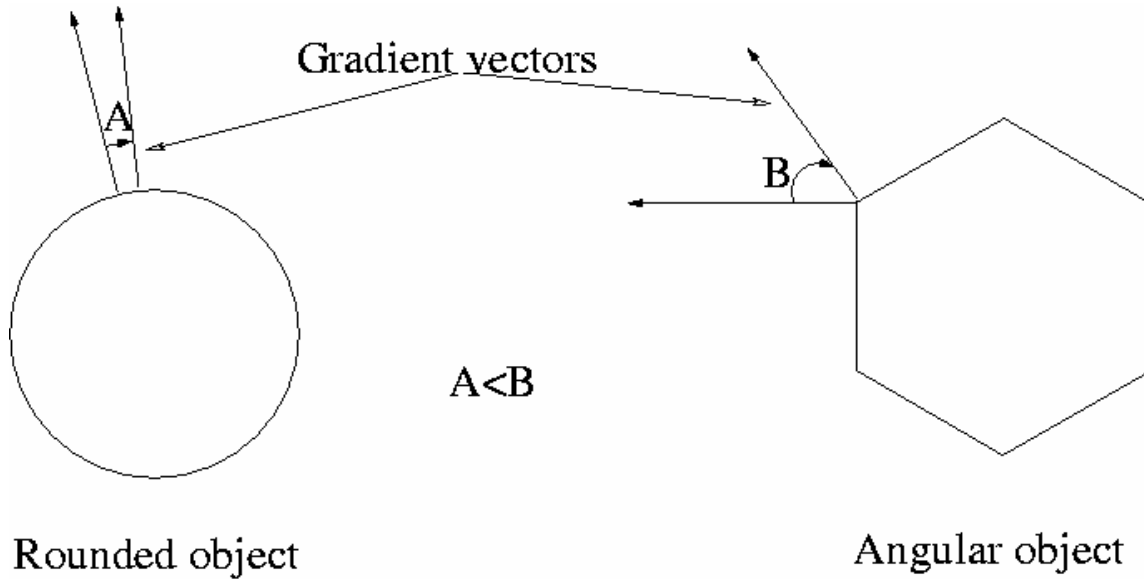


Fig. 2.26. Illustration of the Difference in Gradient between Particles (after Chandan et al. 2004)

Angularity Index

Masad et al. (2001) proposed the angularity index, which is described by the following equation:

$$\text{Angularity Index} = \sum_{\theta=0}^{\theta=360-\Delta\theta} \frac{|R_{P\theta} - R_{EE\theta}|}{R_{EE\theta}} \quad (2.21)$$

where $R_{P\theta}$ is the radius of the particle at a directional angle, θ . $R_{EE\theta}$ is the radius of an equivalent ellipse at the same θ . The index relies on the difference between the radius of

a particle in a certain direction and a radius of an equivalent ellipse taken in the same direction as a measure of angularity. By normalizing the measurements to the ellipse dimensions, the effect of form on angularity is minimized (Masad et al. 2001).

Outline Slope Method

Based on image analysis from the images captured by the University of Illinois Aggregate Imaging Analyzer (UIAIA), a quantitative angularity index (AIUI) was developed (Rao et al. 2002). The AIUI methodology is based on tracing the change in slope of the particle image outline obtained from each of the top, side, and front images. Accordingly, the AIUI procedure first determines an angularity index value for each 2-D image. Then, a final AIUI is established for the particle by taking a weighted average of its angularity determined for all three views.

To determine of the Angularity for each 2-D projection, an image outline, based on aggregate camera view projection, and its coordinates are first extracted. Next, the outline is approximated by an n -sided polygon as shown in Fig. 2.27. The angle subtended at each vertex of the polygon is then computed. Relative change in slope of the n sides of the polygon is subsequently estimated by computing the change in angle (β) at each vertex with respect to the angle in the preceding vertex. The frequency distribution of the changes in the vertex angles is established in 10° class intervals. The number of occurrences in a certain interval and the magnitude are then related to the angularity of the particle profile.

Eq. (2.22) is used for calculating angularity of each projected image. In this equation, e is the starting angle value for each 10° class interval and $P(e)$ is the probability that change in angle α has a value in the range e to $(e+10)$.

$$Angularity = A = \sum_{e=0}^{170} e * P(e) \quad (2.22)$$

The UIAI of a particle is then determined by averaging the angularity values (see Eq. 2.22) calculated from all three views when weighted by their areas as given in the following equation:

$$UIAI = \frac{A(front) * Area(front) + A(top) * Area(top) + A(side) * Area(side)}{Area(front) + Area(top) + Area(side)} \quad (2.23)$$

The final UIAI value for the entire sample is simply an average of the angularity index values of all the particles weighted by the particle weight, which measures overall degree changes on the boundary of a particle.

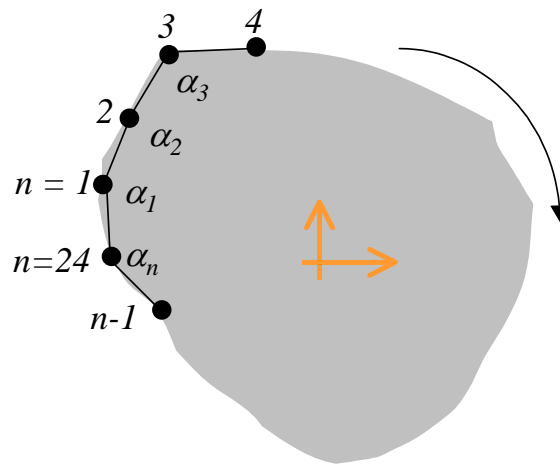


Fig. 2.27. Illustration of an n -Sided Polygon Approximating the Outline of a Particle (after Rao et al. 2002)

Convexity

Convexity is another parameter that can be used to describe angularity of aggregate particles. Convexity can be calculated using the following formula:

$$\text{Convexity} = Conv = \sqrt{\frac{A_{Particle}}{A_{Convex}}} \quad (2.24)$$

Where $A_{Particle}$ is the area of the real projection of the particle, and A_{Convex} is the area of the convex particle's projection.

Minimum Average Curve Radius

This method is described by Maerz (2004) and illustrated in Fig. 2.28. In this method aggregate angularity is defined as the minimum average curve radius of the individual particles. Maerz (2004) described the following procedure to calculate the minimum average curve radius: The radius of a circle containing three points on the profile is calculated from the array of x, y points, each point separated by 10 pixels. An instantaneous curve radius is determined for each point on the profile in this manner, creating an array of curve radii. Then the array of curve radii values are smoothed by a moving average filter. A 5-point Gaussian low-pass filter is used (see Fig. 2.29). The array of smoothed curve radii is examined to find local minima in the curve radius function. A test is performed to ensure that a corner of the aggregate piece does not result in more than one local minimum. Then the list of local minimum curve radii is ordered from smallest to largest. The averages of the four smallest curve radii are averaged to produce the minimum average curve radius of the individual piece.

Typical Analysis of Texture

The analysis of texture has been carried out using both black and white images and gray images. The main disadvantage of using black and white images is the high resolution required for capturing images, which makes it difficult to do using automated systems. In addition, the majority of texture details are lost when a gray image is converted to black and white. The analysis of gray images has the advantage of analyzing more texture data at the surface of a particle, leading to detailed information about texture. However, the main challenge facing this technique is the influence of natural variation of color on gray intensities and, consequently, texture analysis. Some image analysis techniques have the potential to separate the actual texture from color variations. The following sections discuss some of the techniques used to analyze the texture of aggregates.

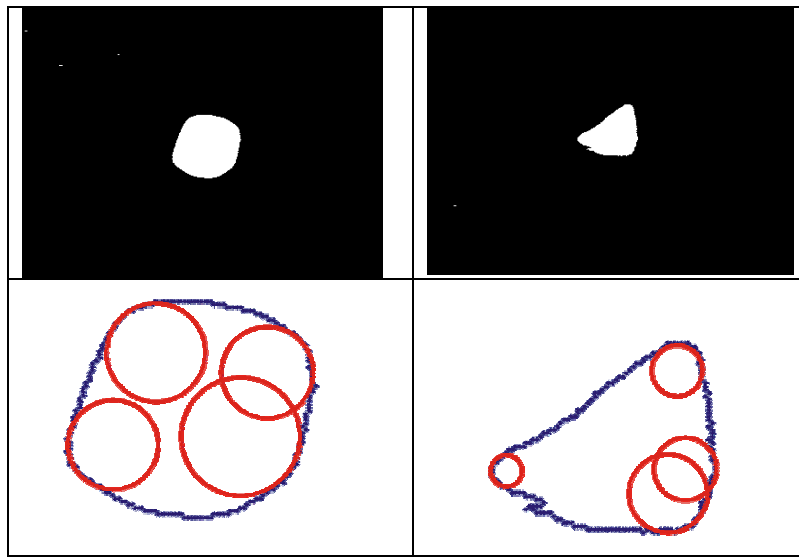


Fig. 2.28. Average Minimum Curve Radius Calculations. Left: Rounded Aggregate. Right: Angular Aggregate. Bottom: Aggregate Profile with Inscribed Curve Radii (after Maerz 2004)

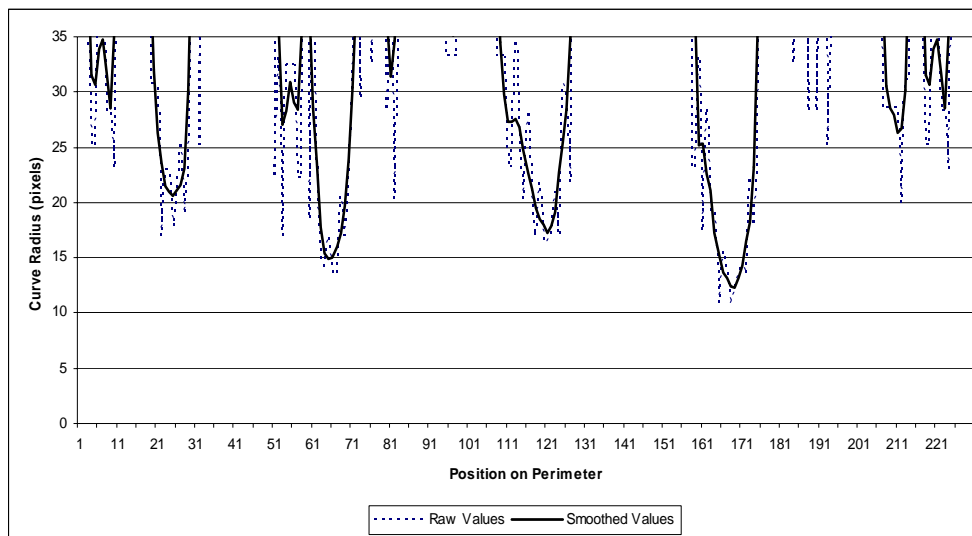


Fig. 2.29. Curve Radius Measurements around the Profile of the Rounded Particle in Fig. 2.28; Raw and Smoothed Values (After Maerz 2004)

Fourier Series Analysis of Texture

As mentioned earlier in the previous section, Fourier series analysis can be used to analyze texture of aggregates. The shape signature for texture as formulated by Wang et al. (2003) is given by:

Texture Signature: $26 \leq n \leq 180$

$$\alpha_t = \sum_{j=26}^{180} \left[\left(\frac{a_n}{a_0} \right)^2 + \left(\frac{b_n}{a_0} \right)^2 \right] \quad (2.25)$$

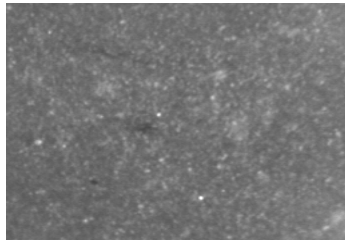
where a_0 , a_n , and b_n are found using Eqs. (2.9 to 2.11). Texture is captured using harmonics with frequencies that are higher than angularity and form.

Intensity Histogram Method

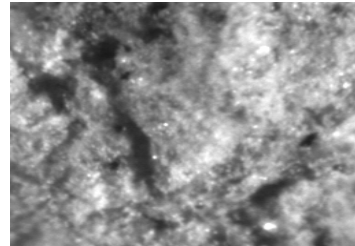
An intensity histogram evaluates the variation in the gray intensity of the gray-scale image over the entire image. The mean and standard deviation of the variations are the output from the intensity histogram. There is a correlation between the standard deviation of gray intensity and the surface texture of the particle (Masad et al. 2001). Standard deviations are typically much lower for smooth particles compared to those for rough particles. Fig. 2.30 shows images of smooth and rough particles and their intensity histograms.

Fast Fourier Transform Method

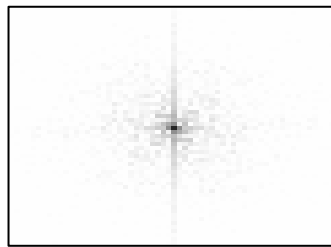
This is a well-known method in the sciences for converting data from the time or spatial domain to the frequency domain. Dominant frequencies become apparent when a Fast Fourier Transform (FFT) is applied to a gray-scale image. Frequency is a measure of reoccurrence of a distinct gray level intensity in the image. The resulting FFT image consists of points of different gray levels, where the distance of a point from the center represents the frequency and the gray level in the FFT image corresponds to the peak intensity at a given frequency (Russ 1998). The number of dominant peaks in the FFT has been found to be a measure of the surface texture (Masad et al. 2001) (Fig. 2.30).



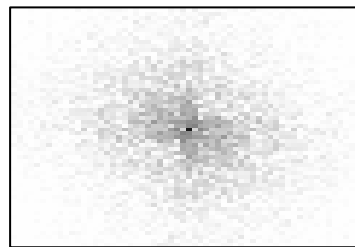
(a) Smooth texture



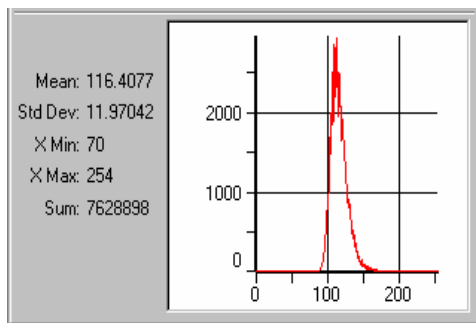
(b) Rough texture



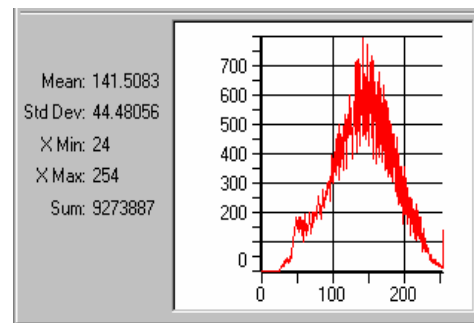
(c) FFT of smooth texture



(d) FFT of rough texture



(e) Histogram of smooth texture



(f) Histogram of rough texture

Fig. 2.30. Images of Smooth-and Rough-Textured Aggregates and Their Fast Fourier Transforms and Histograms (after Masad 2001)

Wavelet Analysis

Texture in an image is represented by the local variation in the pixel gray intensity values. Although there is no single scale that represents texture, the histogram and FFT analyses of texture capture only a single scale. Wavelet theory offers a mathematical framework for multi-scale image analysis of texture (Mallat 1989). This is advantageous to determine the texture scale or a combination of them that has the most influence on the aggregate performance in pavement layers

The wavelet transform works by mapping an image onto a low-resolution image and a series of detail images. An illustration of the method is presented here with the aid of Fig. 2.31. The original image is shown in Fig. 2.31(a). It is decomposed into a low-resolution image (Image 1 in Fig. 2.31(b)) by iteratively blurring the original image. The remaining images contain information on the fine intensity variation (high frequency) that was lost in Image 1. Image 2 contains the information lost in the y-direction, Image 3 has the information lost in the x-direction, and Image 4 contains the information lost in both x- and y-directions. Image 1 in Fig. 2.31b can be further decomposed similarly to the first iteration, which gives a multi-resolution decomposition and facilitates quantification of texture at different scales. An image can be represented in the wavelet domain by these blurred and detailed images. The texture parameter used is the average energy on Images 2,3, and 4 at each level. Texture index is taken at a given level as the arithmetic mean of the squared values of the detail coefficients at that level (level 6 is used):

$$Texture\ Index_n = \frac{1}{3N} \sum_{i=1}^3 \sum_{j=1}^N (D_{i,j}(x, y))^2 \quad (2.26)$$

where N denotes the level of decomposition and i takes values 1, 2, or 3, for the three detailed images of texture, and j is the wavelet coefficient index. More details on this method can be found in other references (Mallat 1989; Fletcher et al. 2002; Chandan et al. 2004). Owing to the multi-resolution nature of the decomposition, the energy signature, or equivalently, the texture content has a physical meaning at each level. Energy signatures at higher levels reflect the “coarser” texture content of the sample,

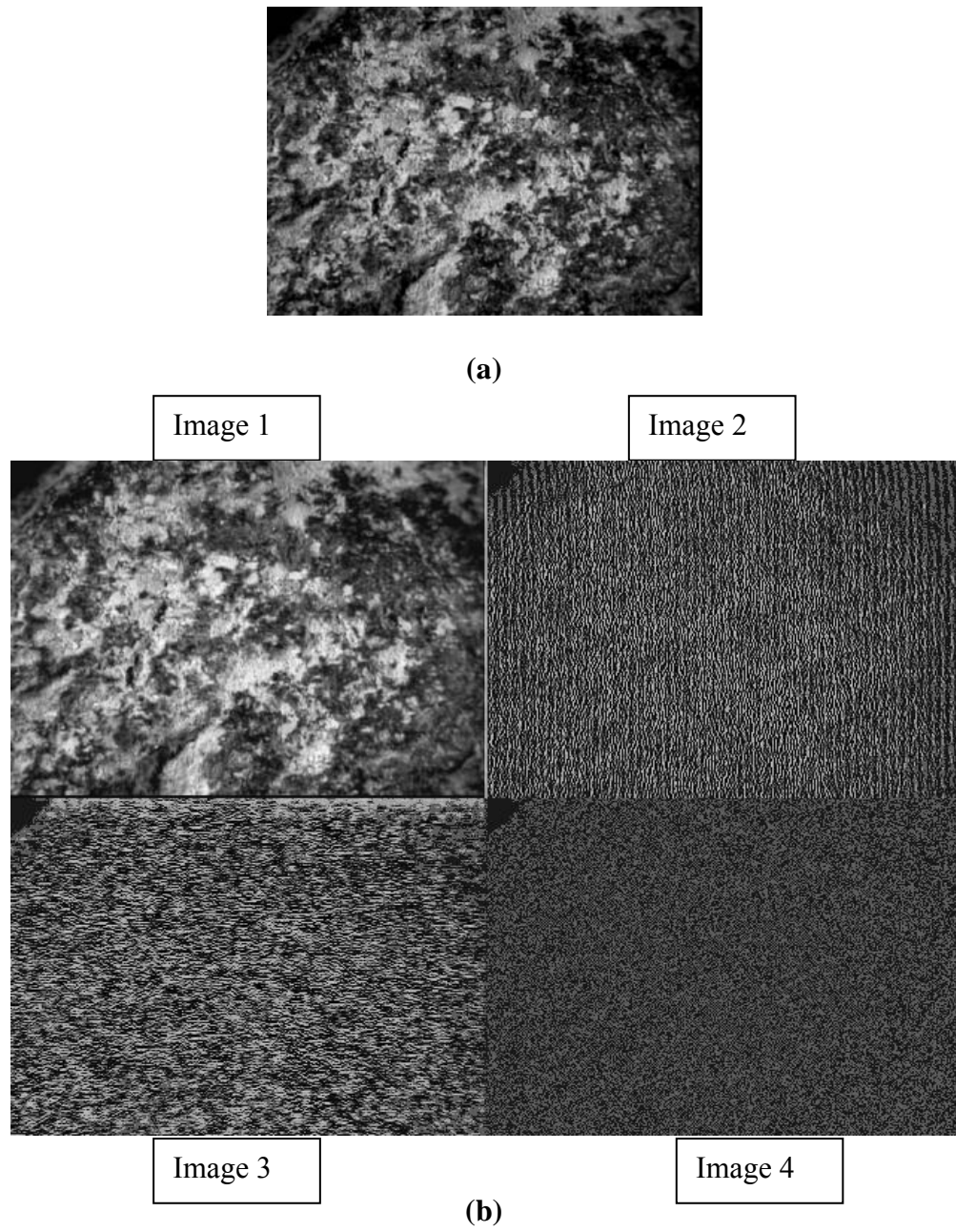


Fig. 2.31. Illustration of the Wavelet Decomposition (after Chandan et al. 2004)

while those at lower levels reflect the “finer” texture content.

Direct Measurements of Particle Dimensions

Kuo and Freeman (2000) proposed the texture parameter, which is expressed as follows:

$$\text{Texture Parameter} = \left(\frac{P}{P_{convex}} \right)^2 \quad (2.27)$$

Where, P is the perimeter of a particle measured on a black and white image and P_{convex} is the perimeter of a bounding polygon.

SUMMARY

The focus of this chapter was on presenting the findings of previous studies that are relevant to the influence of aggregate shape on performance of different types of pavements, and on identifying aggregate characteristics affecting performance. This chapter also included a brief description of the available test methods (direct and indirect) used for measuring aggregate shape characteristics. Image analysis techniques, that some of the imaging systems uses were also discussed in this chapter.

The comprehensive literature review revealed that the shape properties of coarse and fine aggregates used in hot-mix asphalt, hydraulic cement concrete, and unbound base and subbase layers are very important to the performance of the pavement system in which they are used. Aggregate shape can be decomposed to three independent characteristics: form, angularity and texture. Current methods used in practice for measuring these characteristics have several limitations; they are laborious, subjective, lack direct relation with performance parameters, and limited in their ability to separate the influence of angularity from that of texture. A number of research studies have shown that aggregates that exhibit high texture do not necessarily have high angularity, especially in coarse aggregates. Consequently, it is important to develop methods that are able to quantify each of the aggregate characteristics rather than a manifestation of their interactions.

CHAPTER III

IMPROVED AGGREGATE IMAGING SYSTEM (AIMS) FOR MEASURING SHAPE PROPERTIES

INTRODUCTION

This chapter describes the improvements made to the Aggregate Imaging System (AIMS). AIMS was developed to capture images and analyze the shape of a wide range of aggregate types and sizes, which covers those used in asphalt mixes, hydraulic cement concrete, and unbound layers of pavements. Improvements were made in this study to AIMS hardware and both the control and analysis softwares. The improvements addressed the operational characteristics, lighting scale, and automation capabilities.

DESCRIPTION OF THE AGGREGATE IMAGING SYSTEM “AIMS”

Details of the main components and design of the prototype aggregate imaging system have been reported in different publications (Fletcher 2002, Fletcher et al. 2003, Masad 2003). Fig. 3.1 shows a 3-D graphical model of AIMS illustrating the various components of the system.

AIMS was developed to capture images and analyze the shape of a wide range of aggregate types and sizes, which cover those used in HMA, hydraulic cement concrete, and unbound aggregate layers of pavements. AIMS uses a simple setup that consists of one camera and two different lighting schemes to capture images of aggregates at different resolutions, from which aggregate shape properties are measured using image analysis techniques that are based on sound scientific concepts.

The system operates based on two modules. The first module is for the analysis of fine aggregates (smaller than 4.75 mm (#4 sieve)), where black and white images are captured. The second module is devoted to the analysis of coarse aggregate (larger than 4.75 mm (#4 sieve)). In the coarse module, gray images as well as black and white images are captured. Combining analysis of both the coarse and fine aggregate analysis into one system is considered an advantage to reduce the cost of developing the system.

It also allows using the same analysis methods to quantify aggregate shape irrespective of size to facilitate relating aggregate shape to pavement performance.

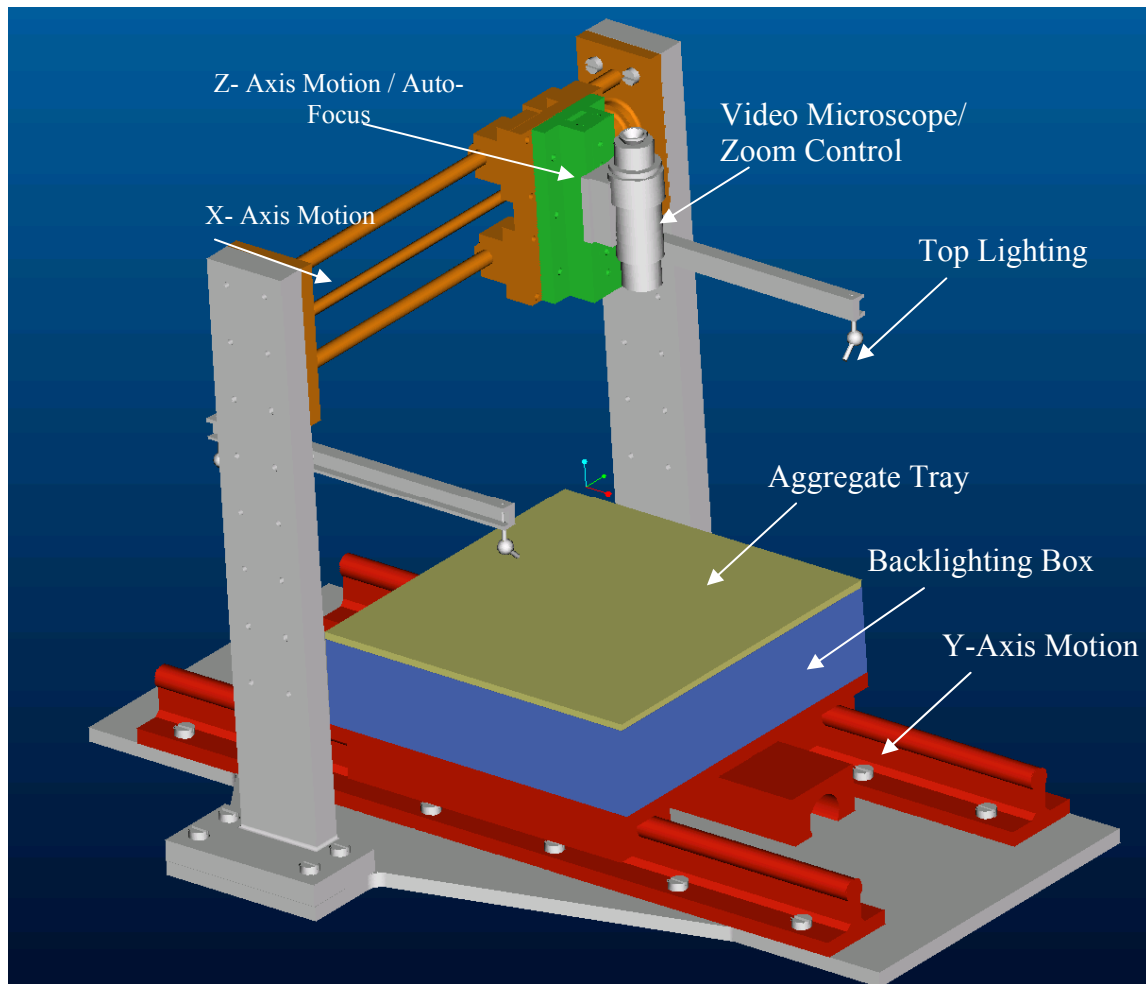


Fig. 3.1. 3-Dimensional Graphical Model of AIMS (after Fletcher 2002)

The fine aggregates are analyzed for form and angularity using black and white images captured using backlighting under the aggregate sample tray. This type of lighting creates a sharp contrast between the particle and the tray, thus giving a distinct outline of the particle. A study by Masad et al. (2001) clearly showed that a high correlation exists between the angularity (measured on black and white images) and texture (measured on gray-scale images) of fine aggregates. Since it was easier to capture black and white images for angularity analysis than the high resolution images required for texture, this helped to simplify the AIMS operation for conducting angularity analysis only.

AIMS is designed to capture images for measuring fine aggregate angularity and form at a resolution such that the pixel size is less than 1% of the average aggregate diameter and the field of view covers 6-10 aggregate particles (Masad et al. 2000). In other words, the resolution of an image is a function of aggregate size. The image acquisition setup was configured to capture a typical image of 640 by 480 pixels at these resolutions in order to analyze various sizes of fine aggregates.

For coarse aggregates, it was found that there is a distinct difference between angularity and texture, and these properties have different effects on performance (Fletcher et al. 2003). In accordance with this finding, AIMS analyzes coarse aggregates for form, and angularity using black and white images and analyzes texture using gray images. The black and white images are captured using a backlighting table, while top lighting is used to capture gray images of particles surfaces. As for fine aggregates, the image acquisition setup captures images at a resolution of 640 by 480 pixels. In the coarse aggregate module, only one particle is captured per image in order to facilitate the quantification of form, which is based on 3-D measurements. As described later in this chapter, the video microscope is used to determine the depth of a particle, while the images of 2-D projections provide the other two dimensions to quantify form. Texture is determined by analyzing the gray images using the wavelet method that was described earlier in Chapter II. The system is computer controlled and achieves motion in x-, y-, and z-directions as well as magnifies images.

IMPROVEMENTS MADE TO HARDWARE COMPONENTS AND FUNCTIONS

In this section the main improvements made to the hardware components are reported. The improvements were directed to enhance the operational characteristics of the system, reduce human involvement, and enhance its automation capabilities. This section also includes a very concise description of the procedures and measurements used in the fine and coarse modules.

Hardware Improvements

AIMS utilizes a closed-loop direct current (DC) servo control unit for precise positioning of the x-, y-, and z-axes and highly repeatable focusing (GTS-1500). The x- and y-axes travel distance is 37.5 cm (15 inches); and z-axis travel distance is 10 cm (4 inches). These travel distances were improved compared to the previous prototype system which achieved x- and y-axis travel distance of 25 cm (10 inches); and a z travel distance of 5 cm (2 inches). This improvement in the x- and y-axes travel distance made it possible to more than double the size over the first prototype system. Increasing the lighting table size made it possible to analyze larger aggregate sample and helped to reduce the time required to analyze more aggregates. The increase in the z-axis travel distance allows the improved AIMS system to analyze larger aggregate sizes. Figs 3.2 and 3.3 show pictures of the AIMS system first prototype and the improved version, respectively. The difference in the size of the lighting table can be easily noticed by comparing the two figures.

AIMS uses Optem Zoom 160 video microscope. The Zoom 160 has a zoom range of X16, which means that an image can be magnified 16 times. This allows capturing wide range of particle sizes without changing parts. The first prototype version of AIMS used a linescan camera (LC-150) black and white video camera with an external controller. The unit utilizes the ICX088DLA Charged-Coupled Device (CCD), which is a 12.5 mm (1/2 inch) interline CCD. The LC-150 offers high sensitivity and more than 600 TV lines horizontal resolution. The external controller is housed in a small 15 X 10 cm (6 x 4 inch) case. The controller offers both manual and automatic

gain control and enhances black level and contrast control. The improved AIMS system is equipped with a Pulnix TM-9701 progressive scan video camera with a 16.9 mm (2/3 inch) CCD imager. It has an adjustable shutter speed from 1/60 sec to 1/16,000 sec. The progressive scan video camera allows capturing images at higher speeds than line scan cameras, and it is less affected by noise. A small vibration in the system caused some noise that affected the image quality when a line scan camera was used. The progressive scan camera is much less affected by these vibrations and provides more consistent quality of images. The same video controller functions are used in the improved AIMS system but without automatic gain control (AGC) and gain functions that no longer apply with Pulnix cameras. This camera is also equipped with its own power supply, rather than using the controller to power the camera, as was the case for the first prototype version.

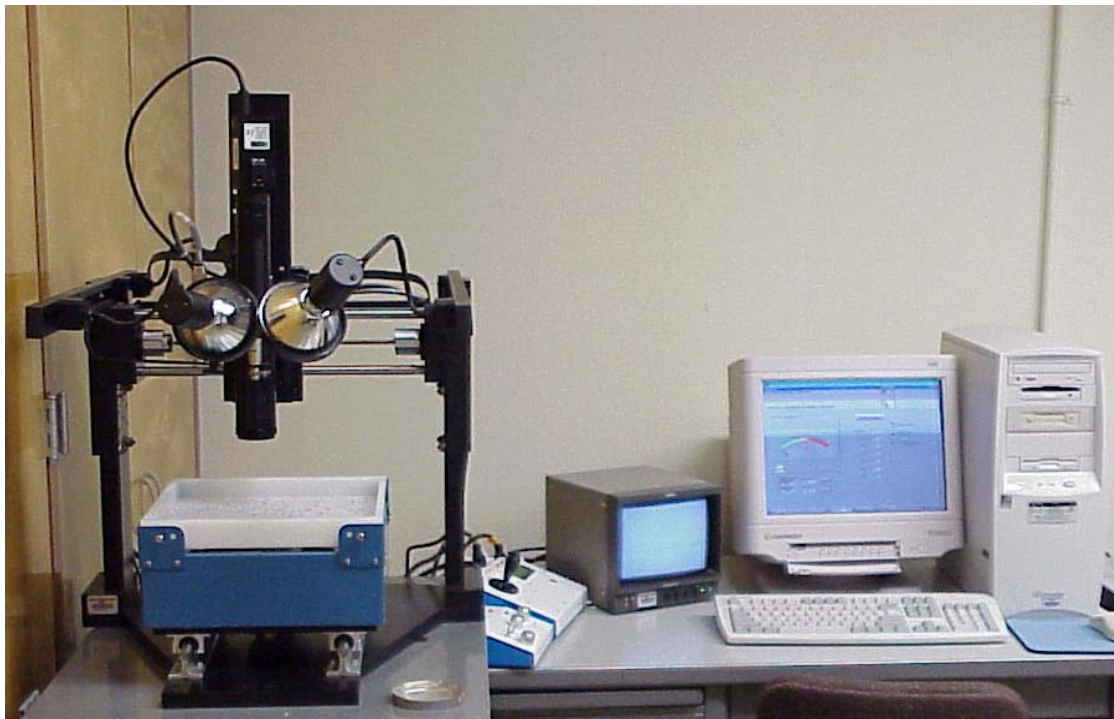


Fig. 3.2. First Prototype of Aggregate Imaging System (AIMS)



Fig. 3.3. Improved Aggregate Imaging System (AIMS)

The existence of two controllers (GTS-1500 and video controller) required several wire connections from and into these controllers (see Fig. 3.2). Consolidating the number of wires is desirable to simplify the AIMS assembly, reduce the number of power outlets, and reduce the noise generated by these wires. In order to overcome these problems, the two controllers are now housed in one bigger case as shown in Fig. 3.3. A fan was installed in the new controller case to reduce the generated heat, which might cause a malfunction when using the system for long periods of time. In addition to the above, some of the video controller functions (enhancement and black level) are fixed inside the box to reduce human involvement and make the system easier to set and use. The new controller still provides manual and automatic control of motion in x, y, z, and magnification axes.

The first prototype version of AIMS had four halogen lights for the top lighting and two fluorescent bulbs for the backlighting (see Fig. 3.2). It was noticed that the uniformity of the light in an image produced by these sources was affected by the

location of the particle on the lighting table. Improvements were made to the lighting schemes where a new large array of light-emitting diodes (LEDs) is used for bottom lighting as shown in Fig. 3.4. These LEDs provide a uniform and variable backlighting source. Top lighting is accomplished in the improved AIMS system with a fiber-optic ring-light mounted on the video microscope. The ring light provides uniform illumination of the region directly in the view of the microscope. It also has a variable intensity control so the desired degree of illumination can be adjusted. Fig. 3.5 shows the top lighting used in the improved AIMS. Fig. 3.6 shows the top lighting sources used in the two versions of AIMS.

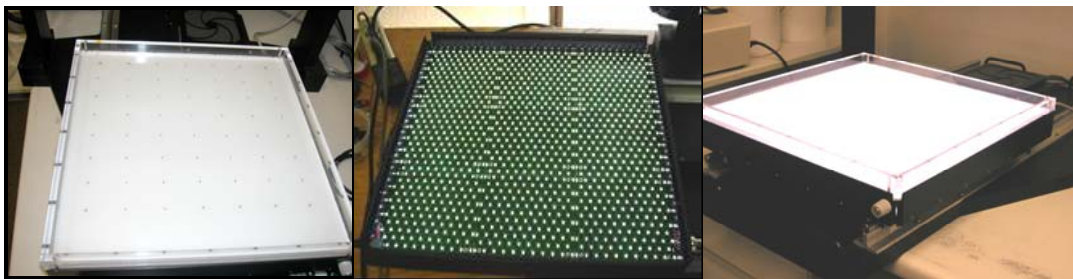
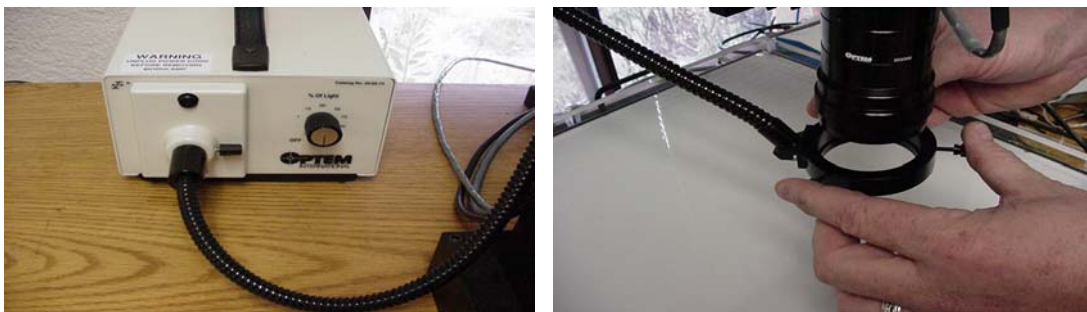


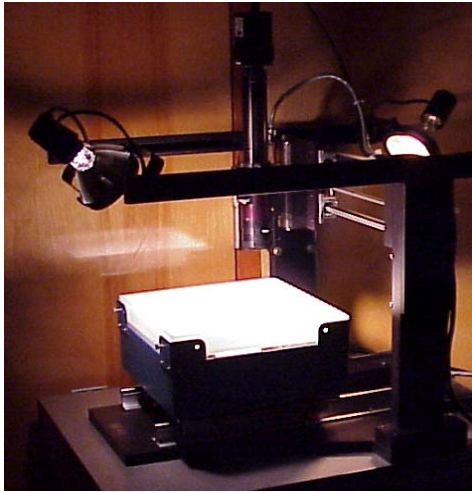
Fig. 3.4. Lighting Table Using LEDs for Backlighting Source



a) Top Lighting Source

b) Fiber-Optic Ring-Light

Fig. 3.5. Top Lighting Used in the Improved AIMS



a) First Prototype



b) Improved System

Fig. 3. 6. Top Lighting in Different Versions of AIMS

In order to ensure longer service life for the LEDs a ventilation system was added. A fan was installed to circulate air inside the lighting table to reduce the heat generated from the LEDs while the system is in use. The LEDs are expected to last longer as generated heat is reduced. The new ventilation system is shown in Fig. 3.7.

An important issue, especially when capturing images of fine particles, is to keep images in focus and acquire sharp images. This can be achieved using the auto focus option of the microscope. Auto focusing is implemented in capturing coarse aggregates; however, it was found to be time consuming in capturing images of fine aggregates. An alternative solution is to determine a head of time the location of the microscope to capture sharp images. In doing so, the lighting table has to be leveled. An inclination in the lighting table causes the images to be out of focus. The allowable inclination is a function of the optical system depth of field (DOF). The DOF is defined as the axial distance that the object can be moved toward or a way from the lens without

objectionable loss of sharpness (Thales-Optem Zoom brochure; (www.thales-optem.com/pdf/Zoom160Brochure.pdf). In order to achieve a leveled table with respect to the video microscope, the table was designed with four tray leveling screws as shown in Fig. 3.8. The leveling process can be easily accomplished by focusing on the surface of the tray on the lighting table in one corner at maximum magnification. Then the optical system is moved to another corner without disturbing the zoom and the leveling screw at the corner is adjusted to maintain the image in focus. This procedure is repeated for the other corners.

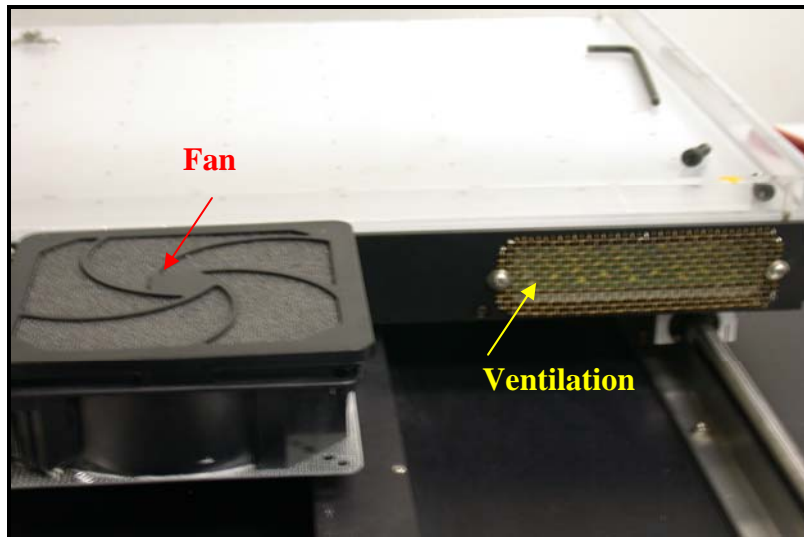


Fig. 3.7. Ventilation System

The first prototype version of AIMS used National Instruments (NI) IMAQ-PCI 1407 image acquisition hardware. PCI 1407 is simple to configure and has the advantage of low cost and high accuracy. It has a single monochrome video input for standard video and features gain calibration, high-impedance mode, and an 8-bit flash analog-to-digital converter (ADC) that converts video signal to digital form.

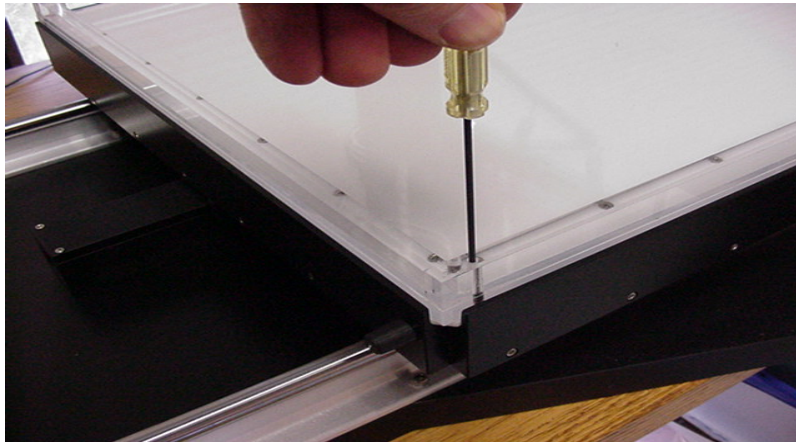


Fig. 3.8. Adjusting Sample Tray Level

The improved version of AIMS uses IMAQ-PCI 1409 image acquisition hardware instead of IMAQ-PCI 1407. PCI 1409 has the advantage of being able to digitize analog images to 10 bits per pixel and 8 bits per pixel. The 10 bits per pixel is useful for obtaining higher-precision images that have 1024 gray-scale instead of 256. PCI 1409 has more board memory to store images, and PCI 1409 supports a wider range of video types including double-speed progressive scan, video cassette recorder (VCR), and analog line scan that the 1407 does not support. PCI 1409 exposes four additional control lines that can be used for additional pattern generation to control cameras. More details are available at the National Instrumentation website (www.ni.com).

Both IMAQ-PCI devices are controlled through the NI-IMAQ driver software. This software serves as the link between the board and the application software. More details can be found at the National Instruments website.

The optical system performance specifications that AIMS uses are presented in Table 3.1 below.

Table 3.1. Optical System Performance Specifications

Objective Lens		0.25X	0.5X
Dovetail Tube		1X	1X
Camera Format (inch)		2/3	2/3
Working Distance (W.D.) (mm)		370	181
Numerical Aperture (N.A.)	Low	0.0022	0.0045
	High	0.038	0.076
Magnification	Low	0.13	0.25
	High	2	4
Depth-of-Field (D.O.F.) (mm)	Low	108.8	27.2
	High	0.38	0.1
Field-of-View (F.O.V.) (mm)	Low	52.8 x 70.4	26.4 x 35.2
	High	3.3 x 4.4	1.6 x 2.2

The terms and factors used in the Table 3.1 above are defined by Thales-Optem Zoom 160 brochure, which can be found at (www.thalesoptem.com/pdf/Zoom160Brochure.pdf), as follows:

- Dovetail Tube: The link between the upper zoom module and the video camera.
- Camera Format: Impacts magnification and field of view. As camera format increases field of view also increases. It is a set factor based on the chip size of the camera.
- Working Distance: The distance in (mm) from the specimen being viewed and the bottom-most mechanical components of the optical system.
- Numerical Aperture (N.A.): A measurement of the light collecting ability of the lens. A higher (N.A.) translates to a brighter image, better resolution, and shorter depth of field.
- Magnification (MAG.): The ratio of image size to actual object size.
- Depth of Field (D.O.F.): The axial depth in (mm) of the space on both sides of the object plane within which the object can be moved without objectionable loss of sharpness.

- Field of View (F.O.V.): The maximum area that can be seen through the optical system. There are two field-of-view extremes. One at high magnification and one at low magnification.

Fine Aggregate Module Operation Procedure

The analysis of fine aggregate starts by randomly placing an aggregate sample (ranging from a few grams for small fine aggregate sizes up to a couple of hundred grams for the larger fine aggregate size) on the aggregate tray with the backlighting turned on. A camera lens of 0.5X object is used to capture the images. The 0.5X objective lens provides a field of view of (26.4 x 35.2 mm) with a 1X Dovetail tube and a 2/3 inch camera format at a working distance of 181 mm. The camera and video microscope assembly moves incrementally in the x-direction at a specified interval capturing images at every increment. Once the x-axis range is complete, the aggregate tray moves in the y-direction for a specified distance, and the x-axis motion is repeated. This process continues until the whole area is scanned. An illustration of the camera path is shown in Fig. 3.9.

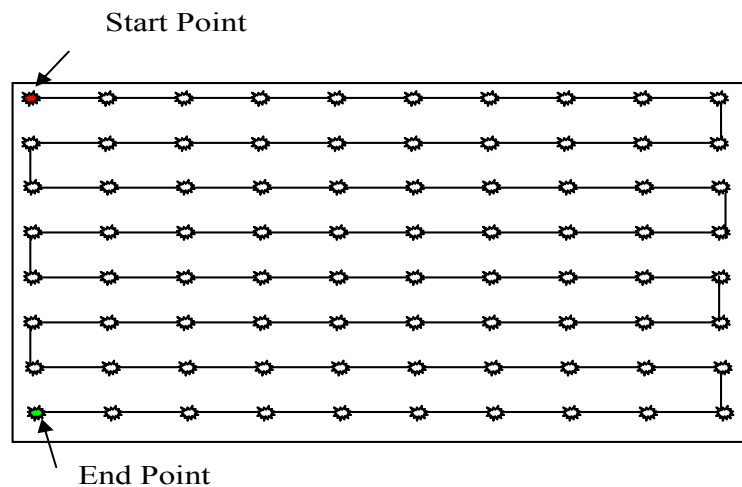


Fig. 3.9. Illustration of the Camera Path

Depending on the size of aggregates to be analyzed, the z-location of the camera is specified in order to meet the resolution criteria in Table 3.2. These criteria are established such that the images for measuring fine aggregate shape and angularity are captured with pixel size less than 1% of the average aggregate diameter and the field of view is large enough to cover 6-10 aggregate particles. This is a very important feature because the results are not influenced by size. The system is designed in such a way that aggregates that are not within the size for which the scan is conducted and, consequently those that do not meet the criteria in Table 3.2, are removed from the image.

Table 3.2. Resolution and Field of View Used in Angularity Analysis for Different Fine Sieve Sizes Using 0.5X lens

(1) Particle Size (mm) Pass - Retain	(2) Average Particle diameter (mm)	(3) Magnification	(4) Field of View (mm)	(5) Resolution = 640/ 70.4 or 480/ 52.8 (Pixel/mm)	Average Particle diameter in Pixels (2) * (5)	Size range Upper – Lower (Pixels) (1) * (5)
4.725 - 2.36	3.56	2.00X	13.2 x 17.6	36.36	129.45	172 - 86
2.36 - 1.18	1.77	4.125X	6.4 x 8.5	75.29	133.26	178 - 88
1.18 - 0.6	0.89	8.25X	3.2 x 4.3	148.84	132.46	176 - 89
0.6 - 0.30	0.45	16X	1.65 x 2.2	290.91	130.9	175 - 73
0.30 - 0.15*	0.225	16X	1.65 x 2.2	290.91	65.45	72 - 44
Gradation		2.75X	9.6 x 12.8	50.0		

* Resolution criterion does not apply for this size range

Coarse Aggregate Module Operation Procedure

The analysis starts by placing the aggregates on the sample tray with marked grid points. The camera lens used in capturing the coarse aggregate has a 0.25X objective. The maximum F.O.V achieved in the coarse aggregate module is 52.8 x 70.4 mm with a 1X Dovetail tube and a 2/3 inch camera format at a working distance of 370 mm. The camera and microscope move as for fine aggregates, but with different distances and

intervals. In this module only one particle is captured in each image. Backlighting is used to capture images for the analysis of angularity while top lighting is used for capturing images for texture analysis. Two scans are conducted for the coarse aggregate.

Backlighting is used in order to capture black and white images. These images are analyzed later to determine angularity, and the major (longest axis) and minor (shortest axis) axes on these 2-D images. The analysis of coarse aggregate angularity starts by placing the aggregate particles in a grid pattern with a distance of 50 mm in the x-direction and 40 mm in the y-direction apart center to center. The z-location of the camera is fixed for all aggregate sizes. Resolutions used in the coarse aggregate angularity analysis are presented in Table 3.3.

Table 3.3. Resolution and Field of View Used in Angularity Analysis of Different Coarse Sieve Sizes Using 0.25X lens

(1) Particle Size (mm) Pass - Retain	(2) Average Particle diameter (mm)	(3) Magnification	(4) Field of View (mm)	(5) Resolution = 640/ 70.4 or 480/ 52.8 (pixel/mm)	Average Particle diameter in Pixels (2) * (5)	Size Range Upper - Lower (Pixels) (1) * (5)
9.5 – 4.75	7.1125	1	52.8 X 70.4	9.12	64.87	86 - 43
12.7 – 9.5	11.1	1	52.8 X 70.4	9.12	101.23	116 - 87
19.0 – 12.7	15.85	1	52.8 X 70.4	9.12	144.55	173 - 117
25.4 – 19.0	22.2	1	52.8 X 70.4	9.12	202.46	231 - 174
> 25.4	25.4	1	52.8 X 70.4	9.12	231.65	> 232

Note: Size range applied for all size ranges was > 43 pixels.

Capturing of images for the analysis of coarse aggregate texture is very similar to the angularity except that top lighting is used instead of backlighting in order to capture gray images. The texture scan starts by focusing the video microscope on a marked point on the lighting table while the backlighting is turned on. The location of the camera on

the z-axis at this point is considered as a reference point (set to zero coordinate). Then an aggregate particle is placed over the calibration point. With the top light on, the video microscope moves up automatically on the z-axis in order to focus on the aggregate surface. The z-axis coordinate value at this new position is recorded. Since the video microscope has a fixed focal length, the difference between the z-axis coordinate at the new position and the reference position (zero) is equal to the aggregate depth. This procedure is repeated for all particles. The particle depth is used along with the dimensions measured on black and white images to analyze particle form, as discussed later.

One of the major improvements made to AIMS that enhanced its automation capabilities is adding the capability to capture images for texture analysis with different resolutions based on aggregate sizes.. A criterion was set that required images to be captured so that the area is proportional to 25% of the aggregate. Table 3.4 presents the resolution criteria for capturing images of coarse aggregates for texture analysis.

Table 3.4. Resolution and Field of View Used in Texture Analysis for Coarse Sieve Sizes Using 0.25X lens

Particle Size (mm) Pass - Retain	(Average Particle diameter (mm)	Particle Min. Expected Area (mm ²)	%25 of particle Min. Expected Area (mm ²)	Suggested Magnif.	Field of View (mm)	Covered Area (mm ²)	Resolution = 640/ 70.4 or 480/ 52.8 (Pixels/mm)
*9.5 – 4.725	7.1125	22.32	5.58	16X	3.3 X 4.4	14.52	145.45
12.7 – 9.5	11.1	90.25	22.56	12X	4.4 X 5.9	25.96	108.00
19.0 – 12.7	15.85	161.29	40.32	9X	5.9 X 7.8	43.68	82.10
25.4 – 19.0	22.2	361	90.25	6X	8.8 X 11.7	102.96	54.70
> 25.4	25.4	645.16	161.29	5X	10.6 X 14.1	149.46	45.40

* Resolution criteria can not be achieved with this size.

DEVELOPMENT OF TEXTURE LIGHTING SCALE

Lighting is an important factor influencing the quality of an image and analysis results. During the preliminary use of the AIMS system it was noted that texture results were influenced significantly by the intensity of the top lighting. This section describes the experiment that was conducted to develop a standard lighting scale for the improved AIMS system that uses a new source of top lighting.

In the past, similar lighting scales were developed by fixing the type, location and angle of lighting with respect to an aggregate sample. This approach was found to be impractical as the parameters (location and angle) have to be changed as the type of the lighting source changes. Therefore, there was a need to develop a lighting scale based on a parameter measured on the captured images rather than the specifics of the lighting hardware components.

In order to develop a standard lighting scale for the improved AIMS system, gray images of coarse aggregate particle surfaces of different types (slag, traprock, limestone, dolomite, gravel, and granite) and colors (dark gray, light gray, white, pink, yellow, and others) were captured using variable top light intensities. Then, these particles were cut using a saw to create smoother surfaces and were imaged again. The AIMS control software was used to record the mean of the gray scale histogram for each particle during scanning. The histogram gives the distribution of the different gray shades in an image from zero for black to 255 for white. The mean of the histogram reflects the average light reflection by a particle.

The histogram mean values resulting from the scanned particles before and after cutting are shown in Fig. 3.10. On average, the cut sections had an intensity mean 30 points higher than the original sections. However, this difference is not significant, especially when the variation of the mean within particles from the same source prior to cutting is taken into consideration. In Fig. 3.10 the horizontal bars shown for three of the aggregates indicate the range of variability within the same aggregate source.

The measured texture was plotted as a function of the histogram mean intensity as shown in Fig. 3.11. It can be seen that light intensity can have a significant effect on

the measured texture. Moreover, particles with high texture in the original form maintained high texture after being cut. This was expected since cutting would produce surface texture level dependent on the particle mineralogy.

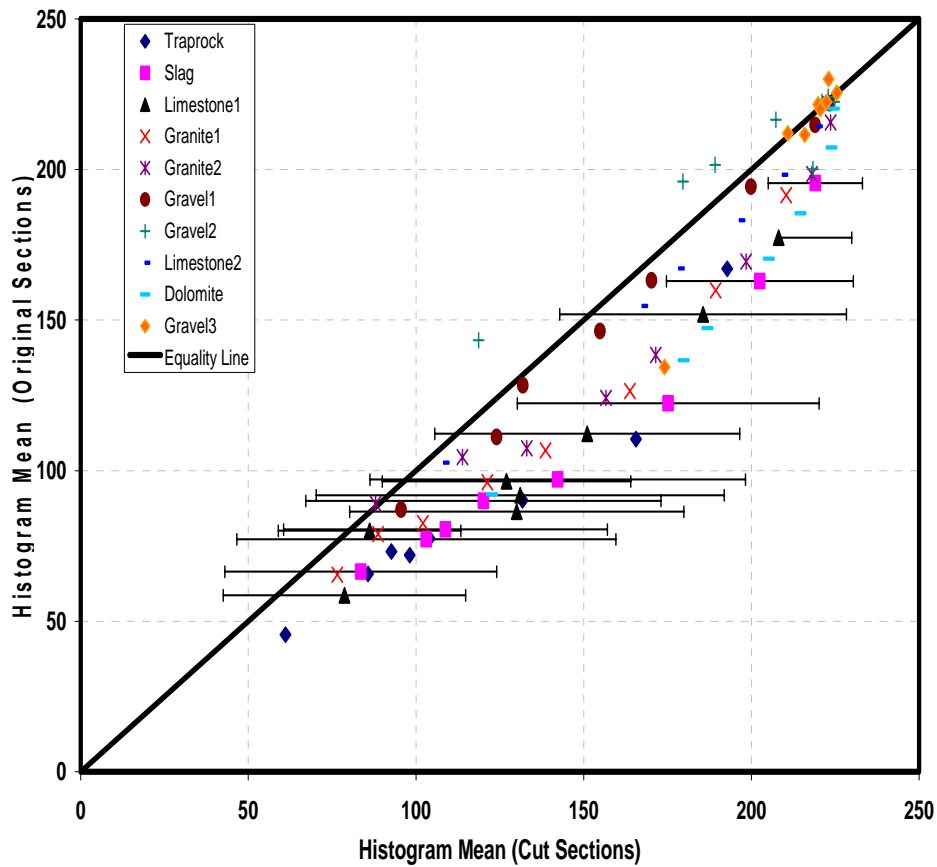


Fig. 3.10. Mean of Gray Scale Intensity Histogram for Different Aggregates with Cut and Original Sections

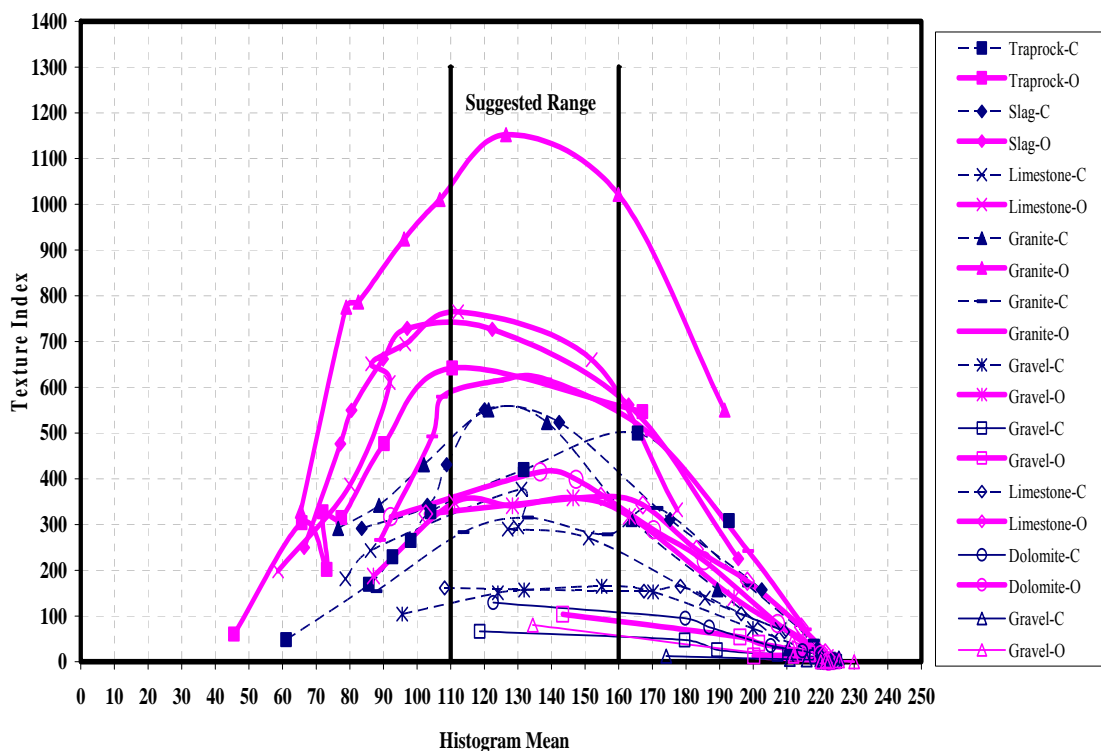


Fig. 3.11. Relation between Surface Texture and Histogram Intensity Mean for Different Aggregates (O: Original, C: Cut)

There is a range of intensity within which the measured texture was fairly uniform (see Fig. 3.11). This facilitates the development of a lighting scale with a reasonable range that accommodates the natural variation within an aggregate sample and the difference between the cut and original sections. This ensures that particle color has a minimal effect on the results. According to Fig. 3.11, an image should be captured such that the histogram intensity mean is between 110 and 160 in order to minimize the influence of color variation on the results.

CONTROL AND ANALYSIS SOFTWARE

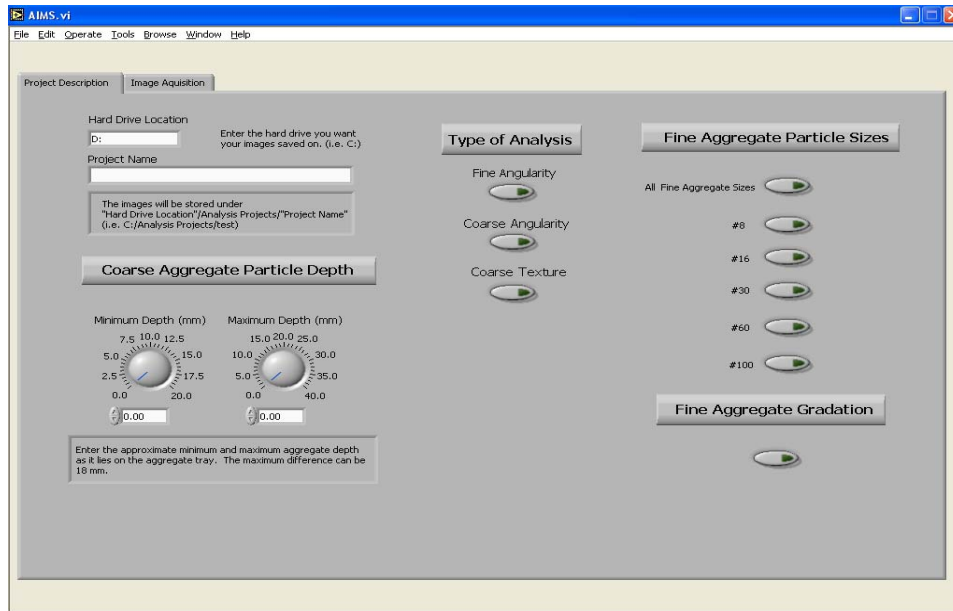
This section includes a brief description of both the control and analysis software.

Control Software

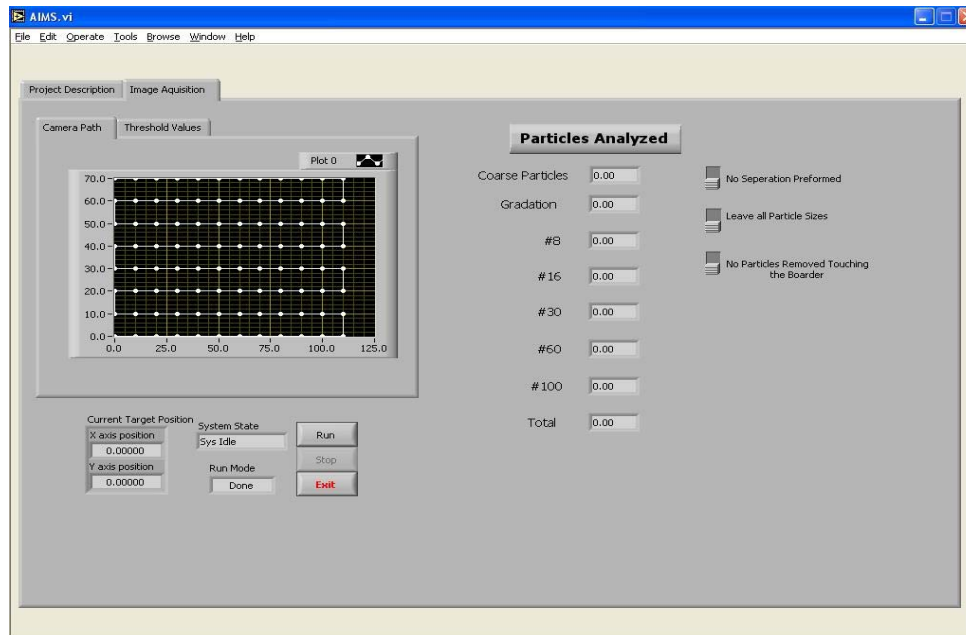
National Instruments LabVIEW™ (version 6.1) and IMAQ Vision (version 2.5) software were used to program motion control and the image acquisition. Both software packages use the LabVIEW Graphical (G) programming language. IMAQ Vision includes a comprehensive set of functions for image processing and analysis. “LabVIEW is a software that is designed for data acquisition and instrument control. It consists of libraries of functions and development tools. A program written in G is called a visual instrument (VI). The VI consists of two main parts; the user interface (main panel) where the program is controlled, and code diagram or block diagram where the G programming instructions are included to carry out the required tasks. Different than any other programming languages where text is used, the LabVIEW (G) programming is done in a pictorial format” (Fletcher 2002). More information on LabVIEW can be found on the Internet or by visiting the National Instrumentation website (www.ni.com).

Figs. 3.12 and 3.13 show the project description user interface and the image acquisition user interface for the original and improved versions of the control program, respectively. As can be seen in Fig. 3.13, a real-time image window is displayed.

In running both coarse and fine modules, the first step is always calibration of the system. The second step is to distribute the entire aggregate sample on the sample tray. On the user interface, “Project Name” and “Hard Drive Location” are entered and the type of scan or analysis to be performed is selected. A list of options for the aggregate sizes and scan types are available to select from. The selection process is very easy to follow as the user is guided by steps and help messages.

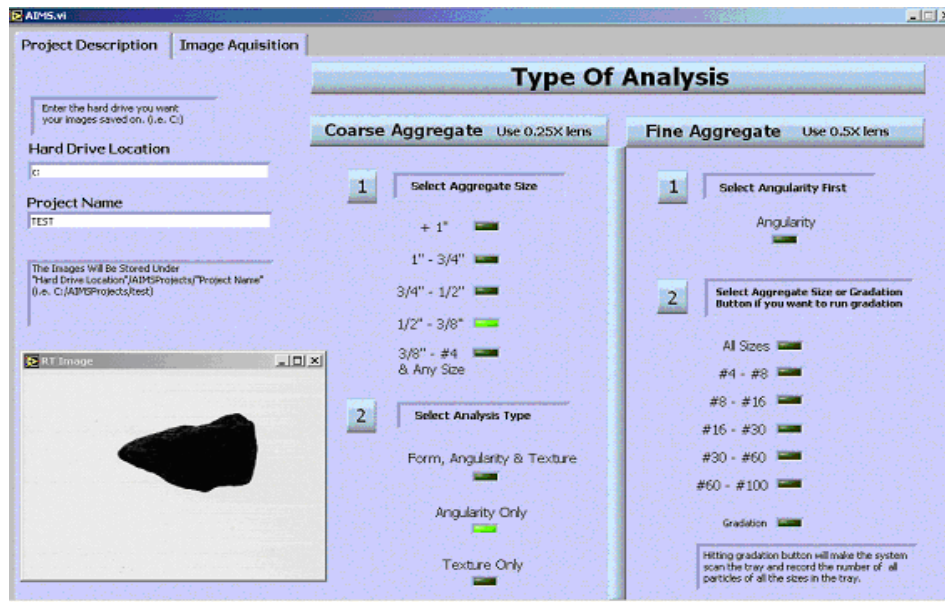


(a)

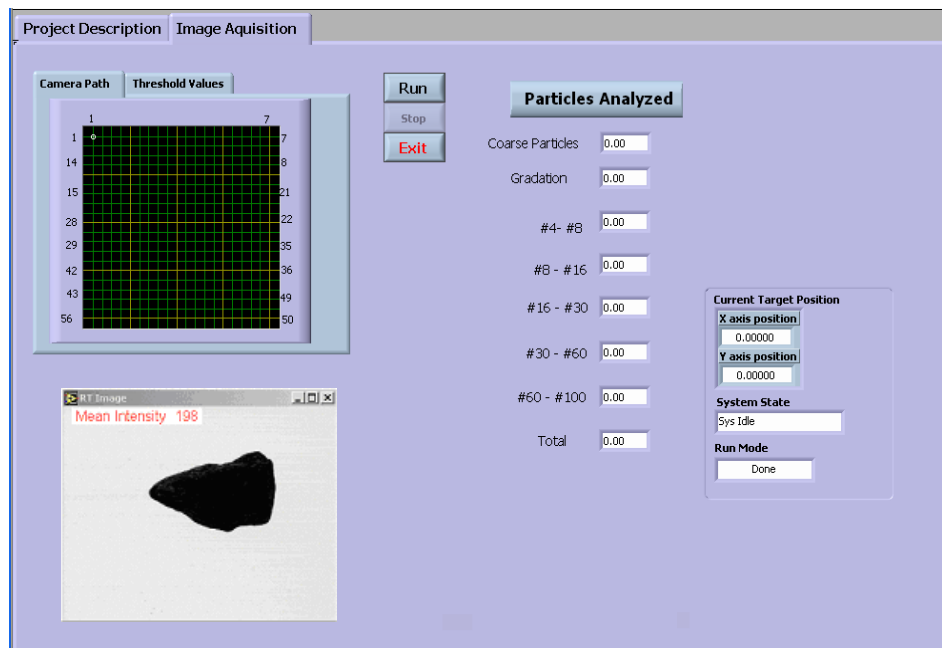


(b)

Fig. 3.12. Front Panel Interface of the Control Program Used by AIMS First Prototype Version. (a) Project Description Interface and (b) Image Acquisition Interface



(a)



(b)

Fig. 3.13. Front Panel Interface of the Control Program Used by AIMS Improved Version. (a) Project Description Interface and (b) Image Acquisition Interface

Once the selections are made and the user clicks the run button the program displays the original and processed images of particles (see Fig. 3.14). After the scan finishes, the program creates a sub directory with the user-specified project on the user-specified hard drive.

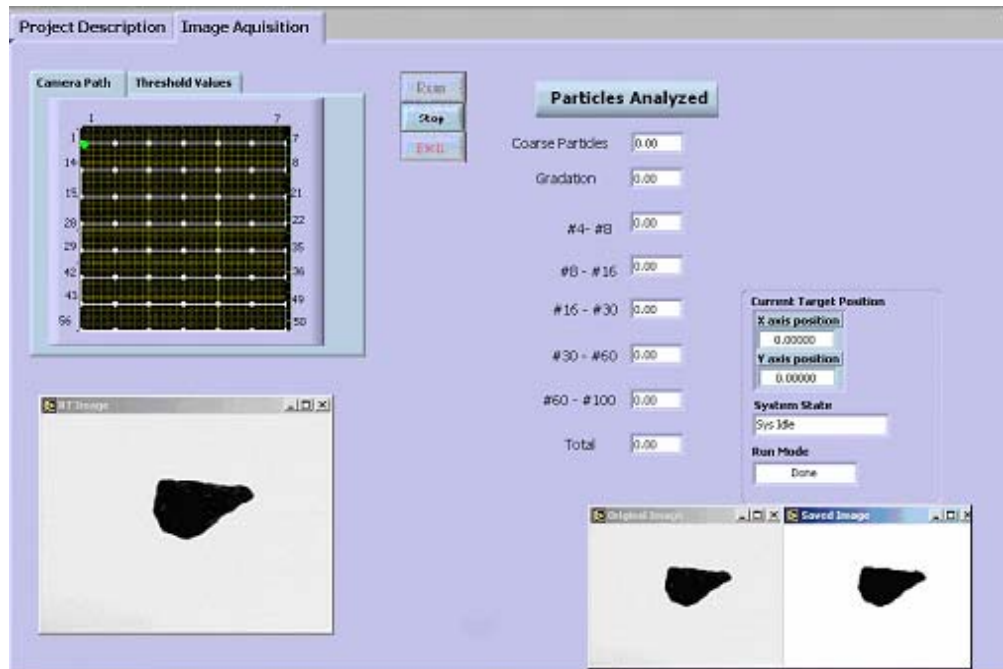


Fig. 3.14. Control Program Interface Showing Original and Processed Images while Running Angularity Analysis Scan

As discussed in the previous section, images for texture analysis are captured such that average gray intensity is within a specified range. This software is capable of showing the value of the mean gray-scale histogram on the real time image. It also plots a bar chart of the mean gray histogram for all images of a particle scanned during the texture analysis scan (see Fig. 3.15). The program shows graph of the camera path and a text window. These new features can show the location and number of the particles on

the lighting table whose their mean gray-scale histogram falls above or below scale limits. Particles with mean gray-scale histograms that fall within scale limits appear with green dots on the chart, as shown in Fig. 3.15. This improvement made it easier for the user to identify the particles that need to be rescanned if the lighting was inappropriate the first time.

The program was developed to be self-guided and to minimize user interruption during measurements. Therefore, the program is features instructional message windows that promptly display to guide the user through successful analysis.

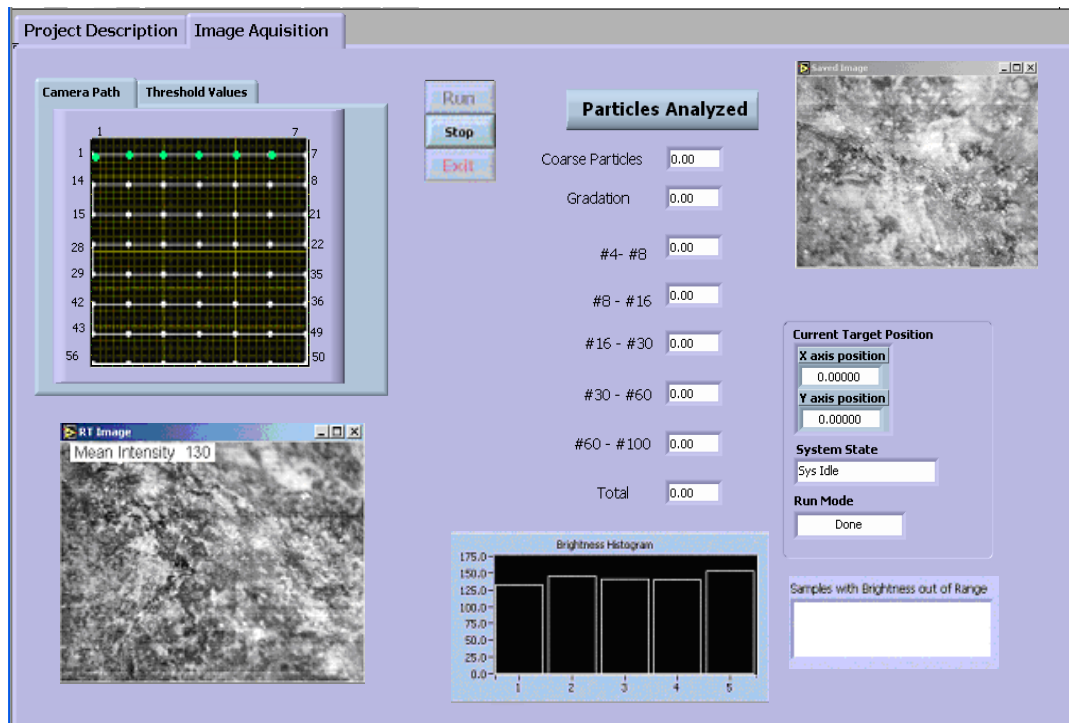


Fig. 3.15. New Features in Control Program while Running Texture Analysis Scan

Analysis Software

A detailed description of the software is provided by Masad (2003). The information is provided here for the completeness of the description of AIMS. The images captured during scanning are analyzed for form, angularity, and texture using the image analysis software. The image analysis software was developed as a standalone application that could be run on any 32 bit Windows platform (Masad 2003). The program was written using the multi-function capabilities (MFC) functionality of C++. The interface enables users to select among two aggregate analysis options (coarse and fine). Then depending on the user choice, various analysis options are offered to select from. For coarse aggregates, analysis of aggregates' texture, angularity (two methods); and form (two methods) can be conducted. For fine aggregates, the analysis options are angularity (two methods), and form.

The analysis methods in the AIMS analysis software are based on a fundamental concept, and their results are easy to interpret. These analysis methods were discussed in Chapter II. The analysis software sorts three dimensions of particles and calculates sphericity. Sphericity is a 3-D measure of coarse aggregate form and is calculated using Eq. 2.1. Form Index is a 2-D measure of form that can be quantified using Eq. 2.4. The analysis software enables users to calculate the form index for both fine and coarse aggregates. Two methods are used to quantify the angularity of coarse and fine aggregates. These methods are gradient angularity and radius angularity, given by Eqs. 2.19 and 2.21, respectively. Texture of coarse aggregate is quantified by the wavelet method as given in Eq. 2.26.

The analysis software stores the results as text files in the same directory as the images. The analysis software also shows results in terms of a cumulative distribution curve along with some statistics such as standard deviation, mean, and values of first, second, and third quartiles, displaying them on a separate interface as shown in Fig. 3.16.

The results interface provides the user with the option of storing the analysis results in an Excel file. When the sample name is entered and the 'OK' button is clicked,

an Excel file opens. In the Excel file the results are processed and presented in different sheets. The original result values are sorted (ranked) and their cumulative percentiles are tabulated. The properties cumulative distribution is plotted on a separate graph, as shown in Fig. 3.17. Statistics and percentage of particles in each aggregate shape property class (discussed in Chapter V) are tabulated in a separate sheet (summary sheet). An example of the data presented in the summary sheet is presented in Fig. 3.18.

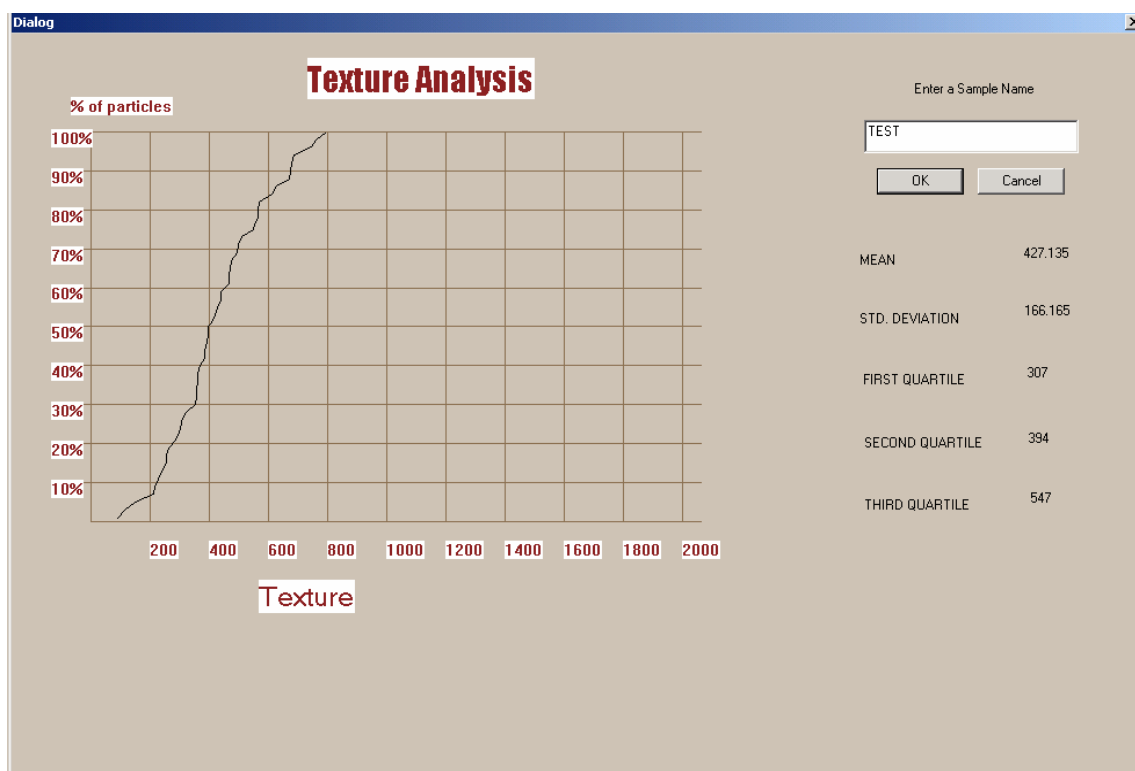


Fig. 3.16. Property Distribution and Statistics Shown on the Software Results Interface

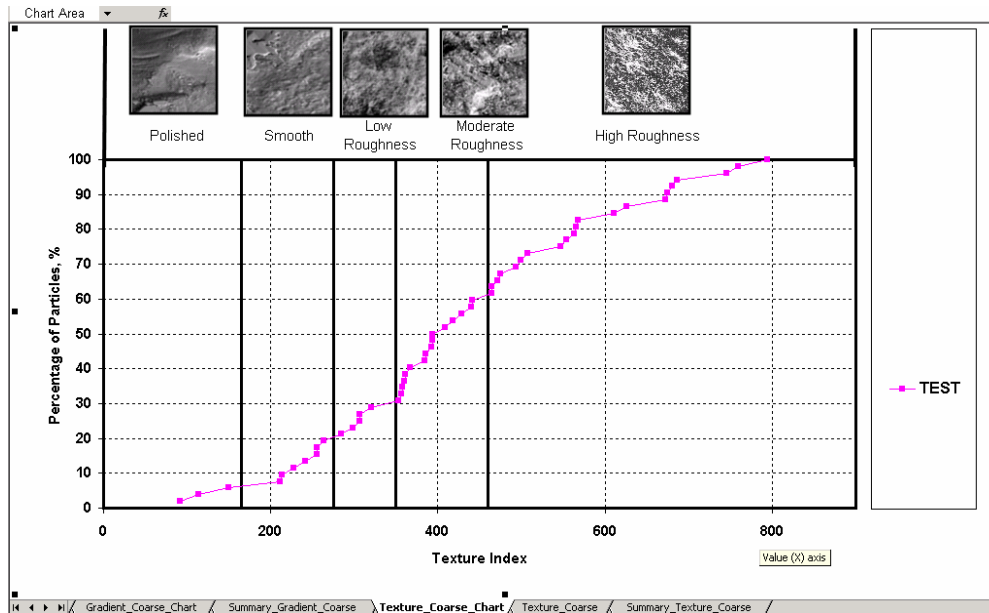


Fig. 3.17. Example of the Cumulative Distribution of Texture

Summary Sheet	
Sample Name	TEST
Mean	427.135
Standard Deviation	166.165
First quartile	307
Second Quartile	394
Third Quartile	547
% Polished Particles	5.76923
% Smooth Particles	13.4615
% Low-Rough Particles	9.61539
% Med-Rough Particles	30.7692
% High-Rough Particles	40.3846
% Total	100

Fig. 3.18. Example of the Data Presented in Summary Sheet

The interface of the AIMS analysis software has good usability features so the user does not need to specify the number of energy levels for texture analysis or the number of erosions for angularity analysis. In this software these values are hard-coded with the most suitable values for each type of analysis, as shown in Fig. 3.19.

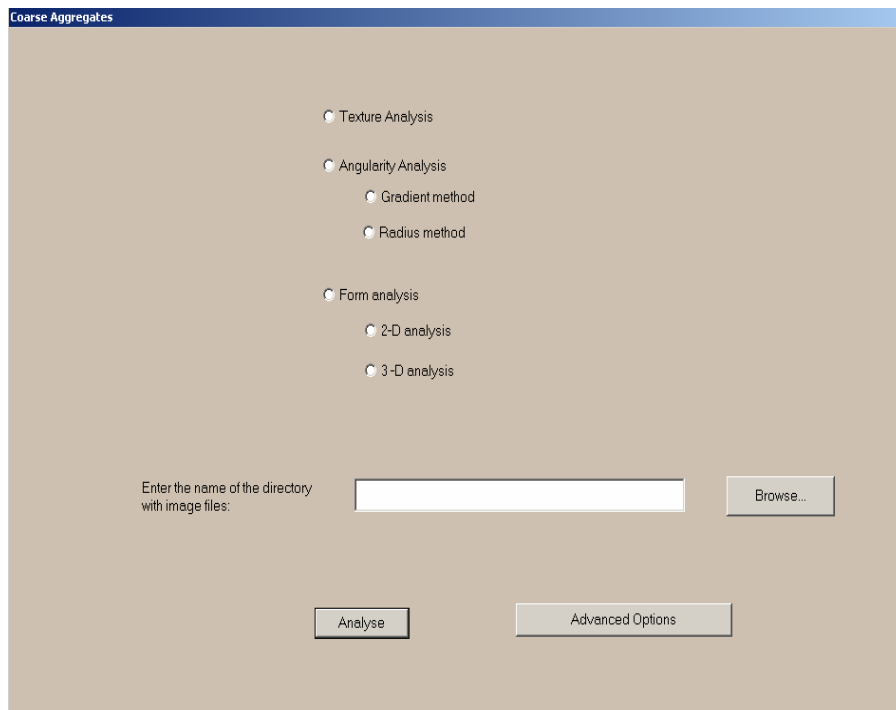


Fig. 3.19. Interface of AIMS Analysis Software

AIMS uses a preliminary set of threshold values to classify the shape properties of coarse and fine aggregates. As discussed in Chapter VI, these values are based on cluster analysis that divides aggregates into groups based on their shape properties. The default threshold values for the limits of different properties are hard-coded in the program. However, the user is given an option to set new ranges for the classification of particles, which makes the software flexible enough to accommodate new threshold

values or classification limits based on future measurements. Fig. 3.20 shows the interface that can be used to change the classification limits of aggregate shape properties. These classification limits are programmed to show on the Excel Charts. This makes it easier to examine what percentage of the aggregate distribution fall within each shape classification.

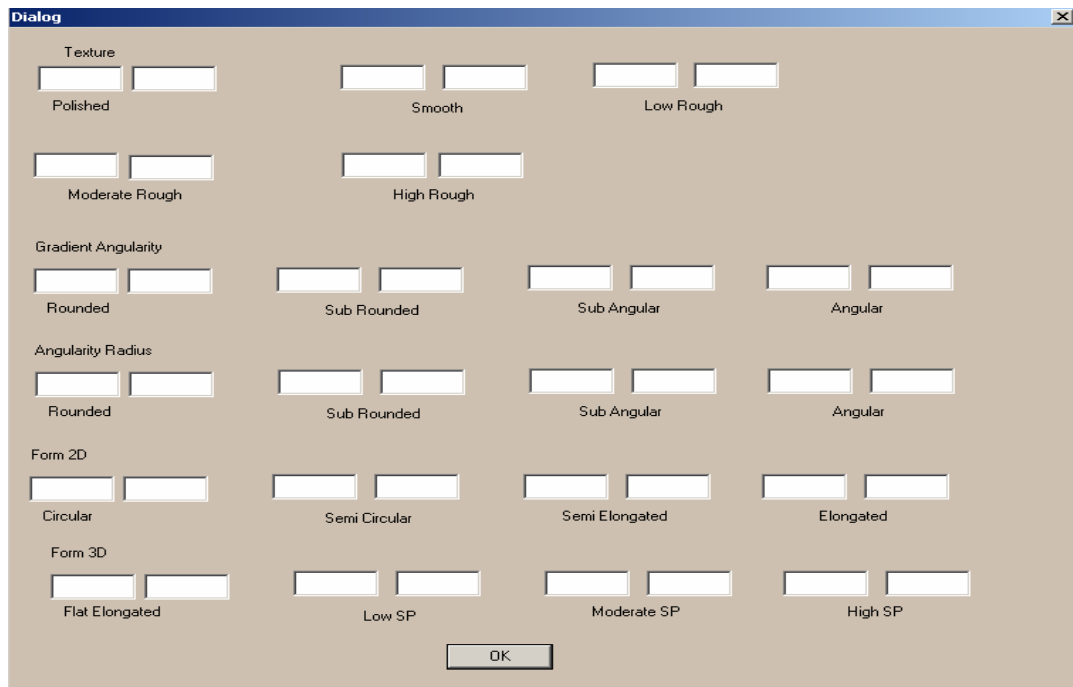


Fig. 3.20. New Feature to Change the Class Limits of Aggregate Shape Properties

SUMMARY

This chapter describes the work that has been done towards achieving the first objective of this study (developing an improved version of AIMS). Several improvements were made in the design of the hardware and software components of AIMS to enhance the operational characteristics of the system, reduce human involvement and errors, and enhance the automation of the test procedure.

One of the important improvements made to AIMS was the development of a standard lighting scale. Lighting is an important factor influencing the quality of an image and analysis results of texture extracted from it. Therefore, a lighting scale based on a parameter measured on the captured images rather than the specifics of the lighting hardware components was developed. The mean of the gray-scale histogram was used as scale parameter, and a range of values was specified so that images can be captured with minimum influence of color variation on the results.

Visualization capabilities were added to the control software to allow the user to specify both the aggregate size and shape characteristics being analyzed and to determine whether an image is captured within the correct lighting scale or not. In AIMS, images for the analysis of angularity and texture are captured based on specified criteria for resolution and magnification in order to significantly reduce the influence of particle size on the shape characterization results.

CHAPTER IV

COMPARATIVE ANALYSIS OF TEST METHODS FOR MEASURING AGGREGATE SHAPE

INTRODUCTION

This chapter documents the experimental evaluation of the characteristics of the available methods used to measure aggregate shape characteristics. The evaluation was conducted in order to compare AIMS to the existing test methods. The first task was to conduct a preliminary evaluation, based on the information available in the literature, of all test methods documented in Chapter II in order to select candidate tests for more in-depth evaluation. The evaluation covered the repeatability, reproducibility, accuracy, cost, and operational characteristics. The first three characteristics were evaluated through statistical analysis of the shape characteristics of a wide range of aggregates from different sources with various shape properties. The accuracy analysis was conducted for the image analysis methods and parameters employed in some of the systems, and for the test methods themselves. The information that pertains to cost and operational characteristics was collected using a survey of vendors, researchers, and operators who have dealt with these systems.

EVALUATION OF MERITS AND DEFICIENCIES OF TEST METHODS

Information gathered from the literature and documented in Chapter II is used here to conduct a comparative analysis of the available test methods. This task served the purpose of identifying test methods that will be subjected to intensive experimental evaluation in this study. A summary of the advantages and disadvantages of the test methods based on information synthesized from the literature is documented in Table 4.1. The table also gives the location where the selected test methods are available for further evaluation.

Table 4.1. Merits and Deficiencies of the Testing Methods Used to Measure Aggregate Shape Properties

Test Method	Estimated Cost (\$)	Aggregate Characteristics	Advantages	Disadvantages
AASHTO T304 (ASTM C1252) Uncompacted Void Content of Fine Aggregate	250	<ul style="list-style-type: none"> • A combination of angularity, texture, and form. 	<ul style="list-style-type: none"> • Simple. • Inexpensive. • Saeed et al. (2001) selected it to measure the properties of aggregates in unbound layers. • Meninger (1998) selected it to measure the properties of aggregates in PCC pavements. • Janoo and Korhonen (1999) recommended it over time index, rugosity, and particle index. • Used in the current Superpave system. 	<ul style="list-style-type: none"> • Lee et al. (1999a) and Chowdhury and Button (2001) reported that the test does not consistently identify angular and cubical aggregates. Also, some fine aggregate with good field performance history did not meet the Superpave criteria. • The results are influenced by form, angularity, texture, and bulk specific gravity.
AASHTO TP56 Uncompacted Void Content of Coarse Aggregate	500	<ul style="list-style-type: none"> • A combination of angularity, texture, and form. 	<ul style="list-style-type: none"> • Simple. • Inexpensive. • Kandhal and Parker (1998) selected it to measure the properties of aggregates in asphalt pavements. • Meninger (1998) selected it to measure the properties of aggregates in PCC pavements. 	<ul style="list-style-type: none"> • The results are influenced by form, angularity, texture, and bulk specific gravity.
ASTM D3398 Standard Test Method for Index of Aggregate Particle Shape and Texture.	400	<ul style="list-style-type: none"> • A combination of angularity, texture, and form. 	<ul style="list-style-type: none"> • Simple. • Inexpensive. 	<ul style="list-style-type: none"> • Saeed et al. (2001) classified this test as having fair performance, predictability, precision, and accuracy. • Meninger (1998) reported that the results have high correlation with the FAA test, which is more practical and easier to use. • Fowler et al. (1996) reported that the method does not provide good correlation with concrete performance. • The results are influenced by form, angularity, texture, and bulk properties.

Table 4.1. Continued

Test Method	Estimated Cost (\$)	Aggregate Characteristics	Advantages	Disadvantages
Compacted Aggregate Resistance CAR Test	500	<ul style="list-style-type: none"> • A combination of angularity, texture, and form. 	<ul style="list-style-type: none"> • Simple. • Inexpensive. • Chowdhury and Button (2001) reported that the CAR test method is more sensitive than FAA and direct shear to changes in shape properties. 	<ul style="list-style-type: none"> • The results are influenced by shape, angularity, texture, and bulk properties.
Florida Bearing Value of Fine Aggregate	1,000	<ul style="list-style-type: none"> • A combination of angularity, texture, and form. 	<ul style="list-style-type: none"> • Simple. 	<ul style="list-style-type: none"> • The results are influenced by form, angularity, texture, and bulk properties. • Less practical and involves more steps than the FAA test. • Operates based on the same concept as the CAR test but requires more equipment and time. • Lee et al. (1999b) stated that FAA test has better correlation with HMA performance than this test.
Rugosity	500	<ul style="list-style-type: none"> • A combination of angularity, texture, and form. 	<ul style="list-style-type: none"> • Simple. • Inexpensive. 	<ul style="list-style-type: none"> • The results are influenced by form, angularity, texture, and bulk properties. • It is based on the same concept as the FAA test and the uncompacted voids in coarse aggregates test. However, it requires more time and is less practical than these tests.
Time Index	500	<ul style="list-style-type: none"> • A combination of angularity, texture, and form. 	<ul style="list-style-type: none"> • Simple • Inexpensive 	<ul style="list-style-type: none"> • The results are influenced by form, angularity, texture, and bulk properties. • It is based on the same concept as the FAA test and the uncompacted voids in coarse aggregates test. However, it requires more time and is less practical than these tests.

Table 4.1. Continued

Test Method	Estimated Cost (\$)	Aggregate Characteristics	Advantages	Disadvantages
AASHTO T 236 (ASTM D3080) Direct Shear Test	10,000	<ul style="list-style-type: none"> • A combination of angularity, texture, and form. 	<ul style="list-style-type: none"> • Simple. • Chowdhury and Button (2001) reported that the test method has good correlation with HMA performance. 	<ul style="list-style-type: none"> • Expensive. • The results are influenced by form, angularity, texture, mineralogy, and particle size distribution. • Nonuniform stress distribution causes discrepancies in the measured internal friction.
ASTM D5821 Determining the Percentages of Fractured Particles in Coarse Aggregate	0	<ul style="list-style-type: none"> • Angularity. 	<ul style="list-style-type: none"> • Simple. • Inexpensive. • Used in the current Superpave system. 	<ul style="list-style-type: none"> • Labor intensive and time consuming. • Depends on the operator’s judgment. • Meininger (1998) classified this method as having low prediction, precision, and medium practicality.
Flat and Elongated Coarse Aggregates ASTM D4791	250	<ul style="list-style-type: none"> • Form. 	<ul style="list-style-type: none"> • Used in current Superpave system. • Able to identify large portions of flat and elongated particles. • Gives accurate measurements of particle dimension ratio. • Found to be related to performance of unbound pavement layers (Saeed et al. 2001). 	<ul style="list-style-type: none"> • Tedious, labor extensive, time consuming to be used on a daily basis (Yeggoni et al. 1996, Rao and Tutumluer 2000). • Limited to test only one particle at a time. • Unable to identify spherical, rounded, or smooth particles. • Doesn’t directly predict performance (Meininger 1998, Fowler et al. 1996).
Multiple Ratio Shape Analysis	1,500	<ul style="list-style-type: none"> • Form. 	<ul style="list-style-type: none"> • Simple. • Inexpensive. • Provides the distribution of dimensional ratio in aggregate sample. 	<ul style="list-style-type: none"> • Does not address angularity or texture.
VDG-40 Videograder	45,000	<ul style="list-style-type: none"> • Form 	<ul style="list-style-type: none"> • Measures the form of large aggregate quantity. • Wiengart and Prowel (1999) and Tutumluer et al. (2000) reported good correlation with manual measurements of flat-elongated particles. 	<ul style="list-style-type: none"> • Expensive. • Does not address angularity or texture. • Assumes idealized particle shape (ellipsoid). • Uses one camera to capture images of all sizes.

Table 4.1. Continued

Test Method	Estimated Cost (\$)	Aggregate Characteristics	Advantages	Disadvantages
Computer Particle Analyzer CPA	25,000	<ul style="list-style-type: none"> • Form. 	<ul style="list-style-type: none"> • Measures the form of large aggregate quantity. 	<ul style="list-style-type: none"> • Expensive. • Does not address angularity or texture. • Assumes idealized particle shape (ellipsoid). • Uses one camera to capture images of all sizes.
Micromeritics OptiSizer PSDA	50,000	<ul style="list-style-type: none"> • Form. 	<ul style="list-style-type: none"> • Measures the form of large aggregate quantity. 	<ul style="list-style-type: none"> • Expensive. • Does not address angularity or texture. • Assumes idealized particle shape (ellipsoid). • Uses one camera to capture images of all sizes. • The system is no longer marketed in the US.
Video Imaging System (VIS)	60,000	<ul style="list-style-type: none"> • Form. 	<ul style="list-style-type: none"> • Measures the form of large aggregate quantity. 	<ul style="list-style-type: none"> • Expensive. • Does not address angularity or texture. • Assumes idealized particle shape (ellipsoid). • Uses one camera to capture images of all sizes.
Buffalo Wire Works PSSDA	35,000	<ul style="list-style-type: none"> • Form. • Angularity. 	<ul style="list-style-type: none"> • Measures the shape of large aggregate quantity. 	<ul style="list-style-type: none"> • Expensive. • Does not address texture. • Assumes idealized particle shape (ellipsoid). • Uses one camera to capture images of all sizes.

Table 4.1. Continued

Test Method	Estimated Cost (\$)	Aggregate Characteristics	Advantages	Disadvantages
Camsizer	45,000	<ul style="list-style-type: none"> • Form. • Angularity. 	<ul style="list-style-type: none"> • Measures the shape of large aggregate quantity. • Uses two cameras to capture images at different resolutions based on aggregate size. 	<ul style="list-style-type: none"> • Expensive. • Assumes idealized particle shape (ellipsoid).
WipShape	35,000	<ul style="list-style-type: none"> • Form. • Angularity. 	<ul style="list-style-type: none"> • Measures the shape of large aggregate quantity. • Measure the three dimensions of aggregates. 	<ul style="list-style-type: none"> • Expensive. • Does not address texture. • Uses two cameras to capture images of all sizes.
University of Illinois Aggregate Image Analyzer (UIAIA)	35,000	<ul style="list-style-type: none"> • Form. • Angularity. • Texture. 	<ul style="list-style-type: none"> • Measures the shape of large aggregate quantity. • Measure the three dimensions of aggregates. 	<ul style="list-style-type: none"> • Expensive. • Uses three cameras to capture images of all sizes.
Aggregate Imaging System (AIMS)	35,000	<ul style="list-style-type: none"> • Shape. • Angularity. • Texture. 	<ul style="list-style-type: none"> • Measure the three dimensions of aggregates. • Uses a mechanism for capturing images at different resolutions based on particle size. • Gives detailed analysis of texture. 	<ul style="list-style-type: none"> • Expensive. • Measures the shape of relatively small amount of aggregates.
Laser-Based Aggregate Analysis System	25,000	<ul style="list-style-type: none"> • Shape. • Angularity. • Texture. 	<ul style="list-style-type: none"> • Measure the three dimensions of aggregates. 	<ul style="list-style-type: none"> • Expensive • Measures the shape of relatively small amount of aggregates.

Note: Prices Listed are Estimates and not absolute.

The experimental evaluation was conducted for AIMS as well as those methods selected based on the preliminary evaluation summarized in Table 4.1. The test methods were selected based on three steps as shown in Fig. 4.1. In the first step, methods were categorized into direct and indirect, as listed in Table 2.1. Then, methods that share the same analysis concept were grouped together. This step ensured that the selected candidate methods represent different analysis concepts. The third step was to select test/tests from each group based on practicality, labor requirements, cost, repeatability, versatility, and field applicability. The preliminary evaluation was necessary in order to ensure that resources were not spent evaluating multiple tests that share the same analysis methods and operational characteristics. Table 4.2 summarizes the outline of the approach for the preliminary evaluation. It should be noted that some of the test methods currently used in practice were included in the intensive evaluation in order to compare them with the results of the candidate methods. Such comparison is necessary to see if any of the available methods are similar or better than methods currently used in the practice.

All indirect methods in the first group in Table 4.2 rely on packing of aggregates that flow through a given-sized orifice. Uncompacted void content of fine aggregates (also known as Fine Aggregate Angularity [FAA] test) and uncompacted void content of coarse aggregates were selected since they are more popular and widely used and are cheaper and easier to use than other tests in the same group. Janoo and Krohonen (1999) concluded that the FAA test was the easiest to implement and use when compared to time index, rugosity, and particle index. Time index was not selected since it is a time consuming test (Janoo and Korhonen 1999). Saeed et al. (2001) evaluated this test and classified it as having fair performance, predictability, precision, and accuracy.

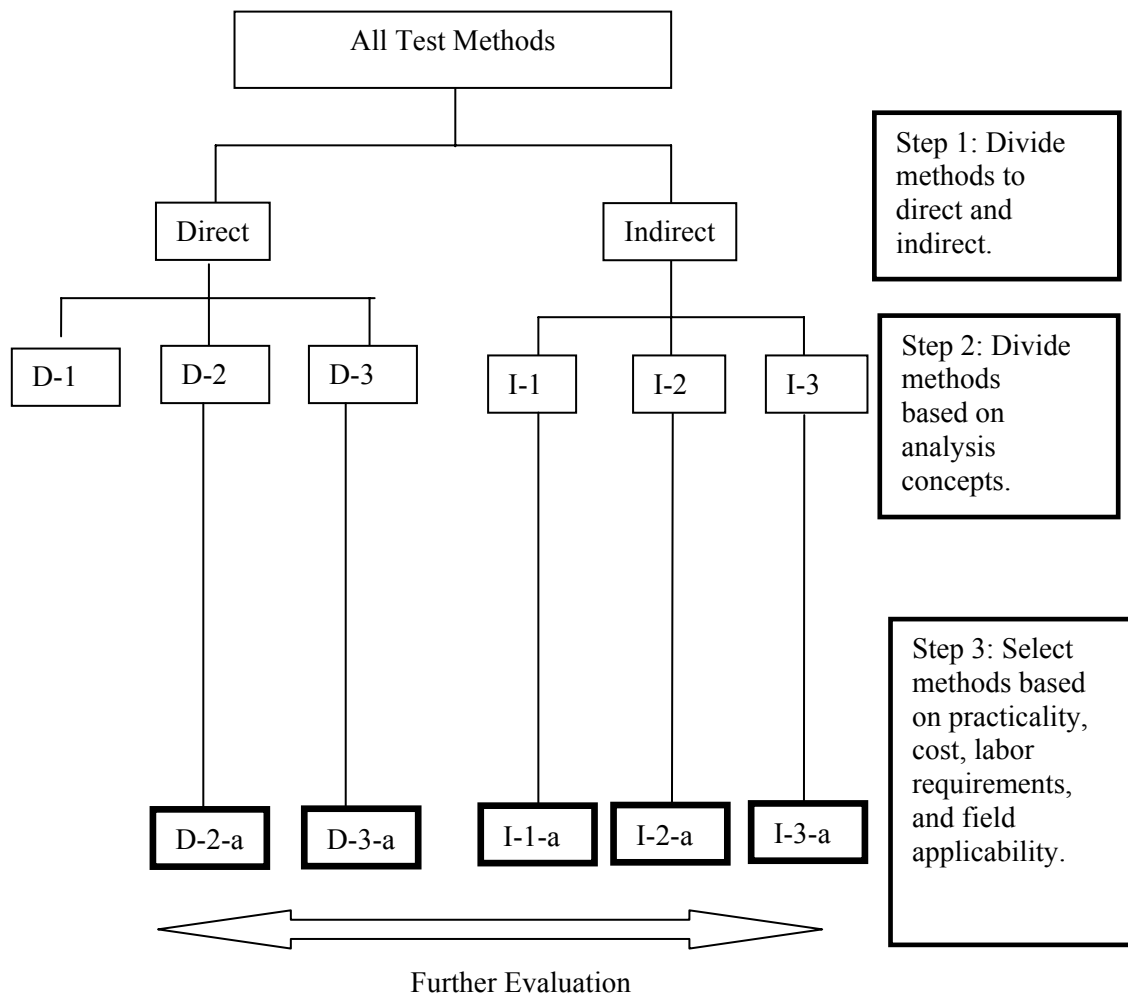


Fig. 4.1. Outline of the Approach for Preliminary Evaluation, Screening, and Prioritization of Test Methods

Table 4.2. Criteria for Selecting Test Methods for Intensive Evaluation

Test	Direct (D) or Indirect (I) Method	Analysis Concept	Selected Test for Further Intensive Evaluation
Uncompacted Void Content of Fine Aggregates AASHTO T304	I	Packing of aggregate that flow through a given sized orifice	Yes
Uncompacted Void Content of Coarse Aggregates AASHTO TP56	I		Yes
Rugosity	I		No
Time Index	I		No
Index for Particle Shape and Texture ASTM D3398	I	Packing of aggregate in a mold using two levels of compactions	No
Compacted Aggregate Resistance CAR	I	Exposing a compacted specimen to pressure or shear forces	Yes
Florida Bearing Ratio	I		No
Angle of Internal Friction from Direct Shear Test	I		No
Percentage of Fractured Particles in Coarse Aggregate ASTM D5821	D	Visual inspection of particles	Yes
Flat and Elongated Coarse Aggregates ASTM D4791	D	Measuring particle dimension using caliper	Yes
Multiple Ratio Shape Analysis	D		Yes
VDG-40 Videograder	D	Using one camera to image and evaluate particles in the sample as they fall in front of a backlight	Yes
Computer Particle Analyzer	D		No
Micromeritics OptiSizer PSDA	D		No
Video Imaging System (VIS)	D		No
Buffalo Wire Works PSSDA	D		Yes
Camsizer	D		Uses two cameras to image and evaluate particles in the sample as they fall in front of a back light
WipShape	D	Uses two cameras to capture image of aggregates passing on a mini conveyor system	Yes
University of Illinois Aggregate Image Analyzer (UIAIA)	D	Uses three cameras to capture three projections of a particle moving on a conveyor belt	Yes
Laser-Based Aggregate Analysis System	D	Uses a laser scan	Yes

The second group of tests includes those in which a compacted specimen is exposed to pressure or shear forces. Of these methods, the CAR test was selected. Chowdhury and Button (2001) concluded that the CAR test method offers much more sensitivity than either the FAA test or the direct shear test. This method has more advantages than the Florida Bearing Ratio and direct shear tests have (see Table 4.1).

Moreover, the CAR test is a relatively new test and has not received enough evaluation in the past.

The percentage of fractured particles in coarse aggregate method (ASTM D5821) was selected since it is currently included in the Superpave system. Rao and Tutumluer (2000) described this method as being time consuming, labor intensive, and subjective in nature. Also, it was classified as having low prediction and precision, with medium practicality (Meininger 1998).

The ASTM D4791 test for measuring flat and elongated coarse aggregates and the multiple ratio shape analysis method were both selected. The multiple ratio shape analysis method is capable of providing more detailed measurements in terms of the distribution of the dimensional ratio. ASTM D4791 was selected since it is included in the Superpave system. According to Yeggoni et al. (1996) and Rao and Tutumluer (2000) ASTM D4791 is considered tedious, labor extensive, and time consuming. The test method is also reportedly unable to identify spherical, rounded, or smooth particles, and is limited to testing only one particle at a time (Meininger 1998; Fowler et al. 1996).

The next group of tests that share the same analysis concept includes the VDG-40 Videograder, Computer Particle Analyzer, Micromeritics OptiSizer PSDA, Video Imaging System (VIS), and Buffalo Wire Works PSSDA. Of these methods only the VDG-40 Videograder and Buffalo Wire Works PSSDA were selected. The developers of Micromeritics OptiSizer PSDA preferred not to participate in the study, and the developers of the VIS declared the suspension of their research for the time being. The VDG-40 Videograder was selected because it is capable of analyzing every particle in the sample. In addition, the VDG-40 Videograder showed good correlation with manual measurements of flat and elongated particles (Weingart and Prowel 1999; Tutumluer et al. 2000). The Buffalo Wire Works PSSDA method was selected because it is reported to analyze particles with a wide range of sizes from those passing sieve #200 to 1.5 inches.

The Camsizer system uses two cameras to capture images at different resolutions and evaluates a large number of particles in the sample as they fall in front of a

backlight. Using two cameras makes this method unique and improves the accuracy of measuring the characteristics of both coarse and fine aggregates. The system has the capability to automatically produce particle size distribution and particle shape characteristics.

The WipShape system uses two cameras to capture images of aggregates passing on a mini-conveyor or on a rotating circular lighting table. This system was selected because it can analyze large quantities of particles in a short time. The system has the potential to measure and report various shape factors including sphericity, roundness, and angularity (Maerz and Lusher 2001; Maerz and Zhou 2001). The system is small in size, which makes it usable in field laboratories.

The University of Illinois Aggregate Image Analyzer (UIAIA) uses three cameras to capture black and white images for a particle from three orthogonal directions and build a 3-D shape construction of each particle. It has automated determination of flat and elongated, coarse aggregate angularity, and gradation. The use of three images for each particle makes it feasible to accurately compute the volume of each aggregate particle. It also provides information about the 3-D characteristics without assuming an idealized shape, such as an ellipsoid.

The Laser-Based Aggregate Analysis System (LASS) uses a laser scan to determine particles' form and angularity. This system was selected initially for evaluation, but unfortunately it was not made available to this study during the experimental evaluation period.

LABORATORY TESTING PROCEDURES

This section includes a description of the aggregates that were selected and used to evaluate the testing methods and the testing procedures that were followed in conducting each of the selected test methods presented in Table 4.2.

Description of Aggregates

Aggregates were selected to cover a wide spectrum of origin, rock type, and shape characteristics. Thirteen coarse aggregates and five fine aggregates were used in this study, as shown in Table 4.3. Three coarse aggregate sizes and three fine aggregate sizes were used to perform the evaluation (see Table 4.3). Experienced individuals from the industry and highway agencies assisted in selecting and providing these aggregates.

Table 4.3. Aggregate Sources and Sizes

Label	Source	Aggregate Description	Aggregate Sizes					
			25.4 - 19.0 mm (1- 3/4")	12.5 - 9.5 mm (1/2- 3/8")	9.5 - 4.75 mm (3/8"- #4)	4.75 - 2.36 mm (#4 - #8)	2.36 - 1.18 mm (#8 - #16)	0.6 - 0.3 mm (#30 - #60)
1	Montgomery AL	Uncrushed River Gravel	X	X	X	X	X	X
2	Montgomery AL	Crushed River Gravel	X	X	X	X	X	X
3	Childersburg AL	Limestone	X	X	X			
4	Auburn AL	Dolomite	X	X	X			
5	Birmingham AL	Slag	X	X	X	X	X	X
6	Brownwood TX	Limestone	X	X	X	X	X	X
7	Fairfield OH	Crushed Glacial Gravel	X	X	X			
8	Fairfield OH	Uncrushed Glacial Gravel	X	X	X			
9	Forsyth GA	Granite	X	X	X			
10	Ruby GA	Granite	X	X	X	X	X	X
11	Knippa TX	Traprock	X	X	X			
12	San Antonio TX	Limestone	X	X	X			
13	Augusta GA	Granite	X	X	X			

Mineralogical content of the thirteen aggregates was also determined using X-ray diffraction (XRD). XRD is a technique for establishing the structures of crystalline solids by directing X-rays of a single wavelength at a crystal and obtaining a diffraction pattern from which interatomic spaces can be determined. “In 1912, W. L. Bragg recognized a predictable relationship among several factors including: 1) the distance between similar atomic planes in a mineral (the interatomic spacing) also called the d-spacing; 2) the angle of diffraction which is called theta angle; and 3) the wavelength of the incident X-radiation. Bragg combined these factors in what is known as Bragg’s law where interatomic spacing can be quantified using the wavelength and the angle of diffraction” (www.geosci.ipfw.edu/). Knowing the interatomic spacing and the other two factors, an unknown mineral can be identified or the atomic-scale structure of an already identified mineral can be characterized.

In this study, what is known as powder XRD was used. As the name indicates, the sample analyzed in is in a powder form, consisting of fine grains of single crystalline material. Aggregates of the size 9.5 – 4.75 mm (3/8”- sieve #4) were ground to a powder form to a size that passes 0.075 mm (sieve #200). A few grams of the powder sample was placed in a holder, and then the sample was illuminated with X-rays of a fixed wave length in the diffractometer. The diffractometer used in this study is a Rigaku Miniflex diffractometer. The intensity of the reflected radiation was recorded. These data were then analyzed for the reflection angle to calculate the interatomic spacing (d-value in angstrom units - 10^{-8} cm). The intensity was measured to discriminate the various d-spacing, and the results were compared to specific tables to identify possible matches with mineral phases. The mineralogical content of the aggregates used in this study is presented in Table 4.4

The ASTM C-702 test procedure was followed to obtain representative samples of reasonable sizes. It is important to employ randomization when dividing the aggregate into smaller representative samples. The purpose of randomization is to reduce bias due to unforeseen factors that would affect measurements. All samples of coarse aggregates were washed prior to evaluation.

Aggregates selected for evaluation were sieved, reduced into smaller samples, and washed according to ASTM and AASHTO standard procedures. The main goal was to prepare these aggregates so they could be used to evaluate the selected methods in Table 4.2 in terms of repeatability, reproducibility, and accuracy.

Table 4.4. Mineralogical Content of Aggregates Using X-Ray Diffraction

Aggregate	Aggregate Description	Minerals Present
1	Uncrushed River Gravel	Quartz, Dolomite (trace)
2	Crushed River Gravel	Quartz
3	Limestone	Calcite, Dolomite, Quartz
4	Dolomite	Dolomite
5	Slag	Akermanite, Calcite, Quartz
6	Limestone	Calcite, Quartz, Dolomite
7	Crushed Glacial Gravel	Dolomite, Calcite, Quartz
8	Uncrushed Glacial Gravel	Dolomite, Calcite, Quartz
9	Granite	Quartz, Biotite, Albite, Labradorite
10	Granite	Quartz, Chlorite, Albite, Amesite, Anorthite, Phlogophite (Mica), Muscovite
11	Traprock	Tephrite, Diopside, Augite, Anorthite
12	Limestone	Calcite
13	Granite	Quartz, Albite, Calcite, Anorthite, Microcline, Kaolinite

It was decided to use the same sample for nondestructive tests by all operators and for all test replicates. It was also decided to consider the aggregate sample as a specific sample weight, 1 kg sample for coarse aggregates and 0.5 kg for fine aggregates. In conducting the tests, the operators were asked to return the aggregates to the sample after running a test, mix the sample, and acquire material randomly for each test.

Testing Methods Procedures

This section presents the test methods that were used in this study in addition to AIMS. As indicated earlier, some of the selected methods have been in practice for years and they are usually performed using standard procedures. On the other hand, there are some methods that have been developed recently. For these methods, the manufacturer's or the developer's instructions were followed to perform the testing. It was necessary in some cases to perform the standard tests with minor modifications in order to conduct the tests on the selected aggregate sizes. Description of the test methods were presented in Chapter II. In this section, only brief descriptions of the testing procedures and modifications, if any, are reported. A summary of aggregate sizes and measured shape parameters obtained from each of the selected test methods is shown in Table 4.5. Also, the last column in Table 4.5 lists the names of the indices, parameters or analysis methods used to present the measurements.

AASHTO 3304 (ASTM C1252) Uncompacted Void Content of Fine Aggregate

This test method was conducted at the Texas Transportation Institute (TTI). Method B of this test procedure was performed, where individual size fractions are tested on the smaller two sizes of the proposed fine aggregate sizes: 2.36 - 1.18 mm (sieve #8 - #16) and 0.6 - 0.3 mm (sieve #30 - #50). The size of 4.75 - 2.36 mm (sieve #4 - #8) was not tested for two reasons: First, this size was not included in the specifications, and second, this aggregate particles size did not pass through the orifice of the test apparatus freely. Complying with the standards, a 190 g sample size was used. In this study, the results are reported using the individual sizes, a slight modification from the Method B procedure, which requires that the average uncompacted void content from the three sizes to be reported. The test measures angularity of fine aggregates by measuring the loose uncompacted void content (UCVCF) in a sample that falls from a fixed distance through a given size orifice. Higher void content is associated with more angular particles. The apparatus used for this study is shown in Fig. 2.5.

Table 4.5. Aggregate Size and Shape Parameters Measured Using the Test Methods

Test	Aggregate Size						Shape Property		
	C 1	C 2	C 3	F 1	F 2	F 3	Form (Abbreviation)	Angularity (Abbreviation)	Texture (Abbreviation)
Uncompacted Void Content of Fine Aggregates AASHTO T304					X	X		% Loose Uncompacted Void Content (UCVCF)	
Uncompacted Void Content of Coarse Aggregates AASHTO TP56		X	X					% Loose Uncompacted Void Content (UCVCC)	
Compacted Aggregate Resistance CAR				X	X	X		Max Shear Resistance (CAR)	
Percentage of Fractured Particles in Coarse Aggregate ASTM D5821	X	X	X					% of Fractured Faces (PFF)	
Flat and Elongated Coarse Aggregates ASTM D4791	X	X	X				Flat Elongated Ratio (FER)		
Multiple Ratio Shape Analysis	X	X	X				Dimensional Ratio (MRA)		
VDG-40 Videograder	X	X	X	X			Flat Ratio (VDG- 40 FLAT) & Slenderness ratio (VDG-40 SLEND)		
Buffalo Wire Works PSSDA- Large	X	X	X				Roundness (PSSDA-Large ROUND)	Roundness (PSSDA-Large ROUND)	
Buffalo Wire Works PSSDA- Small				X	X	X	Roundness (PSSDA-Small ROUND)	Roundness (PSSDA-Small ROUND)	
Camsizer		X	X	X	X	X	Sphericity (CAMSPHT), Symmetry (CAMSYMM), Ratio of Length to Breadth (CAML/B)	Convexity (CAMCONV)	

Table 4.5. Continued

Test	Aggregate Size						Shape Property		
	C 1	C 2	C 3	F 1	F 2	F 3	Form (Abbreviation)	Angularity (Abbreviation)	Texture (Abbreviation)
WipShape	X	X	X				Dimensional Ratio (WSFER)	Minimum Average Curve Radius (WSMACR)	
University of Illinois Aggregate Image Analyzer (UIAIA)	X	X	X				Flat Elongated Ratio (UIFER)	Angularity Index (UIAI)	Surface Texture Index (UISTI)
Aggregate Imaging System (AIMS)	X	X	X	X	X	X	Sphericity (AIMSSPH) & Form 2-D Index (AIMSFORM)	Gradient Angularity Index AIMSGRAD), Radius Angularity Index (AIMSRAD)	Texture Index (Wavelet) (AIMSTXTR)

Aggregate sizes:

C1 = 25.4 - 9.0 mm (1 - 3/4"); C2 = 12.5-9.5 mm (1/2 - 3/8"); C3 = 9.5-4.75 mm (3/8" - #4);

F1 = 4.75 - 2.36 mm (#4 - #8); F2 = 2.36 - 1.18 mm (#8 - #16); F3 = 0.6 - 0.3 mm (#30 - #60).

AASHTO TP56 Uncompacted Void Content of Coarse Aggregate (as Influenced By Particle Shape, Surface Texture, and Grading)

This test method was conducted at TTI. Method B of this test procedure was performed, where individual size fractions are tested. This test was conducted on the smaller two sizes of the proposed coarse aggregate sizes; 12.5 – 9.5 mm (1/2 - 3/8 inches) and 9.5 – 4.75 mm (3/8" - #4). The larger size of 25.4 – 19.0 mm (1 - 3/4 inches) was not tested because it was not included in the test procedure. A sample size of 5000 g was used. In this study, the results are reported using the individual sizes, a slight modification from the Method B procedure, which requires that the average uncompacted void content from the three sizes to be reported. The test measures angularity of coarse aggregates by measuring the loose uncompacted void content (UCVCC) in a sample that falls from a

fixed distance through a given size orifice. Higher void content is associated with more angular particles. The apparatus used in this test method is shown in Fig. 2.6.

Compacted Aggregate Resistance (CAR) Test

The CAR test was conducted at TTI with some modification to the procedure provided by Mr. David Jahn. The procedure suggested by Mr. Jahn was to use the fine aggregates of a blend used in the preparation of the asphalt mix in their as-received condition. Two options were available. The first was to test the individual aggregate sizes. This option was dismissed after consultation with Mr. Jahn since these individual particles would not have the shear resistance that would develop from using combined sizes. The second option, which was followed in this study, was to develop a blend using the three fine aggregate sizes used in this study. The blend used here is given in Table 4.6 below. The sample size was 1200 g. The aggregate sample was oven-dried, and then 3.5% moisture was added to the specimen. The sample was placed in a mold, and 50 blows were applied on one face only. The sample was then placed in the Marshall stability and flow machine and tested at 2 inch/min to report shear resistance versus penetration. The test provides information on the shear resistance of compacted fine aggregates (CAR) which is used as a measure of angularity. Higher shear resistance is associated with higher angularity. The CAR testing setup is shown in Fig. 2.7.

Table 4.6. Fine Aggregate Blend Used in CAR Test

Size	Percentage
4.75 – 2.36 mm (sieve #4-#8)	40%
2.36 – 1.18 mm (sieve #8-#16)	20%
0.6 – 0.3 mm (sieve #30-#60)	40%

ASTM D5821 Determining the Percentages of Fractured Particles in Coarse Aggregate

In this test method, which was conducted at TTI, the size of the sample was chosen such that the number of particles exceeded 50 for aggregate sizes 25.4 – 19.0 mm (1- 3/4 inches) and 12.5 – 9.5 mm (1/2 - 3/8 inches). For the smaller size of 9.5 – 4.75 mm (3/8”- #4) a sample size of 200 grams, as recommended by specifications, was used. The total sample weight from each aggregate type always exceeded 500 g, as specified by ASTM D5821. This method provides information on the angularity of coarse aggregate by visually examining each particle and counting the number of fractured or crushed faces (PFF). A high percent of crushed faces (one face, two or more faces) is associated with higher angularity.

ASTM D4791 Flat and Elongated Coarse Aggregates

This test method was also conducted at TTI. The test specification does not provide a procedure for testing samples of one size. It was decided to use the same aggregate sample size that was used in conducting ASTM D5821. This method provides the percentage by number or weight of flat, elongated, or both flat and elongated particles in a given sample of coarse aggregates. The procedure uses a proportional caliper device, as shown in Fig. 2.13, to measure the dimensional ratio of aggregates. Following Superpave specifications, the ratios of length to thickness or the maximum dimension to the minimum dimension were reported in this study (FER).

Multiple Ratio Shape Analysis (MRA)

This test was conducted at TTI. In this method, aggregates were classified according to their dimensional ratios into five different categories instead of one (<2:1, 2:1 to 3:1, 3:1 to 4:1, 4:1 to 5:1, >5:1). The device consists mainly of a digital caliper connected to a data acquisition system and a computer. A particle is placed on a press table, and the press is lowered until it touches the aggregate particle and stops. The device records the gap between the press and the table, which is equal to the particle dimension. The particle is then rotated in another direction and the procedure is repeated to obtain other

dimensions. These readings are recorded in a custom-designed spreadsheet that displays the distribution of dimensional ratios in the aggregate sample. Fig. 2.14 shows the device. There was no specific sample size, as there were no standards for this test; therefore, it was decided, after consulting with Mr. David Jahn, that the same samples and sample sizes that were used in the flat and the elongated test and fractured faces test be used in this test.

VDG-40 Videograder

In this method an electromagnetic vibrator extracts the constituents of the sample in the hopper and directs them along a feed channel toward separator drums. The separator drum orients the aggregates toward the falling plane at the required speed. The system uses a line-scan CCD camera to image and evaluate every particle in the sample as it falls in front of the backlight. All analysis and data reporting are performed in a custom software package. This system provides information on aggregate gradation measurements and particle flatness (VDG-40 FLAT) and slenderness ratios (VDG-40 SLEND). Fig. 2.15 shows the VGD-40 Videograder.

Only coarse aggregate sizes were analyzed using this system. The VDG 40 Videograder has no standard specification for sample size. It was decided to use a 1.0 kg sample size. To ensure that the sample will have at least 50 particles, which is considered a statistically valid number. The system was brought from Turner-Fairbank Highway Research Center to TTI, where the testing was conducted.

Camsizer

The test was conducted at TTI. This system operates in a very similar way to the VDG-40 Videograder. Particles exit the hopper to a vibrating feed channel and fall between the light source and the camera. Particles are detected as projected surfaces and digitized by the computer (see Fig. 2.20). This system automatically produces particle size distributions and some aspects of particle shape characteristics. The system was not capable of analyzing the large size of coarse aggregates 25.4 – 19.0 mm (1 - 3/4 inches),

since these aggregates were too large to pass through the hopper.

The Camsizer measures the following parameters: Aggregate form, sphericity (CAMSPHT), symmetry (CAMSMM), and length to breadth (CAML/B). CAMSPHT is the same as form factor described in Chapter II and is given by Eq. 2.3. Both CAMSMM and CAML/B are described in Chapter II and can be calculated using Eqs. 2.14 and 2.13, respectively. Angularity in the Camsizer is described using convexity (CAMCONV), which was also described earlier in Chapter II and can be quantified using Eq. 2.24.

University of Illinois Aggregate Image Analyzer (UIAIA)

This method was conducted at the University of Illinois. It uses three cameras to capture projections of coarse aggregate particles as they move on a conveyor belt. These projections are then used to reconstruct a 3-D representation of the particles. The system is designed to measure the shape of coarse aggregates. Particles are placed individually on the conveyor belt. Once a particle is detected at a certain location on the conveyor belt using sensors, the cameras capture the three projections of particles individually. The UIAIA and aggregate detection system are presented in Fig. 2.22. Some of the aggregates with dark color were not measured using this system (aggregate 11 in Table 4.3).

The UIAIA measures all three aggregate shape characteristics (form, angularity, and texture). The methods used by UIAIA to measure these properties were presented in Chapter II. Form of aggregate particles is measured by calculating the flat and elongated ratio (UIFER). The UIAIA measures angularity (UIAI) using the outline slope method, while aggregate surface texture (UISTI) is measured using the erosion-dilation method.

WipShape

This test was also conducted at the University of Illinois. WipShape system uses two orthogonal cameras to capture images of each particle individually from two views. The individual particles are placed on a conveyor belt or on a circular rotating lighting table.

The WipShape system is shown in Fig. 2.21. WipShape provides a measure of aggregate form by providing information on the dimensional ratio from particle images (WSFER). WipShape also uses the minimum average curve radius method, described in Chapter II, to quantify aggregates angularity (WSMACR).

Buffalo Wire Works PSSDA

This test was performed at the University of Tennessee. The developer of the system (Dr. Dayakar Penumadu) created two experimental test devices that have the same analysis concept. These devices are called PSSDA-Large and PSSDA-Small. PSSDA-Large is devoted to analyzing coarse aggregate particles while PSSDA-Small is used for analysis of fine aggregates. Similar to the principle of the VDG-40 Videograder and Camsizer, the system uses one line-scan CCD camera to image and evaluate particles as they fall in front of the backlight. The system provides information about gradation and shape. Roundness (ROUND), which is the inverse of Eq. 2.3, is used to describe form. Both PSSDA systems are shown in Fig. 2.19.

EVALUATION OF REPEATABILITY AND REPRODUCIBILITY

Repeatability and reproducibility of test methods were evaluated through measuring the characteristics of aggregate samples several times using single and multiple operators, respectively. The following considerations were taken into account during the experimental evaluation: (1) operators were uniformly trained on the application of the test methods; (2) operators were provided with the same set of instructional guidelines; and (3) they were instructed that accuracy is more desirable than “good numbers” or “favorable results.”

One coarse aggregate size (12.5 - 9.5 mm [1/2 - 3/8 inches]), and one fine aggregate size (2.36 -1.18 mm [sieve #8 - #16]) were used for the repeatability analysis. Therefore, each of the operators measured the properties of these aggregate sizes three times. Reproducibility was assessed by measuring all aggregate sizes listed in Table 4.3 by each of the three operators. All operators conducted measurements using the same

samples.

Detailed information about the repeatability and reproducibility analysis is provided by Bathina (2004). Bathina (2004) used standard deviation and coefficient of variation as measuring parameters to quantify repeatability and reproducibility. Analysis of variance (ANOVA) was used in the statistical analysis according to the ASTM procedures (ASTM E177, ASTM C802, and ASTM C670). The repeatability and reproducibility statistical parameters were pooled over all materials for each test method. In the analysis process, the following steps and equations have been used:

1. Repeatability calculations: For one material size (m), and operator (p), the average of (n) replicates is given by Eq. 4.1, and the variation in measurements is calculated by Eq. 4.2.

$$x_i = \frac{\sum_{j=1}^n x_{ij}}{n} \quad (4.1)$$

$$S_i^2 = \frac{(\sum_{j=1}^n x_{ij}^2 - n\bar{x}_i)^2}{(n-1)} \quad (4.2)$$

Table 4.7 shows the arrangement of variation data within and between operators for one single material using one test method. The repeatability of a test method is evaluated for each aggregate material and all operators by Eq. (4.3):

$$S_r^2 = S_m^2 (pooled) = \frac{\sum_{i=1}^p S_i^2}{p} \quad (4.3)$$

2. Reproducibility Calculations: The average of measurements made by (p) operators for a single material (Eq. 4.4) and the variation between operators (Eq. 4.5) are calculated.

$$\bar{x}_m = \frac{\sum \bar{x}_i}{p} \quad (4.4)$$

$$S_{x_m}^2 = \frac{\sum \bar{x}_i^2 - p(\bar{x}_m)^2}{(p-1)} \quad (4.5)$$

Variations between operators are calculated by:

$$S_{L_m}^2 = S_{x_m}^2 - [S_m^2(pooled)/n] \quad (4.6)$$

Then, reproducibility of a test method is given by:

$$S_R^2 = S_{L_m}^2 + S_m^2(pooled) \quad (4.7)$$

Table 4.7. Arrangement of Variation in Measurements within and between Operators

Operator	Data (replicates) x_j			Average (\bar{x}_i)	Within Operator Variance S_i^2
1	I	II	III	\bar{x}_1	S_1^2
2	I	II	III	\bar{x}_2	S_2^2
3	I	II	III	\bar{x}_3	S_3^2

Repeatability and reproducibility of the test method on all aggregates were estimated by pooling standard deviations and coefficients of variations over all materials according to the guidelines of ASTM C 802 (Bathina 2004). Since each of the selected test methods measure shape properties using different parameters and these measurements had different scales, repeatability and reproducibility were assessed independently (i.e., calculated for each parameter). This assessment implies that repeatability and reproducibility of a test method varies with the measured parameter. The final results of repeatability and reproducibility for all test methods are reported for each shape property and for each aggregate size (coarse and fine) separately. Results of repeatability and reproducibility of test methods used to measure shape properties of coarse and fine aggregates are presented in Tables 4.8 and 4.9, respectively. The notations of the parameters are maintained as they are described in the manuals and

standards of test methods.

Several factors should be taken into consideration in the interpretation of the repeatability and reproducibility results reported in Tables 4.8 and 4.9. First, the methods differ significantly in the level of detail provided in the results. All the indirect methods provide an average index, while the imaging-based methods provide, or at least are capable of providing, the entire distribution of a shape property in an aggregate sample. This advantage of the imaging-based methods is not reflected here since the calculations are all conducted using average values in order to analyze all test methods. Second, the test methods differ in the range of the results from different aggregates. For example, it was found that the Camsizer parameters have a narrow range, where the maximum and minimum values between aggregates differ by about 20%. However, the AIMS parameters have wide range. Third, all the measurements were conducted by trained operators, and it is expected that the results in Tables 4.8 and 4.9 are low compared to wide use by many operators in different laboratories. Finally, all measurements were conducted using a single device, and the results do not reflect the possible differences among different devices for the same test method. To this end, it was recommended to use the results in Tables 4.8 and 4.9 to classify test methods as low (L), medium (M), and high (H) variability rather than comparing the test method based on slight differences in the coefficient of variation. Consequently, the test methods are classified based on variability as shown in Tables 4.10 and 4.11.

Table 4.8. Repeatability and Reproducibility of Test Methods Measuring Coarse Aggregate Shape Properties

Shape Property	Test Method	Parameter Abbreviation Used in This Study	Measure Parameter as Reported by Test Method	Standard Deviation (S)		Coefficient of Variation (CV)	
				Repeatability	Reproducibility	Repeatability	Reproducibility
Angularity	Uncompacted Void Content of Coarse Aggregates	UCVCC	% Uncompacted Void content	0.010	0.013	0.009	0.018
	% Fractured Faces	PFF	0 Fractured Faces	0.075	0.260	0.227	0.766
			1 Fractured Face	0.059	0.156	0.165	0.502
			≥2 Fractured Faces	0.050	0.361	0.123	1.150
	Camsizer	CAMCONV	Conv3	0.00034	0.00032	0.00032	0.00031
	WipShape	WSMACR	Min Avg. Curve Radius	0.001	0.004	0.010	0.037
	University of Illinois Aggregate Image Analyzer UIAIA	UIAI	Angularity Index	9.555	15.384	0.018	0.031
	Aggregate Imaging System AIMS	AIMSGRAD	Gradient Angularity	321.968	357.771	0.084	0.106
		AIMSRAD	Radius Angularity	0.309	0.470	0.031	0.048
	Buffalo Wire Works PSSDA-Large	PSSDA-Large ROUND	Average Roundness	0.046	0.080	0.027	0.049

Table 4.8. Continued

Shape Property	Test Method	Parameter Abbreviation Used in This Study	Measure Parameter as Reported by Test Method	Standard Deviation (S)		Coefficient of Variation (CV)	
				Repeatability	Reproducibility	Repeatability	Reproducibility
Texture	University of Illinois Aggregate Image Analyzer UIAIA	UISTI	Mean Surface Texture Index	0.065	0.093	0.028	0.0556
	Aggregate Imaging System AIMS AIMS	AIMSTXTR	Texture Index	36.037	37.395	0.139	0.163
	Camsizer	CAMCONV	Conv3	0.00034	0.00032	0.00032	0.00031
	Uncompacted Void Content of Coarse Aggregates UCVC	UCVCC	% Uncompacted Void content	0.010	0.013	0.009	0.018
	WipShape	WSMACR	Min Avg. Curve Radius	0.001	0.004	0.010	0.037
	University of Illinois Aggregate Image Analyzer UIAIA	UIAI	Angularity Index	9.555	15.384	0.018	0.031

Table 4.8. Continued

Shape Property	Test Method	Parameter Abbreviation Used in This Study	Measure Parameter as Reported by Test Method	Standard Deviation (S)		Coefficient of Variation (CV)	
				Repeatability	Reproducibility	Repeatability	Reproducibility
Form/ Parameter	Camsizer	CAMSPHT	SPHT3	0.004	0.004	0.003	0.003
		CAMSYM M	Symm3	0.001	0.001	0.002	0.001
	Aggregate Imaging System AIMS	AIMSFOR M	Form 2-D	0.229	0.303	0.031	0.041
		AIMSPH	Sphericity	0.014	0.018	0.020	0.026
	Buffalo Wire Works PSSDA-Large	PSSDA- Large ROUND	Average Roundness	0.046	0.080	0.027	0.049
Form/ Dimensional Ratio	Flat and Elongated Ratio	FER	% of Flat and Elongated Particles	1.000	4.570	0.064	0.317
	Multiple Ratio Analysis MRA	MRA	<Wt. 2:1	0.015	0.025	0.033	0.053
			Wt 2:1- 3:1	0.016	0.025	0.039	0.060
			Wt 3:1-4:1	0.010	0.012	0.374	0.478
			Wt 4:1-5:1	0.005	0.007	0.132	0.312
	VDG-40 Videograder	VDG-40 SLEND	Slenderness Ratio	0.021	0.023	0.013	0.014
		VDG-40 FLAT	Flatness Factor	0.023	0.042	0.016	0.027
	Camsizer	CAML/B	l/b3	0.016	0.016	0.008	0.008
	WipShape	WSFER	<2:1	3.502	8.323	0.052	0.114
			<3:1	2.396	4.506	0.159	0.275
			<4:1	1.334	2.196	0.302	0.405
	University of Illinois Aggregate Image Analyzer UIAIA	UIFER	< 3:1	2.370	3.650	0.024	0.036
			3:1 - 5:1	2.136	3.180	0.204	0.268

Table 4.8. Continued

Shape Property	Test Method	Parameter Abbreviation Used in This Study	Measure Parameter as Reported by Test Method	Standard Deviation (S)		Coefficient of Variation (CV)	
				Repeatability	Reproducibility	Repeatability	Reproducibility
Form/ Dimensional Ratio	Aggregate Imaging System AIMS	AIMSFER	<3 :1	5.061	7.383	0.063	0.091
			3:1 - 5:1	4.753	6.917	0.309	0.398

Table 4.9. Repeatability and Reproducibility of Test Methods Measuring Fine Aggregate Shape Properties

Shape Property	Test Method	Parameter Abbreviation Used in This Study	Measure Parameter as Reported by Test Method	Standard Deviation (S)		Coefficient of Variation (CV)	
				Repeatability	Reproducibility	Repeatability	Reproducibility
Angularity	Uncompacted Void Content of Fine Aggregates	UCVCF	% Uncompacted Void Content	0.002	0.0053	0.004	0.010
	Camsizer	CAMCONV	Conv3	0.0002	0.0002	0.0002	0.0002
	Aggregate Imaging System AIMS	AIMSGRAD	Gradient Angularity	190.779	314.718	0.046	0.071
		AIMSRAD	Radius Angularity	0.319	0.331	0.029	0.032
	Buffalo Wire Works PSSDA-Small	PSSDA-Small ROUND	Average Roundness	0.111	0.101	0.113	0.111
Compacted Aggregate Resistance CAR	CAR	Aggregate Resistance	3241.977	4237.560	0.072	0.073	

Table 4.9. Continued

Shape Property	Test method	Parameter Abbreviation Used in This Study	Measure Parameter as Reported by Test Method	Standard Deviation (S)		Coefficient of Variation (CV)	
				Repeatability	Reproducibility	Repeatability	Reproducibility
Form	Camsizer	CAMPHT	SPHT3	0.0017	0.0018	0.0019	0.002
		CAMSYMM	Symm3	0.00032	0.00065	0.00035	0.0007
		CAML/B	l/b3	0.0015	0.0052	0.0011	0.003
	Aggregate Imaging System AIMS	AIMSFORM	Form 2-D	0.305	0.387	0.032	0.041
	Buffalo Wire Works PSSDA-Small	PSSDA-Small ROUND	Average Roundness	0.111	0.101	0.113	0.111

Table 4.10. Classification of Coarse Aggregate Test Methods Based on Repeatability and Reproducibility.

Shape Property	Test Method	Parameter Abbreviation Used in This Study	Measure Parameter as Reported by Test Method	Coefficient of Variation (CV)	
				Repeatability	Reproducibility
Angularity	Uncompacted Void Content of Coarse Aggregate	UCVCC	% Uncompacted Void Content	L	L
	% Fractured Faces	PFF	0 Fractured Faces	H	H
			1 Fractured Face	M	H
			≥2 Fractured Faces	M	H
	Camsizer	CANCONV	Conv3	L	L
	WipShape	WSMACR	Min Avg. Curve Radius	L	L
	University of Illinois Aggregate Imaging System UIAIA	UIAI	Angularity Index	L	L
	Aggregate Imaging System AIMS	AIMSGRAD	Gradient Angularity	L	L
AIMSRAD		Radius Angularity	L	L	
Buffalo Wire Works PSSDA-Large	PSSDA-Large ROUND	Average Roundness	L	L	
Texture	University of Illinois Aggregate Imaging System UIAIA	UISTI	Mean Surface Texture Index	L	L
	Aggregate Imaging System AIMS	AIMSTXTR	Texture Index	M	M
	Camsizer	CAMCONV	Conv3	L	L
	Uncompacted Void Content of Coarse Aggregate	UCVCC	% Uncompacted Void content	L	L
	WipShape	WSMACR	Min Avg. Curve Radius	L	L
	University of Illinois Aggregate Imaging System UIAIA	UIAI	Angularity Index	L	L

Table 4.10. Continued

Shape Property	Test Method	Parameter Abbreviation Used in This Study	Measure Parameter as Reported by Test Method	Coefficient of Variation (CV)	
				Repeatability	Reproducibility
Form/ Parameter	Camsizer	CAMPHT	SPHT3	L	L
		CAMSYMM	Symm3	L	L
	Aggregate Imaging System AIMS	AIMSFORM	Form 2-D	L	L
		AIMSSPH	Sphericity	L	L
	Buffalo Wire Works PSSDA-Large	PSSDA-Small ROUND	Average Roundness	L	L
Form/ Dimensional Ratio	Flat and Elongated Ratio	FER	% of Flat and Elongated Particles	L	H
	Multiple Ratio Analysis MRA	MRA	<Wt 2:1	L	L
			Wt 2:1- 3:1	L	L
			Wt 3:1-4:1	H	H
			Wt 4:1-5:1	M	H
	VDG-40 Videograder	VDG-40 SLEND	Slenderness Ratio	L	L
		VDG-40 FLAT	Flatness Factor	L	L
	Camsizer	CAML/B	1/b3	L	L
	WipShape	WSFER	<2:1	L	M
			<3:1	M	H
			<4:1	H	H
	University of Illinois Aggregate Imaging System UIAIA	UIFER	< 3:1	L	L
			3:1 - 5:1	H	H
	Aggregate Imaging System AIMS	AIMSFER	<3 :1	L	L
3 :1 - 5:1			H	H	

Low (L) CV<=10%, Medium (M) 10%< CV<=20%, High (H) CV>20%

Table 4.11. Classification of Fine Aggregate Test Methods Based on Repeatability and Reproducibility

Shape Property	Test Method	Parameter Abbreviation Used in This Study	Measure Parameter as Reported by Test Method	Coefficient of Variation (CV)	
				Repeatability	Reproducibility
Angularity	Uncompacted void content of Fine Aggregates	UCVCF	% Uncompacted Void Content	L	L
	Camsizer	CAMCONV	Conv3	L	L
	Aggregate Imaging System AIMS	AIMSGRAD	Gradient Angularity	L	L
		AIMSRAD	Radius Angularity	L	L
	Buffalo Wire Works PSSDA-Small	PSSDA-Small ROUND	Average Roundness	M	M
Compacted Aggregate Resistance CAR	CAR	Aggregate Resistance	L	L	
Form	Camsizer	CAMSPHT	SPHT3	L	L
		CAMSYMM	Symm3	L	L
		CAML/B	l/b3	L	L
	Aggregate Imaging System AIMS	AIMSFORM	Form 2-D	L	L
	Buffalo Wire Works PSSDA-Small	PSSDA-Small ROUND	Average Roundness	M	M

Low (L) $CV \leq 10\%$, Medium (M) $10\% < CV \leq 20\%$, High (H) $CV > 20\%$

The percentage of fractured faces test had very high variability compared to all other test methods. This is in agreement with the evaluation and ratings reported by Meininger (1998) and Saeed et al. (2001). According to the results in Table 4.11, the uncompacted void content test for fine aggregate had low variability. Saeed et al. (2001) rated this test as having a fair precision (ability to repeatedly provide correct results). The results of this test were analyzed using the same specific gravity for each aggregate. The variability of this test comes mainly from error in measuring the specific gravity. Therefore, it is expected that the variability of the uncompacted void content test would increase significantly when the variability in specific gravity measurements is included.

AIMS and most of the image analysis methods had high variability when the percentage of particles with a dimensional ratio of 5:1 were considered. This was mainly due to the small percentages of particles that exhibited this characteristic, such that any slight variation in accounting for these particles was manifested as high coefficient of variation. The variability was reduced by considering the percentage of particles with a dimensional ratio smaller or larger than 3:1. The AIMS angularity indices had low variability, while the texture indices had medium variability. It is expected that this variability would be reduced further through automation of the top lighting.

Comparing the repeatability results for the VDG-40 Videograder and Buffalo Wire Works PSSDA, which are presented in Table 4.8, shows that the VDG-40 Videograder had better repeatability than the Buffalo Wire Works PSSDA. These results are in agreement with the findings of Browne et al. (2001), who found that the repeatability of the VDG-40 Videograder was better than the Buffalo Wire Works PSSDA for size distribution measurements. This is due to the difference in the type of cameras used in these systems. In the VDG-40 Videograder the camera used (line-scan camera) captures successive images with very short delays between them, enabling the system to analyze almost every particle. The Buffalo Wire Works PSSDA use a matrix-scan camera that captures successive images with longer delays between them, allowing the system to analyze only about 10 to 20% of particles while the remainder of particles are missed during the time intervals between the image acquisitions.

EVALUATION OF ACCURACY

Ideally speaking, the accuracy of the test methods can be analyzed by evaluating the correlation of the measurements from these tests with the measurements conducted using standards or reference tests that are accepted to be accurate. The three dimensions of coarse particles can be measured using a digital caliper. This is an accurate, but slow, method of assessing the shape of particles. However, a set of test methods that are accepted to be accurate in quantifying texture and angularity does not exist. The existence of such “accurate” tests would have made the analysis of the accuracy of the test methods evaluated in this chapter an easy task. Therefore, the following approach was adopted to assess, to some extent, the accuracy of the test methods:

1. The accuracy should be evaluated for the test methods based on the procedure recommended by standards and/or by the developers, and for the analysis methods (mathematical functions and indices) employed in the imaging-based systems. This task allows evaluation of the accuracy of the analysis methods irrespective of the characteristics of the image acquisition setup.
2. Accuracy of analysis methods in imaging-based systems is evaluated through:
 - a. Analysis of diagrams of sediments with different shape characteristics. These diagrams were developed by geologists in the past to describe and quantify the two-dimensional form and angularity of sediments. They were plotted based on actual observations of sediments and manual measurements of their form and angularity. This task was used to determine whether the analysis methods are capable of identifying clear differences between particle projections. Also, this task was helpful to determine if an analysis method is able to separate the different characteristics of shape (form, angularity, and texture). This was the first screening test for the analysis methods.
 - b. Analysis of the uniqueness of test methods. It is necessary to evaluate the correlations among the different test methods. This task will serve the

purpose of identifying analysis methods that are able to capture the same characteristics. Consequently, the method that is easier to implement and interpret should be recommended.

- c. Comparison between visual rankings of texture and angularity of aggregates by experienced individuals and results of test methods. This is useful to identify analysis methods that are not capable of discriminating aggregates with extreme angularity and texture characteristics (e.g., uncrushed river gravel vs. crushed gravel, uncrushed river gravel vs. crushed granite).
3. Accuracy of test methods is evaluated through:
 - a. Comparison between the form measurements using the test methods and the measurements of particles' dimensions using a digital caliper.
 - b. Comparison between the texture and angularity visual rankings of aggregates by experienced individuals and results of test methods. This is useful to identify test methods that are not capable of discriminating aggregates with extreme angularity and texture characteristics (e.g., uncrushed river gravel vs. crushed gravel, uncrushed river gravel vs. crushed granite).

Accuracy of Analysis Methods

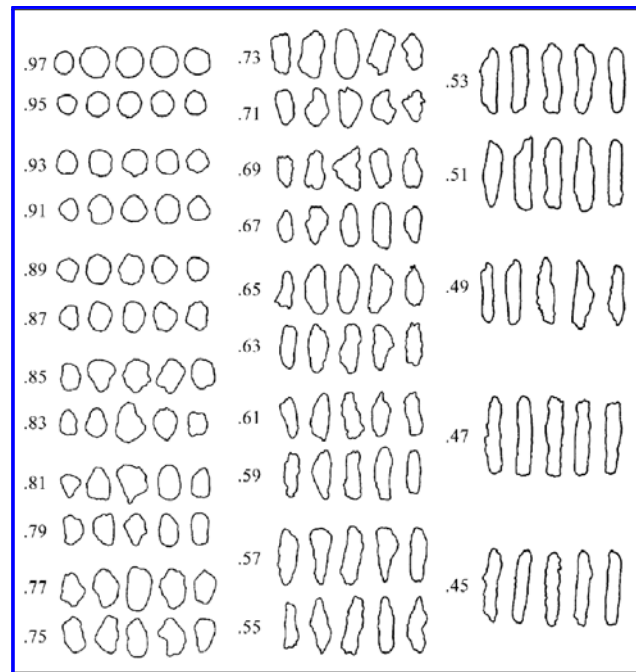
Comparison with Geological Projections

The two dimensional image analysis methods listed in Table 4.12 were used to analyze the particle projections shown in Fig. 4.2. A detailed description of these analysis techniques was presented in Chapter II. These particle projections, shown in Fig. 4.2, were developed by geologist in the past to describe and quantify the 2-D form and angularity of sediments. These diagrams were plotted based on actual observations of sediments and manual measurements of their form and angularity. Fig. 4.2(a) was developed by Rittenhouse (1943) to measure 2-D form (or sphericity). This method is based on the one developed earlier by Wadell (1932, 1935), which is considered a

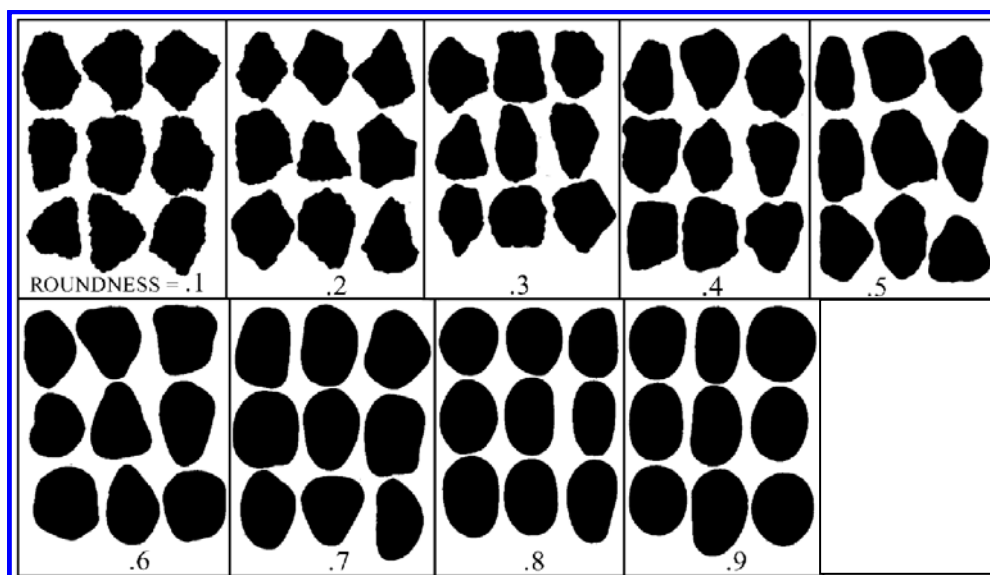
standard and accurate method for evaluating form (Riley 1941; Powers 1953). The method by Rittenhouse (1943) was developed originally for fine particles. It assumes the particle dimension in the third direction to be nearly equal to the shorter of the two dimensions in the projection. Fig. 4.2(b) was developed by Krumbien (1941) to evaluate angularity. This method is also based on the one proposed by Wadell (1932, 1935). This method was originally developed for coarse aggregates.

Table 4.12. Analysis Methods Used in Analyzing Aggregate Images

Method	Description
Texture Index Using Wavelet	Used by AIMS analysis software (AIMSTXTR)
Gradiant Angularity Index	Used by AIMS analysis Software (AIMSGRAD)
Radius Angularity Index	Used by AIMS analysis Software (AIMSRAD)
2-D Form Index	Used by AIMS analysis Software (AIMSFORM)
Sphericity	Used by AIMS analysis Software (AIMSSPH)
Texture Index (Fourier)	(FRTXTR)
Angularity Index (Fourier)	(FRANG)
Form Index (Fourier)	(FRFORM)
Flat & Elongated Ratio	Used By University Of Illinois System (UIFER)
Angularity Using Outline Slope	Used By University Of Illinois System (UIAI)
Surface Texture Using Erosion-Dilation technique	Used By University Of Illinois System (UISTI)
Aspect Ratio	Used in Image Pro Software (ASPTPRO)
Fractal Dimension	Used in Image Pro Software (FRCTLPRO)
Roundness	Used in Image Pro Software (ROUNDPRO)



(a) Rittenhouse (1943)



(b) Krumbein (1941)

Fig. 4.2. Charts Used by Geologists in the Past for Visual Evaluation of Granular Materials

Correlations between analysis method parameters and visual numbers by Rittenhouse and Krumbein are shown in Tables 4.13 and 4.14, respectively. Rittenhouse and Krumbein projections can be used to identify analysis methods capable of capturing changes in form and angularity, respectively. The correlation results in Tables 4.13 and 4.14 suggest that:

- The following methods can be used only to describe form without being affected by angularity of a particle: (a) Flat Elongated Ratio used by University of Illinois test method (UIFER); (b) Form Index measured using Fourier Series (FRFORM); and (c) Aspect Ratio measured using Image Pro software (ASPTPRO).
- The following methods can be used to describe angularity without being affected by form: (a) Gradient Angularity used in the Aggregate Imaging system AIMS (AIMSGRAD); (b) Angularity Index used by the University of Illinois test method (UIAI); (c) Texture Index used by the University of Illinois test method (UISTI); and (d) Fractal technique used in Image Pro software (FRCTLPRO).

Table 4.13. Pearson and Spearman Correlation Coefficients of Rittenhouse Sphericity

Analysis Method Parameter	Pearson Correlation Coefficient	Spearman Correlation Coefficient	Applicability
AIMSGRAD	0.458	-0.54	N
AIMSRAD*	-0.868	-0.894	Y
AIMSFORM*	-0.98	-0.991	Y
FRFORM	-0.918	-0.993	Y
FRANG*	-0.814	-0.99	Y
FRTXTR*	-0.858	-0.999	Y
UIFER	-0.938	-0.993	Y
UIAI	-0.388	-0.368	N
UISTI	0.273	0.425	N
ASPTPRO	-0.938	-0.995	Y
FRCTLPRO	0.256	-0.322	N
ROUNDPRO*	-0.941	-0.996	Y

* Method correlates with two shape properties at the same time.

Table 4.14. Pearson and Spearman Correlation Coefficients of Krumbein Roundness

Analysis Method Parameter	Pearson Correlation Coefficient	Spearman Correlation Coefficient	Applicability
AIMSGRAD	-0.886	-0.983	Y
AIMSRAD*	-0.964	-0.967	Y
AIMSFORM*	-0.958	-0.967	Y
FRFORM	-0.016	-0.033	N
FRANG*	-0.908	-0.883	Y
FRTXTR*	-0.942	-0.967	Y
UIFER	0.486	-0.317	N
UIAI	-0.959	-0.983	Y
UISTI	-0.957	-0.983	Y
ASPTPRO	-0.414	0.317	N
FRCTLPRO	-0.869	-0.867	Y
ROUNDPRO*	-0.959	-0.967	Y

* Method correlates with two shape properties at the same time.

- The Angularity Index (UIAI) has very good correlation with the Texture Index (UISTI). This might suggest that these two parameters are capturing similar geometries on the boundary of particles.
- Roundness measured using Image Pro (ROUNDPRO), and Texture Index using Fourier (FRTXTR), Angularity Index using Fourier (FRANG), Form Index Using AIMS (AIMSFORM), and Radius Angularity using AIMS (AIMSRAD) have good correlation with Rittenhouse sphericity numbers and Krumbein roundness numbers. This indicates that these methods are not as unique as the other methods in distinguishing between angularity and form of particles.

Uniqueness of Test Methods Based on Aggregate Clustering

This task was performed to examine the uniqueness of the analysis methods in capturing aggregate shape characteristics. A simple setup of a camera and a microscope was used to capture images of 50 randomly selected coarse particles (12.5 – 9.5 mm; 1/2 - 3/8

inches), and 50 fine particles (2.36 – 1.18 mm; sieve #8 - #16) of each aggregate type at specific resolution. The setup was equipped with top lighting to capture gray images for texture analysis and a backlighting to capture black and white images for angularity analysis. The resulting images were analyzed using standard image analysis techniques, shown in Table 4.12, which are also employed as analysis techniques in some of the imaging-based tests evaluated in this study.

Using the capabilities of SPSS software, the analysis results from the 50 images of the coarse aggregate size of each aggregate type were used to cluster the analysis methods. The analysis methods were clustered using Ward's Linkage method. Clustering is a widely used pattern recognition method for grouping data and variables. Grouping is done on the basis of similarities or distances. In many areas of engineering and science, it is important to group items into natural clusters. Basic references about clustering methods include most applied multivariate statistical texts (e.g., Johnson and Wichern 2002; Morrison 2004). All clustering methods start from a choice of a metric (a distance or closeness among objects) and a choice of a method for grouping objects. When items (units or cases) are clustered, proximity is usually indicated by some sort of distance. On the other hand, variables are usually grouped on the basis of correlation coefficients or like measure of association (Johnson and Wichern 2002).

In this study, two types of similarities were used. Pearson correlation coefficient, given by Eq. (4.8), is used as a measure of proximity when variables are grouped. The second measure of similarity was the Euclidean distance, given by Eq. (4.9), which is used to cluster cases. The Pearson correlation coefficient of a set of observations $\{(x_i, y_i): i=1, \dots, n\}$ is given by the formula:

$$r = \frac{\sum_{i=1}^n (x_i - \bar{x})(y_i - \bar{y})}{\sqrt{\sum_{i=1}^n (x_i - \bar{x})^2 \sum_{i=1}^n (y_i - \bar{y})^2}} \quad (4.8)$$

and the Euclidean distance is given by:

$$d(\mathbf{x}, \mathbf{y}) = \sqrt{\sum_{i=1}^p (x_i - y_i)^2} \quad (4.9)$$

where \mathbf{x} and \mathbf{y} represent two p -dimensional observations (items) $x = [x_1, x_2, \dots, x_p]$ and $y = [y_1, y_2, \dots, y_p]$.

Ward's Linkage method tries to make the similarity or distance measures sum of squares within groups as small as possible. In this sense, it makes an ANOVA F-test among the clusters as large as possible. Or, in other words, Ward's method groups clusters whose combination results in the smallest increase in the sum of squared deviations from the cluster mean.

Ward's Linkage method with Pearson correlation proximity measure was applied to the analysis results. This type of analysis was needed in order to identify clusters of analysis methods. The results of the cluster analysis are shown in Table 4.15. For each aggregate type, the test methods that have the same number (1, 2, 3, or 4) indicate that these methods are clustered, or they are more correlated with each other than with other test methods. For example, the data from AIMSTXTR analysis of CA-1 is statistically different than the data from all the other test methods, indicating that this analysis method captures an aggregate characteristic different than what is captured by all the other methods. The UIAI and UISTI methods are clustered for 12 of the 13 aggregates. The percentage of aggregates that a test method is clustered with other test methods is shown in Table 4.16. For example, the AIMSTXTR method is clustered alone in 54% of aggregates, clustered with another method in 31% of aggregates, and so on. In other words, an increase in percentage in the cells toward the left of the table is an indication of an increase in the uniqueness of the characteristic measured using this method. Based on the results in Tables 4.15 and 4.16, AIMSTXTR is the most unique among the texture parameters, AIMSGRAD and UIAI are the most unique among the angularity parameters, and AIMSSPH is the most unique among the form parameters.

Table 4.15. Clustering of Analysis Methods (4 Clusters) Based on Pearson Correlation

Analysis Method	Aggregate												
	CA-1	CA-2	CA-3	CA-4	CA-5	CA-6	CA-7	CA-8	CA-9	CA-10	CA-11	CA-12	CA-13
AIMSTXTR	1	1	1	1	1	1	1	1	1	1	1	1	1
AIMSGRAD	2	2	2	2	2	2	2	2	2	2	1	2	2
AIMSRAD	2	2	3	2	2	3	2	1	2	3	2	3	3
AIMSFORM	2	2	2	2	2	3	2	1	2	3	2	3	3
AIMSSPH	3	3	3	3	3	1	3	3	3	1	3	1	4
UIFER	4	4	4	4	4	4	4	3	4	4	4	4	1
UIAI	4	4	4	4	4	4	4	2	4	4	4	4	2
UISTI	4	4	4	4	4	4	4	2	4	4	4	4	1
FRFORM	2	2	2	2	2	3	2	1	2	3	2	3	3
FRANG	2	2	2	2	2	3	2	1	2	3	2	3	3
FRTXTR	2	2	2	2	2	3	2	4	2	3	2	3	3
ASPCTPRO	2	2	2	2	2	3	2	1	2	3	2	3	3
FRCTLPRO	2	2	3	2	2	3	3	1	2	3	2	3	3
ROUNDPRO	2	2	2	2	2	3	2	1	2	3	2	3	3

Table 4.16. Percentage of Clustered Aggregates for Each Analysis Method

Analysis Method	Number of Methods to Cluster With					
	0	1	2	6	7	8
AIMSTXTR	54%	31%	8%		8%	
AIMSGRAD	23%	15%	8%	8%	8%	38%
AIMSRAD			8%		54%	38%
AIMSFORM				8%	54%	38%
AIMSSPH	54%	38%	8%			
UIFER		8%	92%			
UIAI		8%	92%			
UISTI			100%			
FRFORM				8%	54%	38%
FRANG				8%	54%	38%
FRTXTR	8%			8%	46%	38%
ASPCTPRO				8%	54%	38%
FRCTLPRO		8%	8%		46%	38%
ROUNDPRO				8%	54%	38%

Ward's Linkage method was used to cluster aggregates based on their angularity and texture measured using different analysis methods. The results of four clusters are shown in Tables 4.17 and 4.18. This analysis is useful to identify those inaccurate methods that cluster aggregates with distinct shape characteristics.

As shown in Table 4.17, both the FRTXTR and FRACTLRPO parameters show aggregates CA-1 (uncrushed gravel) and aggregates CA-9 and CA-10 (both are granite) in the same cluster. This finding indicates the inability of these methods to detect significant differences between aggregates. UISTI shows both aggregates CA-2 (crushed gravel) and CA-10 (granite) in the same texture cluster.

Table 4.17. Coarse Aggregates in Texture Classes Estimated Using Ward's Linkage

Method	Class 1	Class 2	Class 3	Class 4
AIMSTXTR	1, 2, 12	3, 5, 10, 11, 13	4, 6, 7, 8	9
UISTI	1, 8	2, 3, 7, 10, 11, 13	4, 6, 9, 12	5
FRTXTR	1, 7, 9, 10, 12	2, 4	3, 5, 6, 11, 13	8
FRACTLPRO	1, 4, 9, 10, 12	2, 3, 6, 11, 13	5, 7	8

Table 4.18. Coarse Aggregates in Angularity Classes Estimated Using Ward's Linkage

Method	Class 1	Class 2	Class 3	Class 4
AIMSGRAD	1, 8	2, 4, 6, 7, 12	5, 9, 10	3, 11, 13
AIMSRAD	1, 2, 9	3, 4, 11, 13	5, 6, 7, 10, 12	8
UIAI	1	2, 6, 9	3, 4, 5, 7, 10, 11, 12, 13	8
FRANG	1, 2, 3, 6, 9, 11, 12	4, 5, 7, 10	8	13
FRACTLPRO	1, 4, 9, 10, 12	2, 3, 6, 11, 13	5, 7	8
ROUNDPRO	1, 2, 6, 12	3, 4, 5, 7, 9, 10, 11	8	13

The results in Table 4.18 show that AIMS RAD, FRANG, FRTXTR, and ROUNDPRO methods cluster the uncrushed (CA-1) and crushed gravel (CA-2) in the same group. This result indicates the inability of these methods to capture the influence of crushing on angularity. Recall that these methods are also not unique in distinguishing between angularity and form when used to analyze the geological projections. Table 4.19 shows a summary of the findings about the analysis methods.

Table 4.19. Analysis Methods Used in Analyzing Aggregate Images

Method	Description	Features
Texture Index Using Wavelet	Used by AIMS analysis software (AIMSTXTR)	<ul style="list-style-type: none"> • Capable of separating aggregates with different texture characteristics. • Most unique among the texture parameters.
Gradient Angularity Index	Used by AIMS analysis Software (AIMSGRAD)	<ul style="list-style-type: none"> • Capable of separating aggregates with different angularity characteristics. • Capable of separating angularity from form. • Most unique among angularity parameters.
Radius Angularity Index	Used by AIMS analysis Software (AIMSRAD)	<ul style="list-style-type: none"> • Captures angularity but it is not capable of separating 2-D form from angularity.
2-D Form Index	Used by AIMS analysis Software (AIMSFORM)	<ul style="list-style-type: none"> • Captures 2-D form but it is not capable of separating form from angularity.
Sphericity	Used by AIMS analysis Software (AIMSSPH)	<ul style="list-style-type: none"> • Capable of separating aggregates with different form characteristics. • Captures unique characteristics of aggregates. • Most unique among the form parameters.

Table 4.19. Continued

Method	Description	Features
Texture Index (Fourier)	FRTXTR	<ul style="list-style-type: none"> • Does not separate angularity from form. • Clusters aggregates with distinct characteristics.
Angularity Index (Fourier)	FRANG	<ul style="list-style-type: none"> • Does not separate angularity from form. • Clusters aggregates with distinct characteristics.
Form Index (Fourier)	FRFORM	<ul style="list-style-type: none"> • Capable of separating form from angularity. • Clusters aggregates with distinct characteristics.
Flat & Elongated Ratio	Used By University Of Illinois System (UIFER)	<ul style="list-style-type: none"> • Capable of separating aggregates with different form characteristics. • Capable of separating form from angularity.
Angularity Using Outline Slope	Used By University Of Illinois System (UIAI)	<ul style="list-style-type: none"> • Capable of separating aggregates with different aggregate characteristics. • Capable of separating angularity from form.
Surface Texture Using Erosion-Dilation technique	Used By University Of Illinois System (UISTI)	<ul style="list-style-type: none"> • Clusters aggregates similar to angularity analysis. • Capable of separating angularity from form.
Aspect Ratio	Used in Image Pro Software (ASPTPRO)	<ul style="list-style-type: none"> • Separates angularity from form.
Fractal Dimension	Used in Image Pro Software (FRCTLPRO)	<ul style="list-style-type: none"> • Separates angularity from form. • Clusters aggregates with distinct characteristics.
Roundness	Used in Image Pro Software (ROUNDPRO)	<ul style="list-style-type: none"> • Separates angularity from form. • Clusters aggregates with distinct characteristics.

Accuracy of Test Methods

A digital caliper was used to measure the three dimensions of 100 particles selected randomly from each of the aggregates. Particle sizes passing a 12.5 mm (1/2 inch) sieve and retained on a 9.5 mm (3/8 inch) sieve. The measurements were used to calculate the percentage of particles with a ratio of longest dimension to shortest dimension of 3 : 1, and to calculate sphericity as defined in Eq. (2.1). The results of the digital caliper are shown in Table 4.20. The correlations between the caliper measurements and results of test methods in terms of R^2 are shown in Figs. 4.3 and 4.4. R^2 is the square of the multiple correlation coefficient and the coefficient of multiple determination. It is a statistic that measures how successful the fit is in explaining the variation of the data. It can take on any value between 0 and 1, with a value closer to 1 indicating a better fit. R^2 is defined as the ratio of the sum of squares of the regression (SSR) and the total sum of squares (also known as sum of squares about the mean) (SST). R^2 (coefficient of multiple determinations) is expressed as

$$R^2 = \frac{SSR}{SST} = \frac{\sum_{i=1}^n (\hat{y}_i - \bar{y})^2}{\sum_{i=1}^n (y_i - \bar{y})^2} \quad (4.10)$$

Fig. 4.3 shows that the Multiple Ratio Shape Analysis (MRA) method had the best correlation with the digital caliper. However, considering the irregular shape of the particles and the different methods that can be employed to identify the longest and shortest dimensions, all methods except the WipShape and the flat and elongation caliper tend to give reasonable correlations. The asterisk (*) indicates that not all aggregates were measured using this method. The sphericity measured using the digital caliper had very good agreement with AIMS and PSSDA-Large measurements as shown in Fig. 4.3. Fig. 4.4 shows a comparison between AIMS measurements and digital caliper measurements for sphericity.

Table 4.20. Digital Caliper Results

Aggregate	Average Sphericity	3:1 & Higher (%)
CA-1	0.717	8
CA-2	0.740	2
CA-3	0.675	18
CA-4	0.662	30
CA-5	0.731	2
CA-6	0.711	6
CA-7	0.624	42
CA-8	0.706	6
CA-9	0.643	38
CA-10	0.697	18
CA-11	0.659	22
CA-12	0.666	18
CA-13	0.638	38

Note: CA= coarse aggregate.

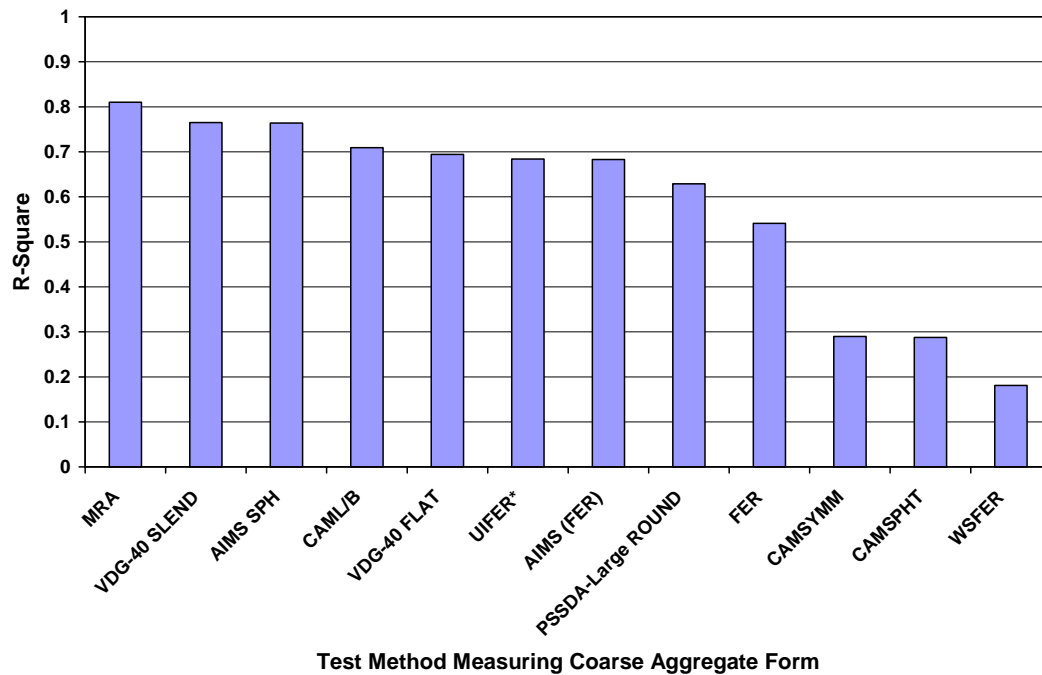


Fig. 4.3. Correlations of Test Methods with the Digital Caliper Results for Coarse Aggregates Form (* : Not all aggregates were measured using this method)

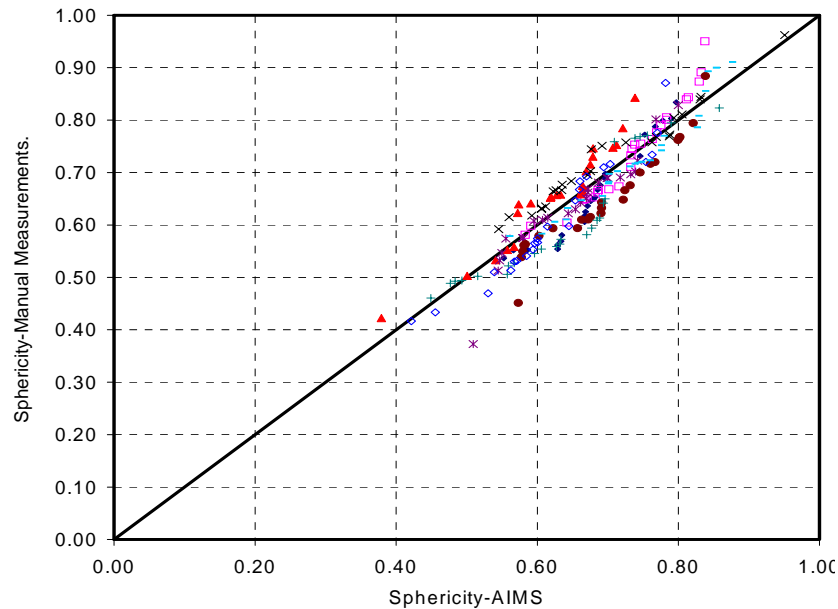


Fig. 4.4. Comparison between Sphericity Measurements of AIMS and the Digital Caliper

Measurements of angularity and texture of coarse aggregates were compared with visual rankings of aggregates by five experienced individuals with backgrounds in asphalt pavements, concrete pavements, geology, and petrographic analysis. These individuals were provided with a form to fill with the rankings. R^2 values between the experienced individuals for texture and angularity rankings are shown in Table 4.21.

The rankings of the “experienced individuals” are more correlated for texture than for angularity. The high correlation between the visual rankings warrants comparing the average of the texture rankings with the experimental measurements. However, this is not the case for the angularity rankings, as the low correlation prevents establishing reliable correlations with the experimental measurements. A follow-up discussion with the experienced individuals revealed that the main difficulty is in visually separating angularity from texture. However, they indicated that it is easier to rank aggregates based on surface irregularity that combined both angularity and texture.

Therefore, it was decided for this study to establish a visual ranking of surface irregularity. The correlation between rankings of surface irregularity is shown in Table 4.21.

Table 4.21. Coefficient of Multiple Determination (R^2) between the Rankings of Experienced Individuals for Angularity, Texture, and Surface Irregularities

Angularity	Evaluator	I	II	III	IV	V
	I	1	0.57	0.58	0.37	0.3
	II		1	0.9	0.41	0.57
	III			1	0.41	0.46
	IV				1	0.41
	V					1
Texture	Evaluator	I	II	III	IV	V
	I	1	0.91	0.92	0.89	0.82
	II		1	0.95	0.79	0.84
	III			1	0.84	0.82
	IV				1	0.74
	V					1
Surface Irregularity	Evaluator	I	II	III	IV	V
	I	1	0.77	0.80	0.76	0.59
	II		1	0.95	0.69	0.79
	III			1	0.70	0.72
	IV				1	0.71
	V					1

The experimental measurements were compared to the visual rankings of surface irregularity and texture. The comparison with surface irregularity is useful since the evaluated tests themselves do not use the same methods to analyze angularity and

texture. In fact, the definition of angularity in a certain test method can be similar to the definition of texture in another test method. Very good correlation was found between the “experienced individuals” in ranking aggregates based on surface irregularity. The average rankings are shown in Table 4.22. Similarly, experts were asked to rank fine aggregate angularity by examining their shape under a microscope. The visual ranking of fine aggregates is shown in Table 4.23.

Table 4.22. Average Visual Rankings of Coarse Aggregates by Experienced Individuals

Aggregate	Texture	Surface Irregularity
CA-1	1.6	1.8
CA-2	4.4	4.2
CA-3	6.8	8.6
CA-4	7.4	8.1
CA-5	12.8	9.8
CA-6	5.2	5.8
CA-7	5.8	6.0
CA-8	1.4	1.2
CA-9	11.4	9.9
CA-10	11.6	10.4
CA-11	9.0	10.3
CA-12	3.6	4.2
CA-13	10.0	10.7

Note: 1- CA= coarse aggregate; 2- Higher rank is associated with higher angularity and/or texture.

Table 4.23. Visual Ranking of Fine Aggregate Angularity by Experienced Individuals

Aggregate	Visual Ranking
FA-1	2
FA-2	4
FA-5	5
FA-6	1
FA-9	3

Note: 1- FA= fine aggregate; 2- Higher rank is associated with higher angularity.

The correlation between the measurements (texture and surface irregularities for coarse aggregate, and angularity for fine aggregates) and the corresponding visual ranking are used to rank the test methods. Figs. 4.5 through 4.7 show these correlations. It is important to emphasize that the correlations were calculated between visual rankings of aggregates and the corresponding average measurements of each test method for each shape property. As discussed in Chapter VII, expressing an aggregate shape based on average only can be misleading due to the high variability in shape within an aggregate sample. However, this is the only available method to get an idea about the ability of these methods to rank aggregates in a reasonable way, or at least identify those methods that are not able to rank aggregates appropriately.

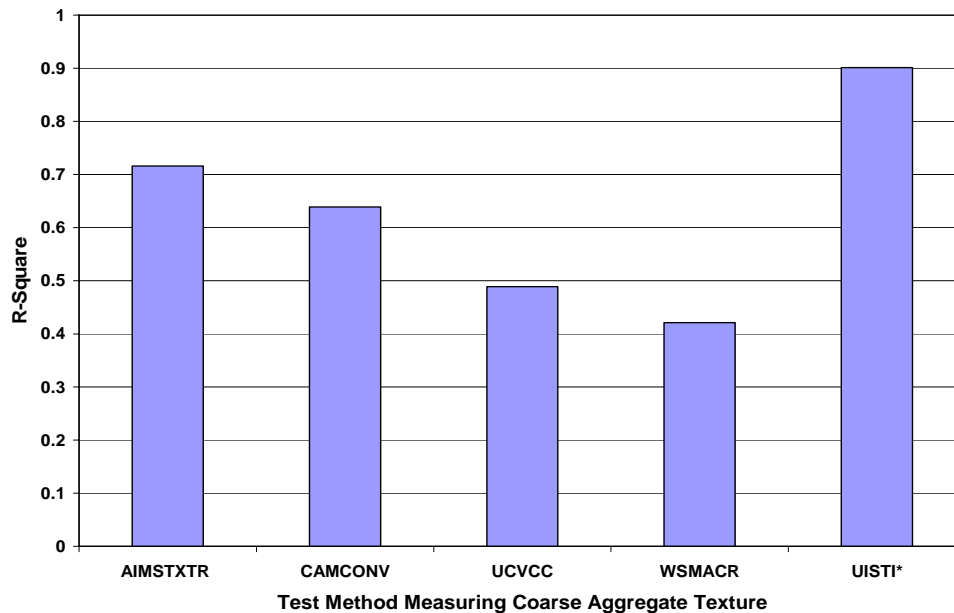


Fig. 4.5. Correlations of Test Methods with Visual Rankings for Coarse Aggregates Texture (* : Not all aggregates were measured using this method)

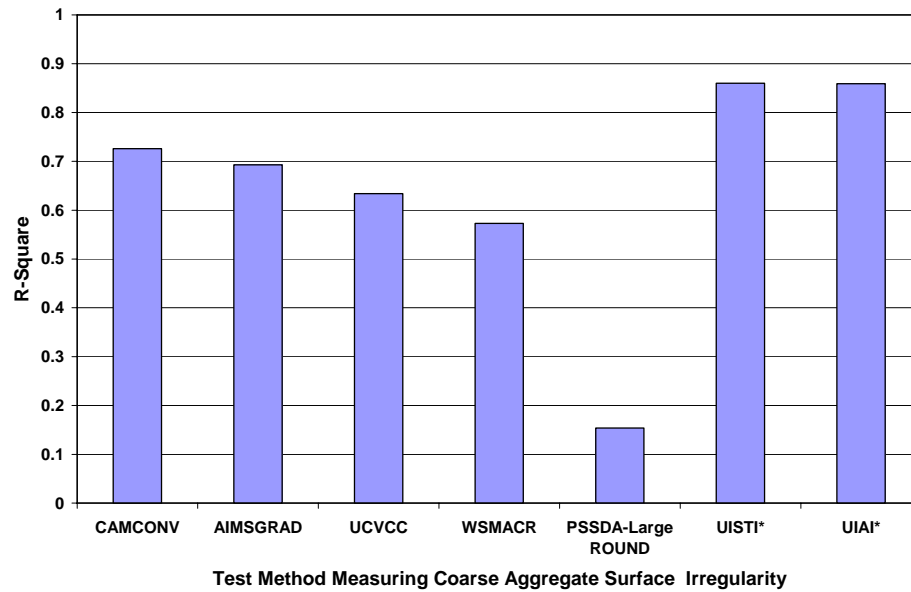


Fig. 4.6. Correlations of Test Methods with Visual Rankings for Coarse Aggregates Surface Irregularity (* : Not all aggregates were measured using this method)

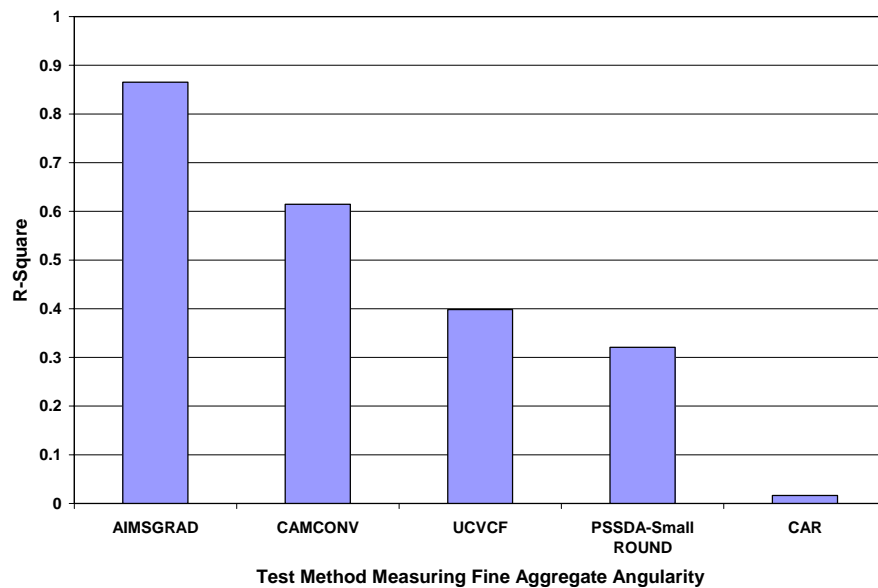


Fig. 4.7. Correlations of Test Methods with Visual Rankings of Fine Aggregate Angularity

Figs. 4.5 through 4.7 clearly show that AIMS is one of the most accurate testing methods available. AIMS is the only test method that is able to operate on all aggregate sizes investigated in this study. AIMS measurements had very good correlation with the rankings of texture and surface irregularity of coarse aggregates, and angularity of fine aggregates.

COST AND OPERATIONAL CHARACTERISTICS OF TEST METHODS

Information about cost and operational characteristics was collected using a survey of vendors, researchers, and operators who have dealt with these systems. The survey aimed at collecting information involving cost, ease of use, portability, ability of interpreting data, readiness for implementation in central laboratories as well as field laboratories, and applicability of test method to measure different aggregate types and sizes. Tables 4.24 through 4.27 show the extracted information from the conducted survey. This information is used in Chapter V in the ranking of test methods.

Table 4.24. Cost and Readiness for Implementation of Test Methods

Test Method	Estimated Price (\$)	Scale of Readiness for Implementation
Uncompacted Void Content of Fine Aggregates AASHTO T304	250	1
Uncompacted Void Content of Coarse Aggregates AASHTO TP56	500	1
Compacted Aggregate Resistance (CAR)	500	1
Percentage of Fractured Particles in Coarse Aggregate ASTM D5821	0	1
Flat and Elongated Coarse Aggregates ASTM D4791	250	1
Multiple Ratio Shape Analysis	1,500	2
VDG-40 Videograder	40,000 - 50,000	2
Buffalo Wire Works PSSDA -Large	30,000 - 40,000	3
Buffalo Wire Works PSSDA -Small	30,000 - 40,000	2
Camsizer	40,000 - 50,000	2
WipShape	30,000 - 40,000	2
University of Illinois Aggregate Image Analyzer (UIAIA)	30,000 - 40,000	3
Aggregate Imaging System (AIMS)	30,000 - 40,000	2

1: Available commercially. Wide use in laboratories.

2: Available commercially. Limited use in laboratories.

3: Not available commercially. Limited use in research laboratories. Can be made available commercially.

Table 4.25. Ease of Use and Data Interpretation of Test Methods

Test Method	Ability to Interpret Data	Ease of Use by Technician
Uncompacted Void Content of Fine Aggregates AASHTO T304	1	1
Uncompacted Void Content of Coarse Aggregates AASHTO TP56	1	1
Compacted Aggregate Resistance (CAR)	1	1
Percentage of Fractured Particles in Coarse Aggregate ASTM D5821	1	1
Flat and Elongated Coarse Aggregates ASTM D4791	1	1
Multiple Ratio Shape Analysis	2	2
VDG-40 Videograder	3	2
Buffalo Wire Works PSSDA-Large	3	3
Buffalo Wire Works PSSDA-Small	3	2
Camsizer	3	2
WipShape	3	3
University of Illinois Aggregate Image Analyzer (UIAIA)	3	3
Aggregate Imaging System (AIMS)	3	3

1: Very Easy

2: Easy

3: Intermediate

4: Difficult

Table 4.26. Portability of Test Methods

Test Method	Portability Scale
Uncompacted Void Content of Fine Aggregates AASHTO T304	1
Uncompacted Void Content of Coarse Aggregates AASHTO TP56	1
Compacted Aggregate Resistance (CAR)	1
Percentage of Fractured Particles in Coarse Aggregate ASTM D5821	1 (NA)
Flat and Elongated Coarse Aggregates ASTM D4791	1
Multiple Ratio Shape Analysis	1
VDG-40 Videograder	2
Buffalo Wire Works PSSDA-Large	3
Buffalo Wire Works PSSDA-Small	2
Camsizer	2
WipShape	2
University of Illinois Aggregate Image Analyzer (UIAIA)	3
Aggregate Imaging System (AIMS)	2

1: Can be used in central and field laboratories. Require less than 1 hr to move it.

2: Can be used in central and field laboratories. Require less than 1-4 hrs to move it.

3: Not portable or require more than 8 hours to move it. Can become portable

Table 4.27. Applicability of Test Methods to Measure Different Aggregate Types and Sizes

Test Method	Applicability Scale
Uncompacted Void Content of Fine Aggregates AASHTO T304	1
Uncompacted Void Content of Coarse Aggregates AASHTO TP56	1
Compacted Aggregate Resistance (CAR)	1
Percentage of Fractured Particles in Coarse Aggregate ASTM D5821	1
Flat and Elongated Coarse Aggregates ASTM D4791	1
Multiple Ratio Shape Analysis	1
VDG-40 Videograder	1
Buffalo Wire Works PSSDA-Large	1
Buffalo Wire Works PSSDA-Small	1
Camsizer	1 / 2*
WipShape	1
University of Illinois Aggregate Image Analyzer (UIAIA)	3
Aggregate Imaging System (AIMS)	1

1: Measure all aggregate sizes and Types.

2: Measure all aggregate types but not all sizes

3: Measure all sizes but not all aggregate types

* Use value of (1) if used in fine aggregates and value of (2) if used in coarse aggregates.

SUMMARY

This chapter documents the experimental evaluation of the characteristics of the available methods to measure aggregate shape properties. In this chapter, the second objective of this study was achieved by evaluating the improved version of AIMS along with other test methods used for measuring aggregate shape properties. The evaluation was conducted based on accuracy, repeatability, reproducibility, cost, ease of use, ease of interpretation of the results, readiness of the test for implementation, and portability. Thirteen different coarse aggregate types and five different fine aggregate types were used in this evaluation.

Analyses of repeatability and reproducibility results were conducted under the

guidelines of ASTM standards E177, C802 and C670. Accuracy of the analysis methods used in the imaging systems was assessed by analyzing some particle projections that have been used by geologists for visual evaluation of particles' shape. Also, all analysis methods were used to analyze images of aggregate particles in order to identify the ability of these methods to accurately rank aggregates and capture unique characteristics of aggregates. The analysis results revealed that some of the available analysis methods are influenced by both angularity and form changes and, consequently, are not suitable to distinguish between these two characteristics. Also, some of the analysis methods are not capable of distinguishing between changes in texture and angularity. The following analysis methods are recommended:

- Texture: Wavelet analysis of gray images of particle surface (implemented in AIMS software),
- Angularity: The gradient method (implemented in AIMS software) and the changes in the slope of a particle outline.
- Two-dimensional form: Aspect ratio.
- Three-dimensional form: Sphericity or the proportions of the three particle dimensions.

Accuracy of test methods was assessed through statistical analysis of the correlations between the results from test methods with measurements of form using a digital caliper and visual rankings of surface irregularity and texture by experienced individuals. AIMS results were ranked at or very close to the top for all shape characteristics.

Information about cost and operational characteristics were collected using a survey of vendors, researchers, and operators who have dealt with these systems.

CHAPTER V
RANKING OF TEST METHODS USING THE ANALYTICAL HIERARCHY
PROCESS (AHP)

INTRODUCTION

It has already been established in previous chapters that AIMS is the only comprehensive test that applies for coarse and fine aggregates, and it can measure the relevant shape characteristics (see Chapter IV). However, it is of interest to compare AIMS to the test methods evaluated in Chapter IV of this study based on certain shape characteristics and aggregate size fractions. In order to do so, a consistent and powerful methodology is needed to rank the test methods according to their repeatability, reproducibility, accuracy, cost, and operational characteristics. To this end, the Analytical Hierarchy Process (AHP) is presented as a mathematical tool to perform rankings of test methods. A brief description of AHP is provided in order to demonstrate its power and flexibility. A program was developed to expedite conducting the calculations involved in AHP. The program provides the decision maker with an enormous amount of flexibility to specify the objectives, ranking criteria, and relative importance or priorities of the different criteria elements. Examples of the rankings of test methods using the AHP are presented.

ANALYTICAL HIERARCHY PROCESS (AHP)

AHP was developed by Dr. Thomas Saaty in 1970s. AHP is a powerful and flexible decision making process that helps people set priorities and make preeminent choices. AHP provides a proven, effective means to deal with complex decision making by dropping these decisions to a series of one-on-one comparisons, then combining the results. In this way, AHP helps decision makers arrive at the best, most justified decision. AHP helps capture both subjective and objective evaluation measures such that the bias in decision making is reduced. AHP has been a well-regarded and widely used decision-making theory. It has been used in several applications that include the

selection of an approach based on defined criteria such as the selection of alternatives, investment distribution, and energy allocation (Saaty 1980).

The AHP method is based on decomposing the goal into its component parts, moving from the general to the specific (i.e., proceeding from the goal to objectives to sub-objectives down to the alternative courses of action). In its simplest form, AHP structure comprises a goal, criteria, and alternative levels. After structuring the hierarchy of all criteria, the next step is to assign a relative weight to each criterion. Weights are assigned based on a pairwise comparison judgment scale, also known as standard preference table, that a decision maker develops (takes values from 1-9). Then the decision maker calculates priorities, using a simple mathematical procedure, throughout the hierarchy to arrive at overall priorities for the alternatives. The sum of all the criteria beneath a given parent criterion in each level of the model must equal one. Each priority list shows its relative importance within the overall structure. From the overall priority list, the decision maker can choose among alternatives by selecting the highest priority alternative. The mathematical functions involved in AHP can be found in Saaty (1980).

AHP PROGRAM DESCRIPTION

A program was developed so that the calculation process conducted in AHP to obtain the overall ranking of test methods was easier and faster. The new program provides the decision maker with an enormous amount of flexibility to change his/her objectives or selection criteria weights before making the final selection from available multiple alternatives. The program was developed with the help of Ms. Aparna Kanungo from the Computer Science Department at Texas A&M University. The program was created using VC++ programming language. The program, when compiled, generates the executable that can be run on any computer irrespective of operating system.

The program uses the crude estimate, specified by Saaty (1980), to calculate the priority vector through the process of averaging over normalized columns technique. The elements of each column are divided by the sum of that column, and then the elements in each resulting row are added and divided by the sum of the numbers in that

row.

This program uses a graphical interface environment where the user is allowed to enter the number of testing methods being compared and the characteristics determining the performance of the test method (see Fig. 5.1(a)). Based on the numbers input by the user, generic text boxes are generated to allow the user to input the names of each of the characteristics and testing methods (see Fig. 5.1(b)). For demonstration purposes, the second example described in the preceding section (fine aggregate angularity) is used to describe the operation steps of the new program.

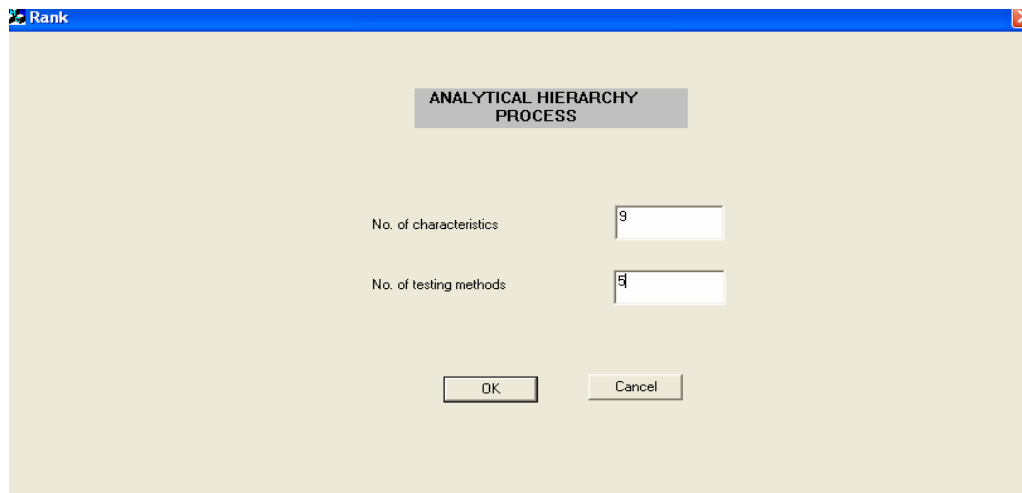
For each of the characteristics, the user is allowed to enter the weights assigned to test methods when pairwise comparison is conducted with respect to each characteristic, as shown in Fig. 5.2(a). Since the lower triangle of these matrices is the reciprocal of the upper triangle with ones along the diagonal, the user can input the upper half of the matrix and the other values are updated automatically. After the values for all weights of all methods in each characteristic have been entered, the user is prompted to enter the weights comparing the various characteristics with respect to overall satisfaction with a method in a new interface, which is shown in Fig. 5.2(b).

After entering all the weights for all methods and characteristics, the program calculates the priority vectors for each of the matrices and displays them in a new interface window, as shown in Fig. 5.3(a). Then the program calculates the overall ranking of the test methods by multiplying the priority matrix of the methods by the priority vector of the characteristics and displays it in a separate interface window, as shown in Fig. 5.3(b).

The program has extra features that enable user to:

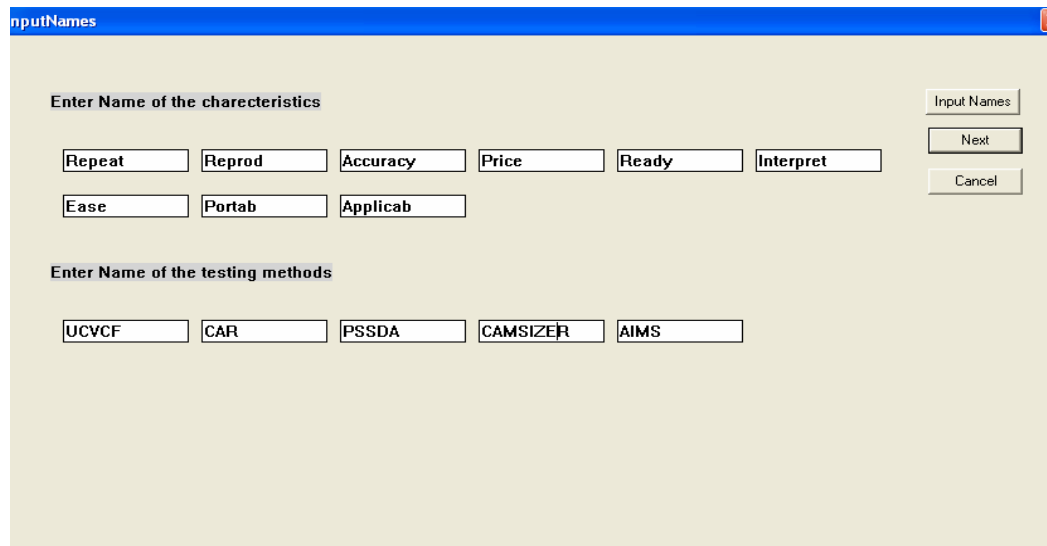
1. Extract the priority vectors and the overall ranking from a text file. The results for the vectors for characteristics and final priority vector are stored in the text file named FinalAnswer.txt on the C: drive.
2. If the user wants to examine the influence of changes in the weights or importance of one or more of the characteristics without changing the remaining ones (i.e., the software has to be executed several times with just one matrix

change), the program enables him/her to do so without a need to enter the unchanged matrices again.



The screenshot shows a window titled "Rank" with a blue header bar. The main content area is light beige and contains a grey box with the text "ANALYTICAL HIERARCHY PROCESS". Below this, there are two input fields: "No. of characteristics" with the value "9" and "No. of testing methods" with the value "5". At the bottom, there are two buttons: "OK" and "Cancel".

(a) Input of Number of Characteristics and Test Methods



The screenshot shows a window titled "InputNames" with a blue header bar. The main content area is light beige and contains two sections: "Enter Name of the characteristics" and "Enter Name of the testing methods". The "Enter Name of the characteristics" section has nine input fields containing the text: Repeat, Reprod, Accuracy, Price, Ready, Interpret, Ease, Portab, and Applicab. The "Enter Name of the testing methods" section has five input fields containing the text: UCVCF, CAR, PSSDA, CAMSIZER, and AIMS. On the right side, there are three buttons: "Input Names", "Next", and "Cancel".

(b) Input Names of Characteristics and Test Methods

Fig. 5.1. Program Graphical Interface to Enter Numbers and Names of Characteristics and Test Methods

Dialog

Enter Input and press Accept Input Button

After entering the value press Accept Input Button

Repeat

Click for Input Accept Input

Display Answer Skip

Cancel

	UCVCF	CAR	PSSDA	CAMSIZER	AIMS
UCVCF	1	1	3	1	1
CAR		1	3	1	1
PSSDA			1	0.33	0.33
CAMSIZER				1	1
AIMS					1

(a) Input Weights Comparing Test Methods to Characteristics

Dialog

Enter Input and press Accept Input Button

After entering the value press Accept Input Button

Weight Matrix for characteristics

Click for Input Accept Input

Display Answer Skip

Cancel

	Repeat	Reprod	Accuracy	Price	Ready	Interpret	Ease	Portab	Applica
Repeat	1		0.2	1	1	1	1	1	1
Reprod		1	0.2	1	1	1	1	1	1
Accuracy			1	5	5	5	5	5	5
Price				1	1	1	1	1	1
Ready					1	1	1	1	1
Interpret						1	1	1	1
Ease							1	1	1
Portab								1	1
Applicab									1

(b) Input Weights Comparing Characteristics

Fig. 5.2. Program Graphical Interface to Enter Weights Comparing Test Methods to Characteristics, and Characteristics with Respect to Overall Satisfaction with Method

	Repeat	Reprod	Accuracy	Price	Ready	Interpret	Ease	Portab	Applicab
UCVCF	0.23	0.23	0.05	0.44	0.33	0.38	0.34	0.33	0.20
CAR	0.23	0.23	0.05	0.40	0.33	0.38	0.34	0.33	0.20
PSSDA	0.07	0.07	0.05	0.05	0.11	0.07	0.12	0.11	0.20
CAMSIZER	0.23	0.23	0.30	0.04	0.11	0.07	0.12	0.11	0.20
AIMS	0.23	0.23	0.54	0.05	0.11	0.07	0.05	0.11	0.20

Priority Vectors of characteristics :

Repeat	0.07
Reprod	0.07
Accuracy	0.38
Price	0.07
Ready	0.07
Interpret	0.07
Ease	0.07
Portab	0.07
Applicab	0.07

(a) Priority Vectors

Final Priority Vector:	
UCVCF	0.21
CAR	0.20
PSSDA	0.08
CAMSIZER	0.20
AIMS	0.29

(b) Overall Ranking

Fig. 5.3. Resulting Priority Vectors and Overall Ranking of Test Methods

While entering the matrix weights, there is a button marked “Skip.” Clicking this button before entering values will cause the program retain the same values as

those in the previous run. For this, the program maintains the values in the immediate previous run in two files called “testread.txt” and “testwrite.txt” on the C: drive.

AHP RANKING OF TEST METHODS

The ranking of test methods depends significantly on the desired outcomes from the test as specified by the user. This section provides an example of how the AHP can be used to determine the ranking of AIMS relative to the other test methods for certain applications such as measuring fine aggregate angularity, and texture and form of coarse aggregates.

The simplest form of AHP structure (i.e., goal, criteria, and alternative levels) is selected in this example. The first level is the overall objective, which is the satisfaction with test methods. The second level consists of the characteristics or criteria elements based on which this satisfaction is measured. These characteristics are repeatability, reproducibility, accuracy, price, readiness for implementation, ability to interpret data and results, ease of use by technician, portability, and applicability to measure different aggregate types and sizes. These criteria are considered to be the most fundamental factors affecting the selection of a test method. They determine the desired characteristics in any test method that meets the satisfaction. The third level of AHP consists of the test methods that are under evaluation using the characteristics in the second level. Fig. 5.4 shows a basic hierarchy for AHP that can be used in this study.

AHP achieves the ranking using pairwise comparisons of the characteristics (level 2) and the test methods (level 3). The first pairwise comparison is conducted among the characteristics in the second level. This is illustrated in Table 5.1. The number in each cell of the table is a weight that reflects the relative importance of the characteristic in the horizontal list compared with the one in the vertical list. If this number is higher than one, it means that the characteristic listed in the row is more important than the characteristic listed in the column. In Table 5.1 accuracy is considered three times as important as repeatability and reproducibility and five times as

important as all the other characteristics. All the remaining characteristics are considered to be equal in their importance. The selection of weights should be based on consultation with researchers and experts in the pavement and aggregate field. The weights in Table 5.1 are assigned following the comparison scale shown in Table 5.2.

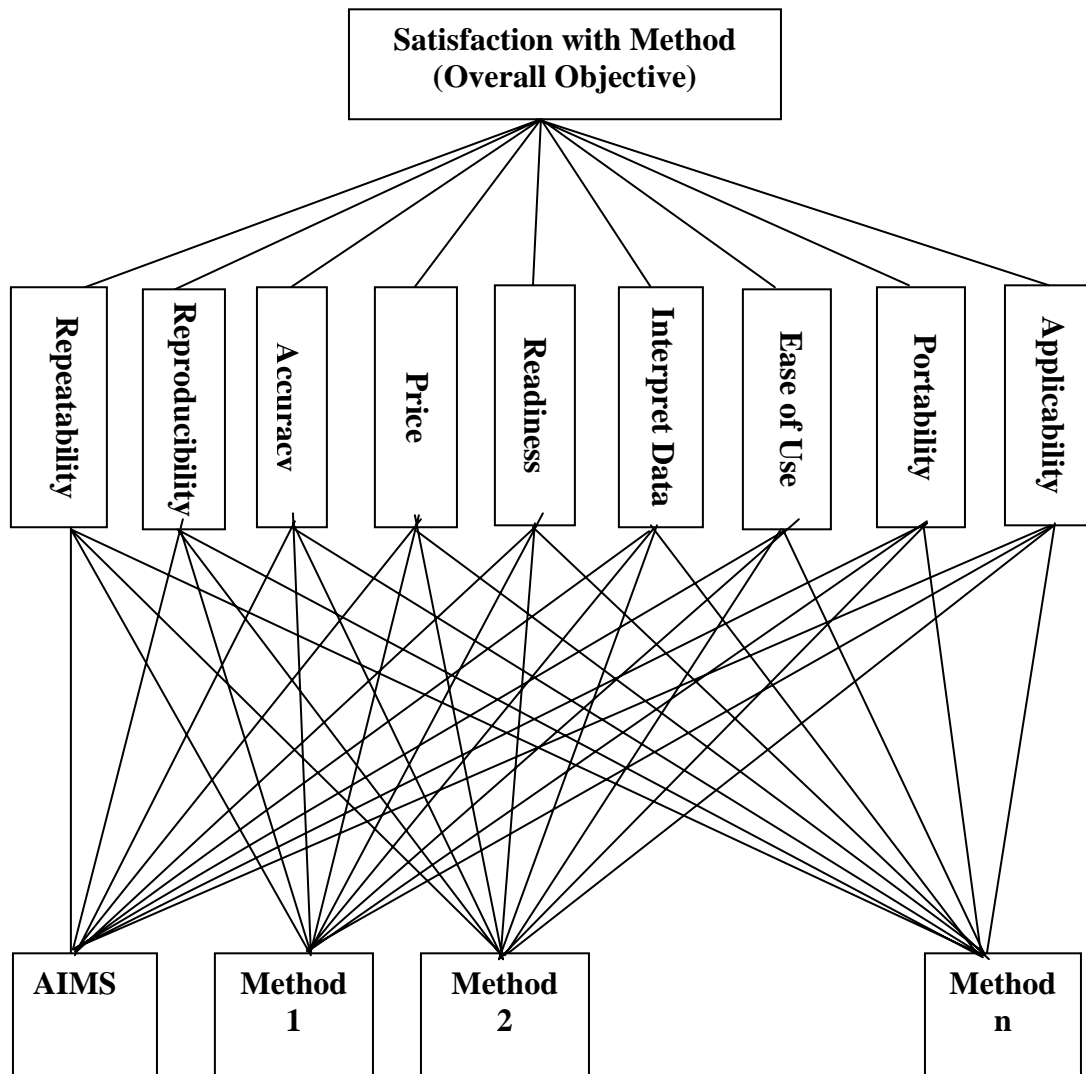


Fig. 5.4. Basic Hierarchy for Analytical Hierarchy Process (AHP) Used in Presented Example

Table 5.1. Example of the Relative Importance of the Characteristic Based on Overall Satisfaction with Method

Characteristics of Test Methods	Repeatability	Reproducibility	Accuracy	Price	Readiness	Interpret Data	Ease of Use	Portability	Applicability
Repeatability	1	1	0.33	1	1	1	1	1	1
Reproducibility	1	1	0.33	1	1	1	1	1	1
Accuracy	3	3	1	5	5	5	5	5	5
Cost	1	1	0.2	1	1	1	1	1	1
Readiness	1	1	0.2	1	1	1	1	1	1
Interpret Data	1	1	0.2	1	1	1	1	1	1
Ease of Use	1	1	0.2	1	1	1	1	1	1
Portability	1	1	0.2	1	1	1	1	1	1
Applicability	1	1	0.2	1	1	1	1	1	1

Table 5.2. AHP Comparison Scale

Verbal Judgment of Preference	Numerical Rating
Equally Important or Preferred	1
Weakly More Important	3
Moderately More Important	5
Strongly More Important	7
Absolutely More Important	9

Weights that compare test methods based on each of the characteristics in Table 5.1 should also be specified. This is accomplished here based on the measurements and data collected and presented in Chapter IV. The weights that compare test methods based on each of the characteristics shown in Table 5.3. The selection of the comparison scale values in Table 5.3 above can be rationalized based on the importance of each of the test characteristics. For example, the values in Table 5.3 can be supported by the following discussion on each of the characteristics:

Table 5.3. Weights that Compare Test Methods Based on Each of the Characteristics

Criterion	Comparison Scale					Table or Figure Where Data is Available
	1	3	5	7	9	
Repeatability/ Reproducibility	1	3	5	7	9	Table 4.10 & Table 4.11
2:1		X				
3:2			X			
3:1					X	
Accuracy Coarse- Form (Ratio of R ² groups)	1	3	5	7	9	Fig. 4.3
2:1		X				
3:1			X			
3:2		X				
4:1					X	
4:2				X		
4:3		X				
Accuracy Coarse- Irregularity (Ratio of R ² groups)	1	3	5	7	9	Fig. 4.6
2:1		X				
3:1			X			
3:2		X				
4:1					X	
4:2				X		
4:3		X				
Accuracy Coarse- Texture (Ratio of R ² groups) Rankings)	1	3	5	7	9	Fig. 4.5
2:1		X				
3:1			X			
3:2		X				
4:1					X	
4:2				X		
4:3		X				
Accuracy Fine- Angular (Ratio of R ² groups)	1	3	5	7	9	Fig. 4.7
2:1		X				
3:1			X			
3:2		X				
4:1					X	
4:2				X		
4:3		X				

Table 5.3. Continued

Criterion	Comparison Scale					Table or Figure Where Data is Available
Cost (Ratio of Cost)	1	3	5	7	9	Table 4.24
<6	X					
>6		X				
<20						
>20			X			
<50						
>50				X		
<80						
>80					X	
Readiness	1	3	5	7	9	Table 4.24
2:1		X				
3:2		X				
3:1			X			
Portability	1	3	5	7	9	Table 4.26
2:1		X				
3:2		X				
3:1			X			
Data Interpretation	1	3	5	7	9	Table 4.25
2:1		X				
3:2		X				
3:1			X			
4:3				X		
4:2					X	
Ease of Use	1	3	5	7	9	Table 4.25
2:1		X				
3:2		X				
3:1			X			
4:3				X		
4:2					X	
Applicability	1	3	5	7	9	Table 4.27
2:1		X				
3:2		X				
3:1			X			

- Repeatability/Reproducibility: As discussed in Chapter IV, repeatability and reproducibility are categorized into three main categories as levels 1, 2, and 3. Levels 1 and 2 can be considered as acceptable scales and some of the test methods can move from level 2 to 1 with some improvements. However, level 3 is

unacceptable since it covers high ranges of coefficient of variations for repeatability and reproducibility. Therefore, the scales are given such that the difference between levels 3 and 2 is less desirable than the difference between levels 1 and 2.

- Accuracy: As indicated earlier, accuracy of test methods was assessed by finding the correlation between the test method and a reference method. In order to assign a scale for accuracy, the R^2 values were divided into four categories as shown in Table 5.4. The ratio between the numbers assigned to each accuracy group is then used to assign the accuracy scale.

Table 5.4. Accuracy Categories Based on R^2 values

R^2	Category
> 0.70	1
0.6 - 0.7	2
0.5 - 0.6	3
< 0.5	4

- Cost: The cost scale is assigned taking into consideration that the lowest price of a test method is about \$250, while the highest price is around \$45,000. If \$250 is taken as the basis for the cost ratio, the following ranges are considered to have the same weight (\$250 - \$1,500, \$1,500 - \$7,500, \$7,500 - \$20,000, and \$20,000 - \$45,000).
- Readiness/Portability: The scale for readiness is assigned to emphasize the importance of recommending a test method that has been used already by research and testing laboratories. Methods that are not available commercially are considered slightly less desirable than those that are available. However, this point is not emphasized in the scale (the maximum possible ratio is only 5) since a method that is supported by state highway agencies can be made available commercially in the future. The same applies for portability, as the portability of those methods that are

given a scale of “3 Not portable or require more than 8 hours to move” (see Table 4.26) can be improved.

- **Interpretation of Data and Ease of Use:** It is essential for a method to be able be simple enough to be used in routine analysis of aggregates. The values assigned in Table 4.25 are based on current knowledge of the test methods. Unless it is labeled (4: difficult), technical training can improve the assigned value from (3: intermediate) to (2: easy) and even (1: very easy). Therefore, the change from 3 to 4 is considered less desirable than the change from 1 to 3.
- **Applicability to Measure Different Aggregate Types and Sizes:** It is essential that any test method be capable of measuring all aggregate types and sizes. If the method fails to measure some sizes or some aggregate types, or both, its applicability should be reduced. The values assigned for the applicability of test method to measure different aggregate types and sizes, as presented in Table 4.27, are based on current knowledge and experience with the test methods. The scale values are assigned assuming that it is weakly more important (assigned a value of 3) to have a method that can measure all aggregate types and sizes than a method that can measure all aggregate types but not all aggregate sizes. It is also considered weakly more important (assigned a value of 3) to have a method that can measure some aggregate sizes for all aggregate types than a method that can measure all sizes for some aggregate types. It is considered moderately more important (assigned a value of 5) to have a method that can measure all aggregate types and sizes than a method that can measure all aggregate sizes but not all aggregate types.

Fine Aggregate Angularity

AHP is used in this example to rank the test methods that measure fine aggregate angularity, which are listed in Tables 4.9 and 4.11. These methods are uncompact void content of fine aggregate (UCVCF); compacted aggregate resistance (CAR); Camsizer; Buffalo Wire Works (PSSDA-Small); and AIMS. The initial priority list is developed

with the same weights for all the characteristics in the second level (i.e., characteristics are equally important), as presented in Table 5.5.

Table 5.5. Comparison of the Characteristic Based on Overall Satisfaction with Method Assuming Characteristics Are Equally Important

Characteristics of Test Methods	Repeatability	Reproducibility	Accuracy	Price	Readiness	Interpret Data	Ease of Use	Portability	Applicability
Repeatability	1	1	1	1	1	1	1	1	1
Reproducibility	1	1	1	1	1	1	1	1	1
Accuracy	1	1	1	1	1	1	1	1	1
Cost	1	1	1	1	1	1	1	1	1
Readiness	1	1	1	1	1	1	1	1	1
Interpret Data	1	1	1	1	1	1	1	1	1
Ease of Use	1	1	1	1	1	1	1	1	1
Portability	1	1	1	1	1	1	1	1	1
Applicability	1	1	1	1	1	1	1	1	1

The second pairwise comparison is conducted on matrices of test methods. Each matrix includes a pairwise comparison of all test methods according to one characteristic from the upper level. Each cell in the matrix includes a number, selected from Table 5.3, which is originally based on Table 5.2. These numbers compare a test method from the horizontal list to that of the vertical list based on the characteristics under consideration. Table 5.6 shows the set of matrices in which pairwise comparison is performed between methods based on each of the characteristics in the second level.

Once the values in Tables 5.5 and 5.6 are assigned, the next step consists of the computation of priority lists from the matrices. From each of the 10 matrices listed in Tables 5.5 and 5.6, a priority list will be calculated. In mathematical terms, the principal eigen vector is computed for each matrix which gives the vector of priority ordering. Saaty (1980) proposed some crude estimates that can be easily followed to calculate

Table 5.6. Comparison of Test Methods Measuring Fine Aggregate Angularity with Respect to the Nine Characteristics

Characteristic		Test Method				
Repeatability		UCVCF	CAR	PSSDA-Small	Camsizer	AIMS
Test Method	UCVCF	1	1	3	1	1
	CAR	1	1	3	1	1
	PSSDA-Small	0.33	0.33	1	0.33	0.33
	Camsizer	1	1	3	1	1
	AIMS	1	1	3	1	1
Reproducibility		UCVCF	CAR	PSSDA-Small	Camsizer	AIMS
Test Method	UCVCF	1	1	3	1	1
	CAR	1	1	3	1	1
	PSSDA-Small	0.33	0.33	1	0.33	0.33
	Camsizer	1	1	3	1	1
	AIMS	1	1	3	1	1
Accuracy		UCVCF	CAR	PSSDA-Small	Camsizer	AIMS
Test Method	UCVCF	1	1	1	0.143	0.11
	CAR	1	1	1	0.143	0.11
	PSSDA-Small	1	1	1	0.143	0.11
	Camsizer	7	7	7	1	0.33
	AIMS	9	9	9	3	1
Price		UCVCF	CAR	PSSDA-Small	Camsizer	AIMS
Test Method	UCVCF	1	1	9	9	9
	CAR	1	1	7	9	7
	PSSDA-Small	0.11	0.14	1	1	1
	Camsizer	0.11	0.11	1	1	1
	AIMS	0.11	0.14	1	1	1
Readiness		UCVCF	CAR	PSSDA-Small	Camsizer	AIMS
Test Method	UCVCF	1	1	3	3	3
	CAR	1	1	3	3	3
	PSSDA-Small	0.33	0.33	1	1	1
	Camsizer	0.33	0.33		1	1
	AIMS	0.33	0.33	1	1	1
Interpretation of Data		UCVCF	CAR	PSSDA-Small	Camsizer	AIMS
Test Method	UCVCF	1	1	5	5	5
	CAR	1	1	5	5	5
	PSSDA-Small	0.20	0.20	1	1	1
	Camsizer	0.20	0.20	1	1	1
	AIMS	0.20	0.20	1	1	1

Table 5.6. Continued

Characteristic		Test Method				
Ease of Use		UCVCF	CAR	PSSDA-Small	Camsizer	AIMS
Test Method	UCVCF	1	1	3	3	5
	CAR	1	1	3	3	5
	PSSDA-Small	0.33	0.33	1	1	3
	Camsizer	0.33	0.33	1	1	3
	AIMS	0.20	0.20	0.33	0.33	1
Portability						
Portability		UCVCF	CAR	PSSDA-Small	Camsizer	AIMS
Test Method	UCVCF	1	1	3	3	3
	CAR	1	1	3	3	3
	PSSDA-Small	0.33	0.33	1	1	1
	Camsizer	0.33	0.33	1	1	1
	AIMS	0.33	0.33	1	1	1
Applicability						
Applicability		UCVCF	CAR	PSSDA-Small	Camsizer	AIMS
Test Method	UCVCF	1	1	1	1	1
	CAR	1	1	1	1	1
	PSSDA-Small	1	1	1	1	1
	Camsizer	1	1	1	1	1
	AIMS	1	1	1	1	1

these vectors. One good estimate method is to divide the elements of each column in the matrix by the sum of that column (i.e., normalize the column). Then elements in each resulting row are added then divided by the number of elements in the row. This is a process of averaging over the normalized column.

The resulting priority vectors from each matrix in Table 5.6 are then combined to create a matrix that represents priority of test method by each characteristic. In order to obtain the overall ranking of the test methods, the priority matrix of the methods by each characteristic will be multiplied by the priority vector of the characteristics resulting from Table 5.5. In other words, the overall ranking of a method can be obtained by multiplying the weight indicating the rank of a test method with respect to the characteristic by the weight of that characteristic then add them up for all characteristics. The resulting priority vectors and the overall ranking of test methods used to measure fine aggregate angularity are presented in Table 5.7.

The results of the above example show that when all characteristics are assumed to be equally important, the uncompact void content of fine aggregate (UCVCF) method was at the top of the priority list, mainly due to the low cost of this test. This priority list changes if the weights assigned to the characteristics or to the methods are changed. Consequently, one can examine the influence of favoring one characteristic on the overall rank of test methods.

Considering a more realistic example, where accuracy of test method is considered more favorable than all other characteristics, the only change made is the weight assigned to the accuracy, which is considered moderately more important than the other characteristics, and is thus assigned a value of 5 based on the scale provided in Table 5.2. The new matrix, where accuracy is 5 times the importance of other characteristics, along with the calculated priority vector is presented in Table 5.8. If the new characteristic's priority vector is multiplied by the matrix of priority vectors resulting from comparing method with respect to the characteristics (presented in Table 5.5), a new overall ranking of test methods will be obtained. Table 5.9 presents the overall ranking of test methods using different accuracy levels of preference.

It is apparent from Table 5.9 that when only accuracy is considered moderately favorable over the other characteristics the ranking of test methods have changed. AIMS, for example, is now ranked first in the priority ordering list using such a preference. Similarly, AIMS is also ranked first when accuracy is considered absolutely more important than the other characteristics (assigned a factor of 9) but with more significant difference between their values or numerical scores in the priority vector.

The results from the two examples suggest that when using AHP it is very important that the weights should be selected based on consultation with researchers and experts in order to truly find the best ranking that meets the objectives or the main goal of the whole process. The selected weights can have a significant influence on the overall ranking of test methods.

Table 5.7. Resulting Priority Vectors and Overall Ranking of Test Methods Measuring Fine Aggregate Angularity Assuming Characteristics Are Equally Important

Priority Vectors for Test Methods with Respect to Characteristics										Priority Vector of Characteristics with Respect to Overall Satisfaction with Method		Overall Ranking	Test Method		
	Repeatability	Reproducibility	Accuracy	Price	Readiness	Interpret Data	Ease of Use	Portability	Applicability						
UCVCF	0.231	0.231	0.051	0.444	0.333	0.385	0.342	0.333	0.20	X	0.111	Repeatability	=	0.283	UCVCF
CAR	0.231	0.231	0.051	0.402	0.333	0.385	0.342	0.333	0.20		0.111	Reproducibility		0.279	CAR
PSSDA-Small	0.077	0.077	0.051	0.052	0.111	0.077	0.130	0.111	0.20		0.111	Accuracy		0.098	PSSDA-Small
Camsizer	0.231	0.231	0.306	0.049	0.111	0.077	0.130	0.111	0.20		0.111	Cost		0.161	Camsizer
AIMS	0.231	0.231	0.540	0.052	0.111	0.077	0.056	0.111	0.20		0.111	Readiness		0.179	AIMS
											0.111	Interpret Data			
											0.111	Ease of Use			
											0.111	Portability			
											0.111	Applicability			

Table 5.8. Comparison of Characteristics with Respect to Overall Satisfaction with Method (Accuracy is Moderately More Important than Other Characteristics)

Characteristic	Repeatability	Reproducibility	Accuracy	Cost	Readiness	Interpret Data	Ease of Use	Portability	Applicability	Priority Vector
Repeatability	1	1	0.2	1	1	1	1	1	1	0.077
Reproducibility	1	1	0.2	1	1	1	1	1	1	0.077
Accuracy	5	5	1	5	5	5	5	5	5	0.385
Cost	1	1	0.2	1	1	1	1	1	1	0.077
Readiness	1	1	0.2	1	1	1	1	1	1	0.077
Interpret Data	1	1	0.2	1	1	1	1	1	1	0.077
Ease of Use	1	1	0.2	1	1	1	1	1	1	0.077
Portability	1	1	0.2	1	1	1	1	1	1	0.077
Applicability	1	1	0.2	1	1	1	1	1	1	0.077

Table 5.9. Overall Ranking of Test Methods Measuring Fine Aggregate Angularity Using Different Accuracy Levels of Preference

Test Method	Accuracy Level of Preference		
	1 = Equally Important	5 = Moderately Important	9 = Absolutely Important
UCVCF	0.28	0.21	0.17
CAR	0.28	0.21	0.17
PSSDA-Small	0.1	0.08	0.08
Camsizer	0.16	0.21	0.23
AIMS	0.18	0.29	0.35

Coarse Aggregate Texture

AHP is used in this example to rank the test methods that are used to measure coarse aggregate texture, which are listed in Tables 4.8 and 4.10. These methods are UCVCC; Camsizer, WipShape; UIAIA, and AIMS. In this example, accuracy is considered moderately more important than applicability of test method to measure all aggregate sizes and types (assigned a value of 5) and absolutely more important than all other remaining

characteristics (assigned a value of 9). At the same time applicability is considered moderately more important than other methods (assigned a value of 5). The priority list for all the characteristics in the second level based on this consideration and the resulting priority vector are presented in Table 5.10.

Table 5.10. Comparison of Characteristics with Respect to Overall Satisfaction with Method (Accuracy is Moderately More Important than Applicability and Absolutely More Important than Other Characteristics)

Characteristic	Repeatability	Reproducibility	Accuracy	Cost	Readiness	Interpret Data	Ease of Use	Portability	Applicability	Priority Vector
Repeatability	1	1	0.11	1	1	1	1	1	0.2	0.046
Reproducibility	1	1	0.11	1	1	1	1	1	0.2	0.046
Accuracy	9	9	1	9	9	9	9	9	5	0.465
Cost	1	1	0.11	1	1	1	1	1	0.2	0.046
Readiness	1	1	0.11	1	1	1	1	1	0.2	0.046
Interpret Data	1	1	0.11	1	1	1	1	1	0.2	0.046
Ease of Use	1	1	0.11	1	1	1	1	1	0.2	0.046
Portability	1	1	0.11	1	1	1	1	1	0.2	0.046
Applicability	5	5	0.2	5	5	5	5	5	1	0.211

Using the weights provided in Table 5.3, the second pairwise comparison is conducted on matrices of test methods. Each matrix includes a pairwise comparison of all test methods according to one characteristic from the upper level. As has been done in the previous examples, after the weights are assigned, the priority lists from the matrices of each characteristic are then computed. The resulting priority vectors for testing methods with respect to characteristics are presented in Table 5.11.

The overall ranking of test methods used to measure coarse aggregate angularity is presented in Table 5.12. It can be clearly seen that AIMS has the highest rank among

all other methods. As discussed earlier in Chapter IV, the wavelet method that AIMS uses in analyzing coarse aggregate texture was found to be unique and most accurate. This fact contributed significantly in ranking AIMS at the top of the priority list although some imaging methods have equal or even better characteristics than AIMS.

Table 5.11. Resulting Priority Vectors of Test Methods Measuring Coarse Aggregate Texture With Respect to Characteristics

Test Method	Priority Vectors for Test Methods with Respect to Characteristics								
	Repeatability	Reproducibility	Accuracy	Price	Readiness	Interpret Data	Ease of Use	Portability	Applicability
UCVCC	0.231	0.231	0.036	0.650	0.442	0.556	0.496	0.442	0.280
Camsizer	0.231	0.231	0.183	0.084	0.165	0.111	0.238	0.165	0.107
WipShape	0.231	0.231	0.036	0.088	0.165	0.111	0.089	0.165	0.281
UIAIA	0.231	0.231	0.372	0.088	0.063	0.111	0.089	0.063	0.051
AIMS	0.077	0.077	0.372	0.088	0.165	0.111	0.089	0.165	0.281

If it is assumed that the imaging methods, after being in practice for some time, may become more practical and easy to use, this will imply that only repeatability, reproducibility, accuracy, and applicability should be considered in comparing test methods. This criterion was applied to the example above, and the overall ranking of test methods measuring coarse aggregate texture is shown in Table 5.12. Again, AIMS shows on the top of the priority list, indicating that it would be the user first choice when measuring coarse aggregate texture.

The overall rankings of test methods presented in Table 5.12 show that UCVCC method has high priority when all characteristics are considered, but this method becomes less favorable when price becomes of less concern to the choice maker.

Table 5.12. Overall Ranking of Test Methods Measuring Coarse Aggregate Texture

Test Method	All Characteristics Considered	Only Repeatability, Reproducibility, Accuracy, and Applicability Considered
UCVCC	0.22	0.10
Camsizer	0.16	0.13
WipShape	0.13	0.10
UIAIA	0.22	0.21
AIMS	0.27	0.24

Coarse Aggregate Form

AHP is used in this example to rank test methods that measure coarse aggregate form (both form parameter and dimensional ratio), which are listed in Tables 4.8 and 4.10. These methods are FER, MRA; VDG-40 Videograder, Camsizer, WipShape, UIAIA, AIMS; and Buffalo Wire Works (PSSDA-Large). The same criterion that was used in the coarse aggregate texture example was also used here. Therefore, the priority list for all the characteristics in the second level and the resulting priority vector for this example will be the same as those presented in Table 5.10.

The second pairwise comparison is conducted on matrices of test methods measuring form of coarse aggregates. The resulting priority vectors for testing methods with respect to characteristics are presented in Table 5.13.

The overall ranking of test methods used to measure coarse aggregate form is presented in Table 5.14. It can be clearly seen that the MRA has the highest rank among all other methods. This method is very accurate, easy to use, and inexpensive, which allows it to be ranked high in the priority list. AIMS and the VDG-40 Videograder were ranked almost the same and came second in the priority list.

Table 5.13. Resulting Priority Vectors of Test Methods Measuring Coarse Aggregate Form with Respect to Characteristics

Test Method	Priority Vectors for Test Methods with Respect to Characteristics								
	Repeatability	Reproducibility	Accuracy	Price	Readiness	Interpret Data	Ease of Use	Portability	Applicability
FER	0.143	0.019	0.041	0.496	0.328	0.408	0.356	0.270	0.180
MRA	0.143	0.183	0.213	0.244	0.125	0.213	0.158	0.270	0.180
VDG-40	0.143	0.183	0.213	0.052	0.125	0.076	0.158	0.105	0.180
Camsizer	0.143	0.183	0.213	0.052	0.125	0.076	0.158	0.105	0.066
WipShape	0.143	0.066	0.019	0.052	0.125	0.076	0.057	0.105	0.180
UIAIA	0.143	0.183	0.088	0.052	0.046	0.076	0.057	0.041	0.034
AIMS	0.143	0.183	0.213	0.052	0.125	0.076	0.057	0.105	0.180
PSSDA-Large	0.143	0.183	0.088	0.052	0.046	0.076	0.057	0.041	0.180

If it is assumed that the imaging methods, after being in practice for some time may become more practical and easy to use, this will imply that only repeatability, reproducibility, accuracy, and applicability should be considered in comparing test methods. This criterion was applied to the example above, and the overall ranking of test methods measuring coarse aggregate form is shown in Table 5.14. Comparing the results in Table 5.14 shows that MRA, VDG-40 Videograder, and AIMS are on the top of the priority list with the same priority values. These results suggest that imaging systems will have a better chance to compete and get higher ranks, especially when price becomes of less concern.

The results from the above three examples suggest that for a choice maker who would consider accuracy and applicability to be more important than any other characteristics required in a test method, his first choice will be AIMS when measuring fine aggregate angularity and coarse aggregate texture. Competing with MRA, AIMS would be a first choice too, when measuring coarse aggregate form, especially when price becomes of less concern. In general, if a choice maker wants a system that can

measure all aggregate shape properties of coarse and fine aggregates of all aggregate types, AIMS will be the best method.

Table 5.14. Overall Ranking of Test Methods Measuring Coarse Aggregate Form

Test Method	All Characteristics Considered	Only, Repeatability, Reproducibility, Accuracy, and Applicability Considered
FER	0.15	0.06
MRA	0.20	0.15
VDG-40	0.18	0.15
Camsizer	0.15	0.13
WipShape	0.08	0.06
UIAIA	0.08	0.06
AIMS	0.17	0.15
PSSDA-Large	0.11	0.09

In summary, AHP can be used to examine the sensitivity of the priority list of test methods to judgment of the relative importance of certain characteristics (the values in Table 5.2) and the relative comparison of test methods for each characteristic (the values in Table 5.3). Also, AHP can be used to develop separate priority lists of tests for fine and coarse aggregates as well as for each of the aggregate characteristics (shape, angularity, and texture).

SUMMARY

The Analytical Hierarchy Process (AHP) was implemented in a program to rank the test methods. AHP is a process of developing a numerical score to rank test methods based on how each of these methods meets certain criteria of desirable characteristics. AHP requires the user to enter numeric values that indicate the relative importance of the different characteristics and numeric values that indicate how the methods compare against each other for each of the characteristics. The measurements of repeatability, reproducibility, and accuracy were used to obtain the input for the AHP. In addition,

information about cost and operational characteristics which was collected using a survey of vendors, researchers, and operators who have dealt with the test methods, was also used as input for the AHP.

AHP was found to be a powerful and flexible tool to rank test methods. It provides flexibility to examine the influence of changes in the importance of the characteristics on the ranking of test methods. It also provides a great deal of information on the relationship between test methods and desirable characteristics. The AHP rankings clearly demonstrated the advantage of AIMS over other test methods as a comprehensive methodology for measuring the shape characteristics of both coarse and fine aggregates.

CHAPTER VI

STATISTICALLY BASED METHODOLOGY FOR AGGREGATE SHAPE CLASSIFICATION

INTRODUCTION

As indicated in the previous chapters, aggregate shape characteristics have long been recognized to influence the structural performance of the pavement system in which they are used. Therefore, the design methodologies used in hot-mix asphalt (HMA), for example, have included tests and specifications to ensure the quality of aggregates used in asphalt pavements. In addition to structural performance, aggregate shape influences the functional properties of asphalt pavements such as pavement surface friction and skid resistance (Yandell 1970; Forster 1981).

The approach that has generally been followed to develop aggregate shape specifications relies almost entirely on the correlation between an indirect measure of aggregate shape and laboratory measurements of HMA physical and mechanical properties (Wedding and Gaynor 1961; Li and Kett 1967; Sanders and Dukatz 1992; Kandahal and Parker 1998; Chowdhury et al. 2001; Masad 2003). This approach tends to inherit the uncertainties of the laboratory methods used to measure performance. There is also the risk of emphasizing a certain material property while ignoring other equally or more important properties. The indirect methods that have been typically used in practice are limited in their ability to separate the fundamental characteristics of shape and their distinct influences on performance (Masad 2003). These limitations have led to discrepancies in the extent that different aspects of shape influence performance (Wedding and Gaynor 1961; Li and Kett 1967; Sanders and Dukatz 1992; Kandahal and Parker 1998; Chowdhury et al. 2001; Masad 2003). As a result, aggregate specifications could be biased toward overemphasizing the need for superior aggregate properties within the framework of certain mix design methodology, or, in contrast, allowing the use of marginal shape properties.

The benefits of developing accurate methods for measuring and classifying

aggregate shape characteristics will be realized in different areas of pavement engineering. In asphalt pavement engineering, for example, the relationships between aggregate shape characteristics, asphalt mix volumetrics, and performance will be better understood and utilized to develop asphalt mix design methodologies that accommodate a wide range of shape characteristics. The link between aggregate shape characteristics and asphalt pavement surface microtexture can be better developed and used to improve the skid resistance of asphalt pavement surfaces. Also, performance prediction models with high reliability can emerge, leading to the development of innovative contractual and construction practices.

A reliable methodology for the classification of aggregate shape should be established based on a number of key aspects. The first aspect is to use a test that is capable of separating the fundamental characteristics of shape (form, angularity, and texture) based on sound scientific methods. In this respect, imaging technologies have been proven to be successful in material characterization in various fields such as material science and geotechnical engineering (Kuo et al. 1996; Masad et al. 2001; Rao et al. 2001). The second aspect is to use aggregates from different sources and sizes that exhibit a wide range of shape characteristics in the development of such a methodology. The third aspect is to employ statistical analysis in identifying aggregate groups based on the distribution of these shape characteristics. Dealing with the distribution of aggregate characteristics rather than average indices is advantageous for the development of reliable specifications given the high variability in shape characteristics within an aggregate sample. Finally, laboratory performance tests and field test sections are needed to support these measurements and the classification of aggregates.

CLASSIFICATION SYSTEM FEATURES

A comprehensive methodology for classification of aggregates based on the distribution of their shape characteristics should exhibit the following features:

- It represents the three characteristics of aggregate shape (three dimensions of coarse aggregates, angularity, and texture), as measured using the recently developed AIMS.
- It unifies the methods used to measure the shape characteristics of fine and coarse aggregates.
- Similar to what is currently done for aggregate gradation; it represents each of the shape characteristics by a cumulative distribution function rather than an average value. Therefore, the methodology is capable of accommodating variations in shape within an aggregate sample and better represents the effects of different processes such as blending and crushing on aggregate shape.
- When developed, it considers statistical analysis of a wide range of aggregate types and sizes.
- It incorporates all the analysis methods and data visualizations in software to facilitate data interpretation and comparative analysis.

CLASSIFICATION SYSTEM DEVELOPMENT METHODOLOGY

This section presents the procedure that was followed to develop the new classification system for aggregate shape. The methodology is based on measuring the shape characteristics of aggregates from a wide range of sources and varying sizes using AIMS. These measurements were described in Chapter IV when AIMS was evaluated for its repeatability and reproducibility. As indicated earlier in Chapter IV, aggregates' form, angularity, and texture were measured using the analysis methods that are part of the AIMS software. These methods, which were discussed in Chapter II, are (1) sphericity as a 3-D measure of coarse aggregates; (2) form Index as a 2-D measure of fine aggregates; (3) gradient angularity for coarse and fine aggregates; and (4) Texture of coarse aggregates quantified by the wavelet method. The measurements were made on aggregates selected to cover a wide spectrum of rock type, shape characteristics, and sizes. These aggregates and their used sizes are listed in Table 4.3.

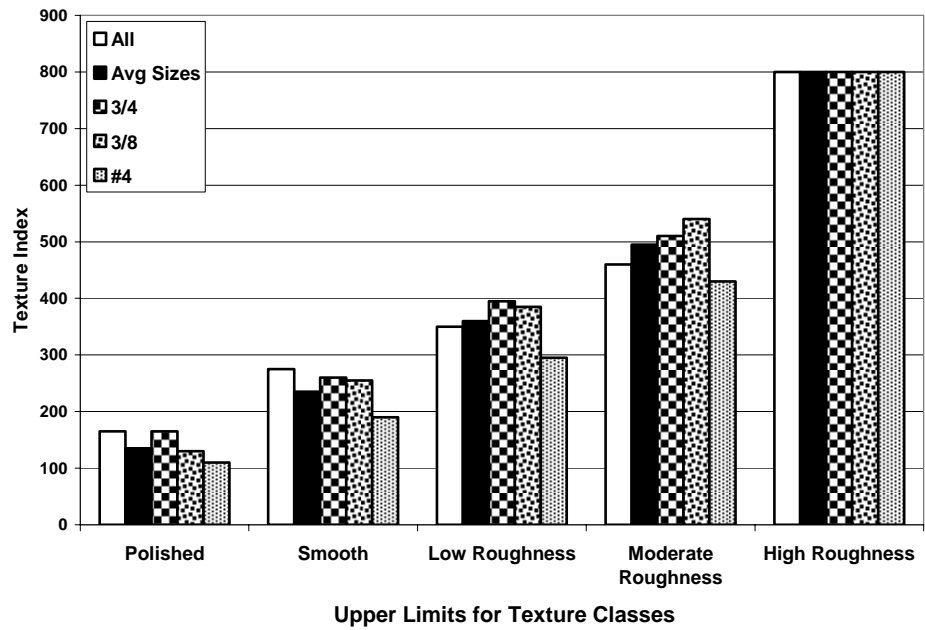
The analysis conducted in the evaluation of repeatability and reproducibility in

Chapter IV generated a total of 195 tests on coarse aggregates and 75 tests on fine aggregates. On average, a coarse aggregate test involved 56 particles while a fine aggregate test involved about 300 particles. All these data were used in the development of the new classification system. The use of different operators and repeated measurements ensures that the classification methodology is developed in such a way that variations in measurements among operators are accounted for in the classification methodology.

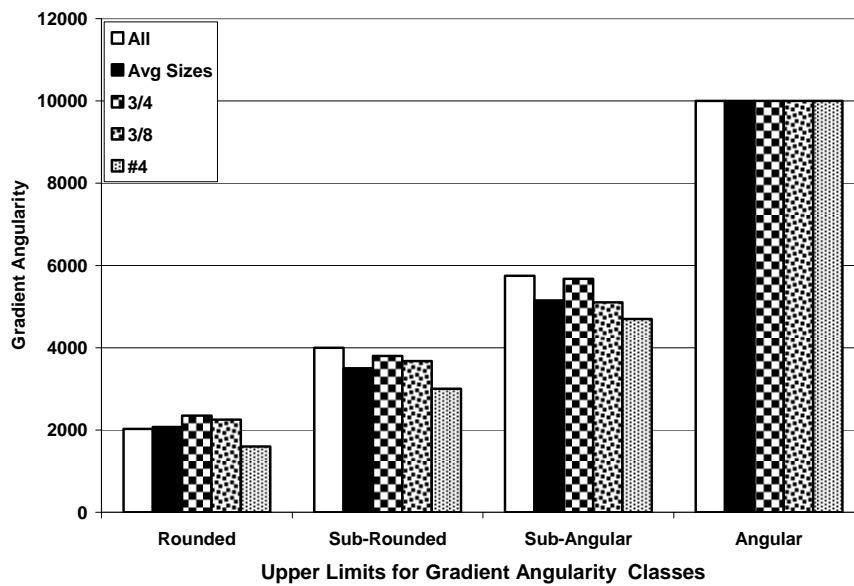
STATISTICAL-BASED AGGREGATE SHAPE CLASSIFICATION

Cluster analysis, discussed earlier in Chapter IV, was used to develop groups (or clusters) of aggregates based on the distribution of shape characteristics. In this study, we chose the usual metric of Euclidean distance (Eq. 4.9) and Ward's Linkage method. The clustering method was applied to the analysis results of each shape property obtained from AIMS.

Three methods for grouping the analysis results were performed with the objective of determining whether common group limits can be obtained for aggregates irrespective of their size. The first method was to find the group limits for each shape property based on measurements by all operators for each size separately. The second method was simply to determine the group limits by averaging those obtained for the three sizes. The third approach was to group the analysis results obtained for each shape property using data from all operators and for all sizes combined. Results of clustering using the three different approaches are shown in Fig. 6.1. Fig. 6.1a shows the groups' limits of the coarse aggregate texture for each size, the average for the limits of three sizes ("Avg. Sizes" label in Fig. 6.1a), and for all sizes combined ("All" label in Fig. 6.1a). The results clearly show that the groups' limits obtained using the three approaches were very close. The same conclusion was reached by examining the results in Figs. 6.1b, c, d, and e for the other shape characteristics. In other words, the groups' limits are similar for all sizes within the coarse and fine fractions.

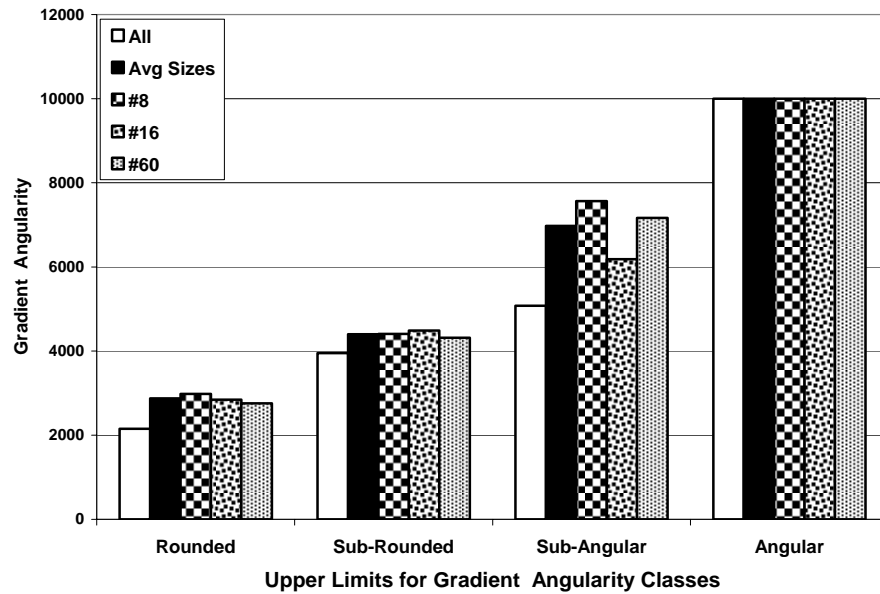


(a) Coarse Aggregates Texture

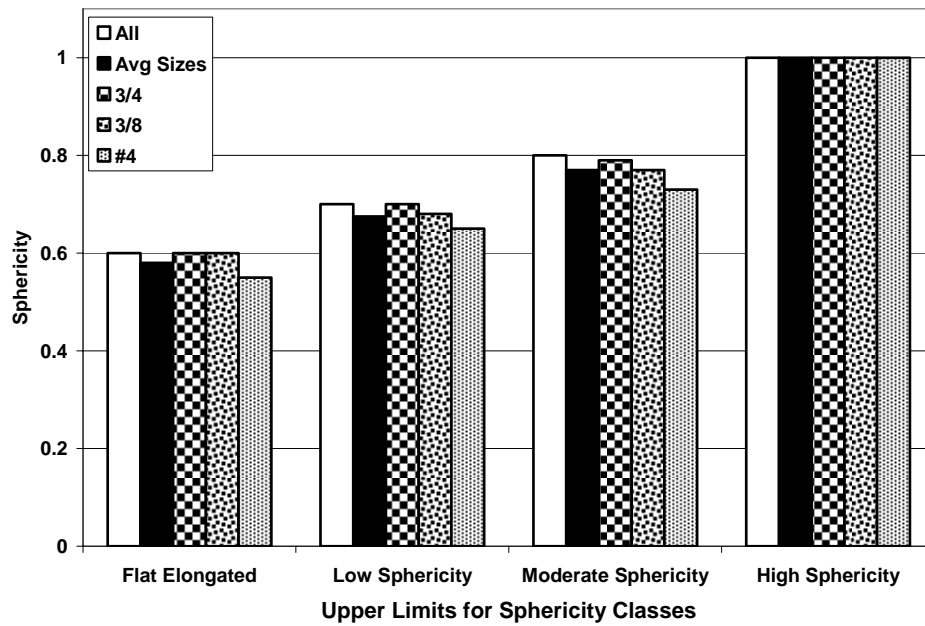


(b) Coarse Aggregates Angularity

Fig. 6.1. Shape Properties Groups for Individual and Combined Aggregates

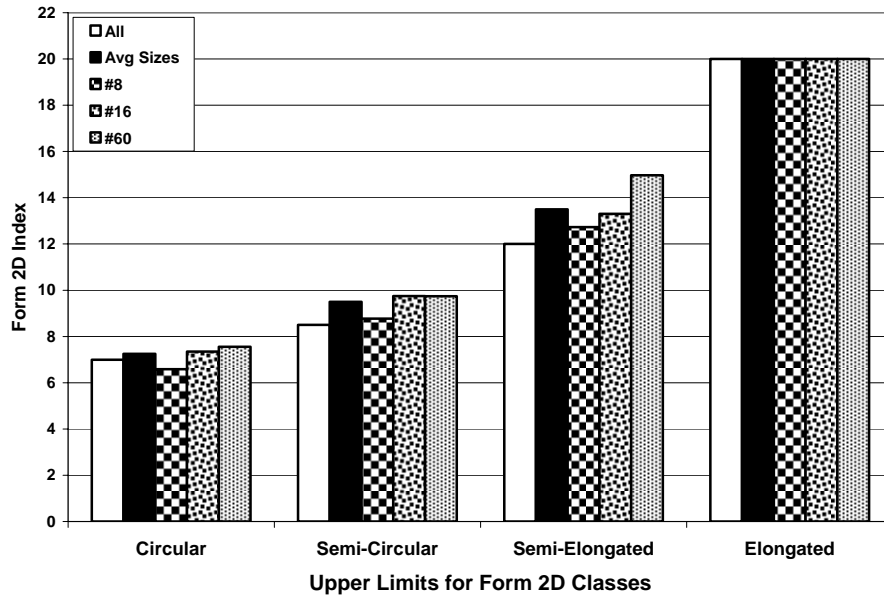


(c) Fine Aggregate Angularity

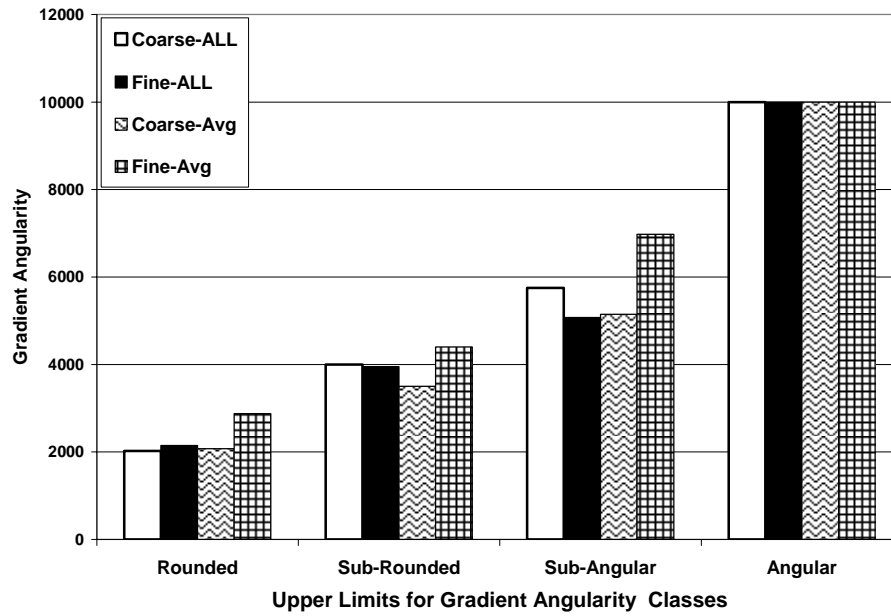


(d) Coarse Aggregates Form (Sphericity)

Fig. 6.1. Continued



(e) Fine Aggregates Form



(f) Coarse and Fine Aggregates Angularity

Fig. 6.1. Continued

Further analysis was also conducted to determine whether it is feasible to unify the angularity groups' limits of both the fine and coarse fractions. The groups' limits for the angularity of fine and coarse aggregates were determined and plotted in Fig. 6.1f. As can be seen, slight differences existed between the limits of fine and coarse fractions, with the largest difference being in the third group. However, it was determined that this difference is still small compared to the actual angularity values, and it would warrant unifying the limits. The results in Fig. 6.1 significantly simplified the development of the classification methodology, as the same limits can be used irrespective of aggregate size. The new aggregate shape classification limits are shown in Fig. 6.2.

ANALYSIS AND RESULTS

The AIMS software was used to calculate the percentages of each aggregate that belong to the different groups in Fig. 6.2. The results are shown in Figs. 6.3 and 6.4. These figures are convenient to rapidly examine the distribution of a certain shape property in a number of aggregate samples. The variability in shape characteristics within and between aggregates indicates that comparing or classifying aggregates based on percent of particles in a single group could be misleading. This is also true for the classification based on average values, especially when an aggregate sample includes a small percent of particles that have extremely high or low values. As such, the new classification methodology considers the distribution rather than an average value. The discussion provided in the following sections is intended to highlight the implications of using the developed methodology on aggregate shape classification with emphasis on examining the effects of different factors such as crushing on shape characteristics.

Aggregate Texture versus Angularity

The shape classification methodology incorporates measurements of texture and angularity for coarse aggregates, while it uses angularity measurements only for fine aggregates. A study by Masad et al. (2001) clearly showed that a high correlation exists between angularity (measured on black and white images), and texture (measured on

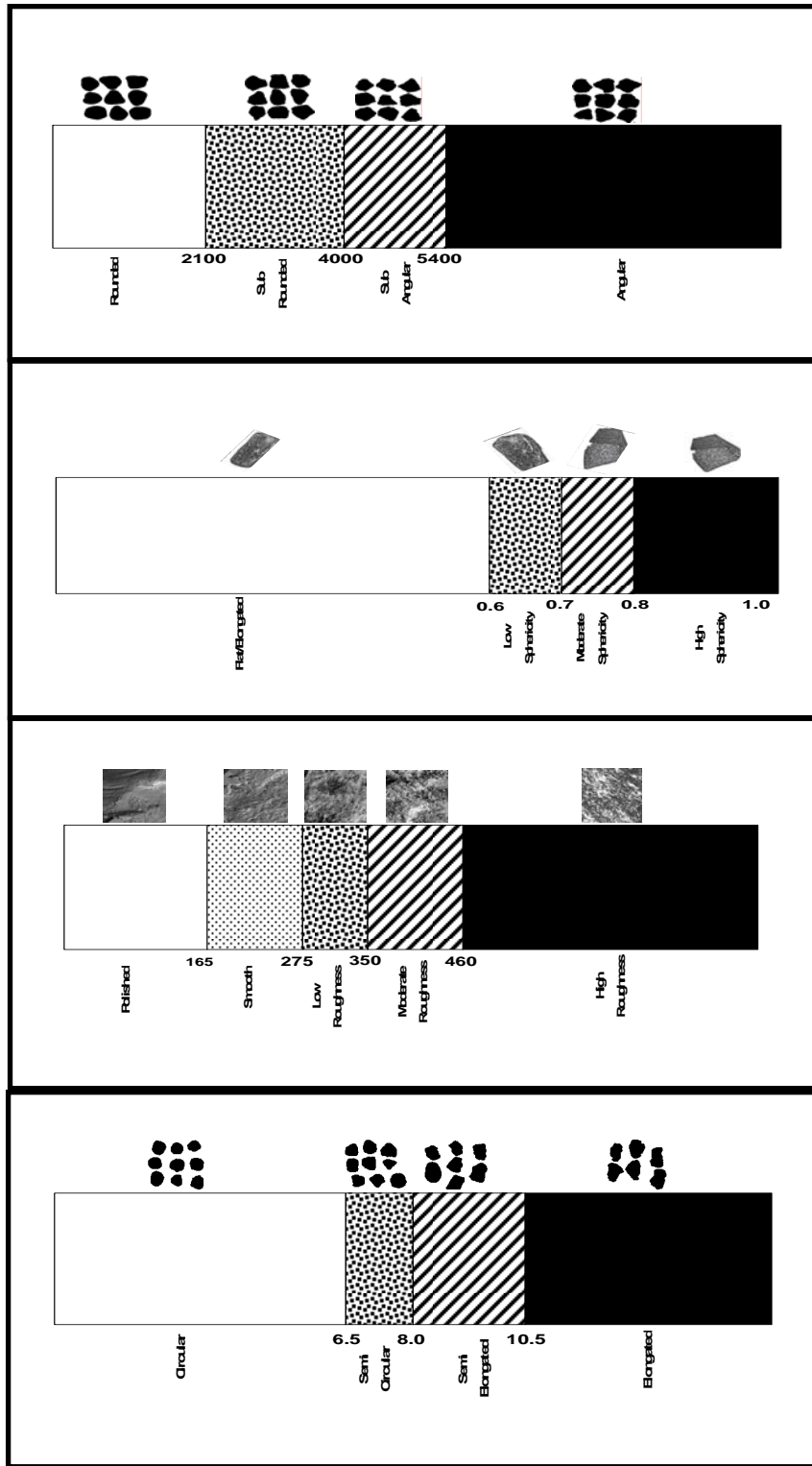
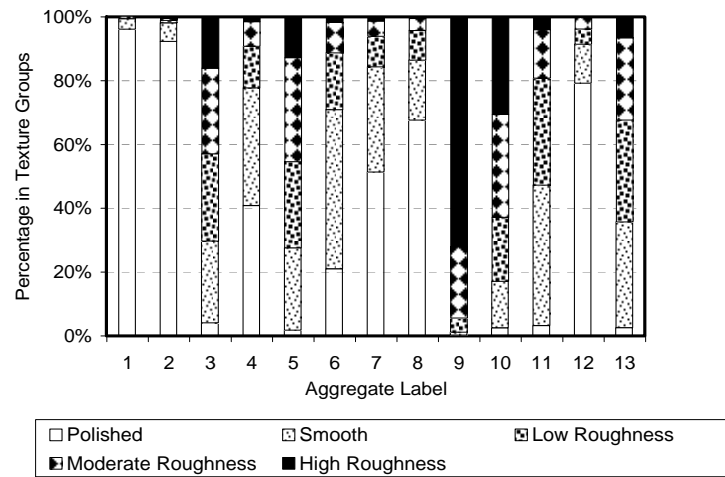
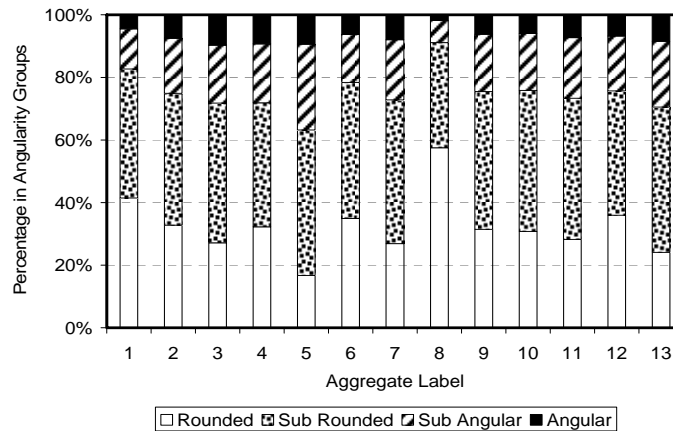


Fig. 6.2. Aggregate Shape Classification Chart

(a) Texture in Coarse Aggregate



(b) Angularity in Coarse Aggregate



(c) Form in Coarse Aggregate

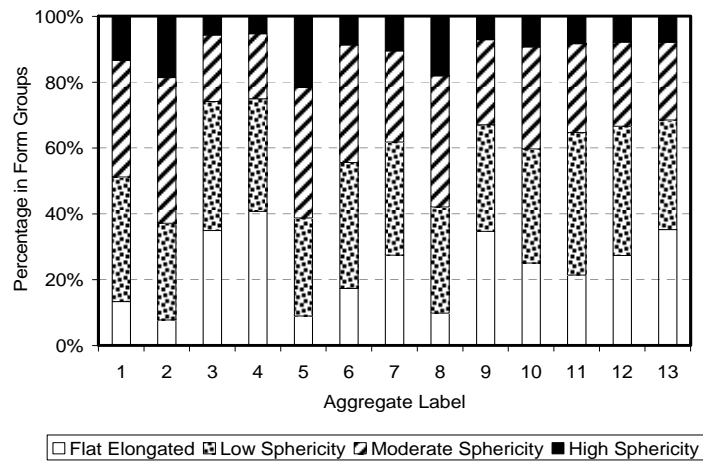
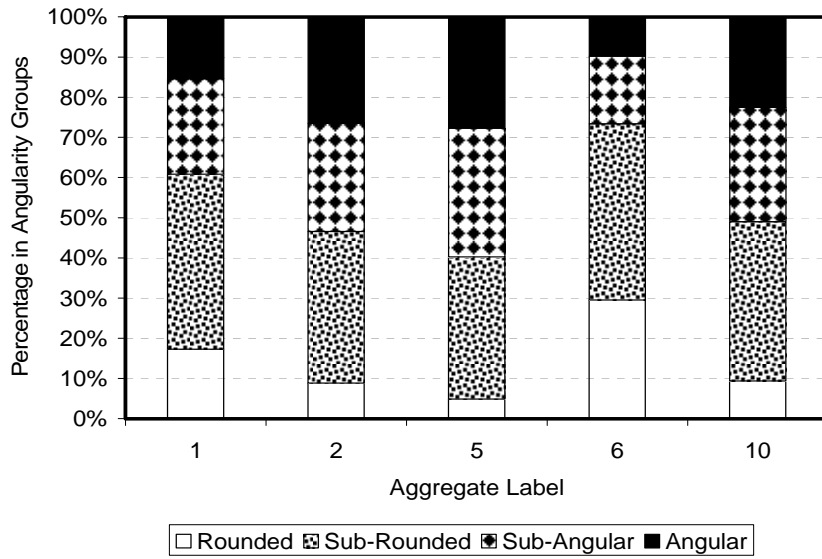
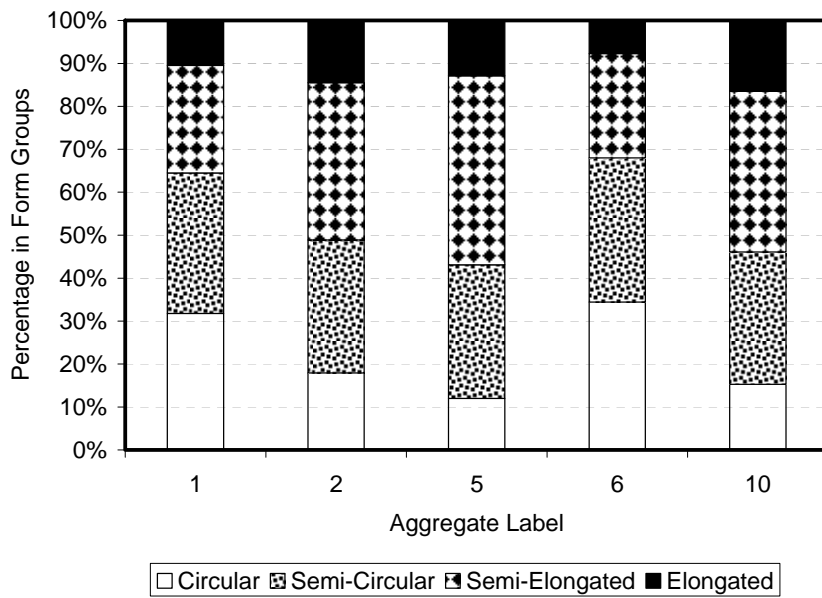


Fig. 6.3. Distributions of Shape Characteristics in Coarse Aggregates



(a) Angularity in Fine Aggregate



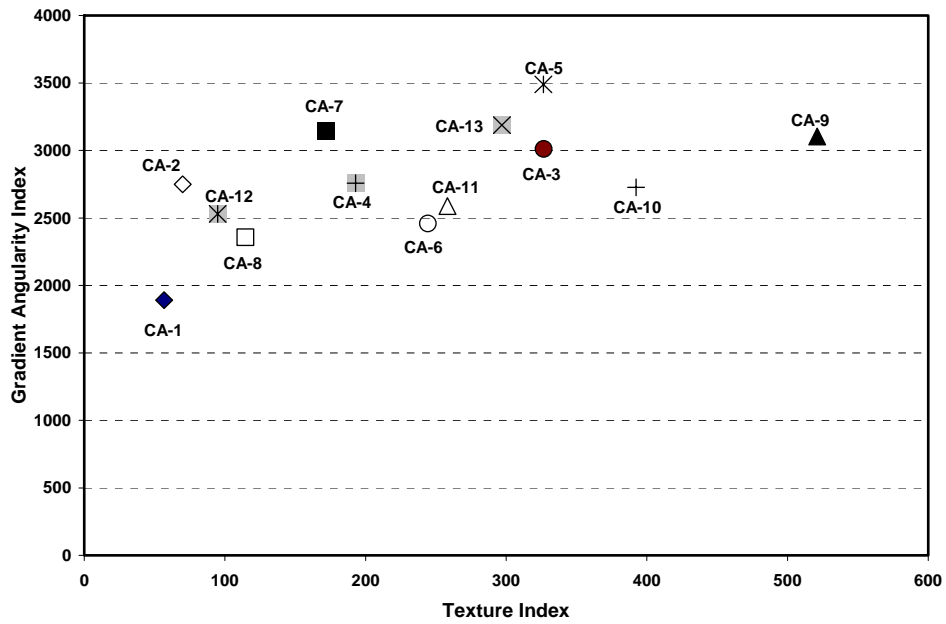
(b) Form in Fine Aggregates

Fig. 6.4. Distributions of Shape Characteristics in Fine Aggregates

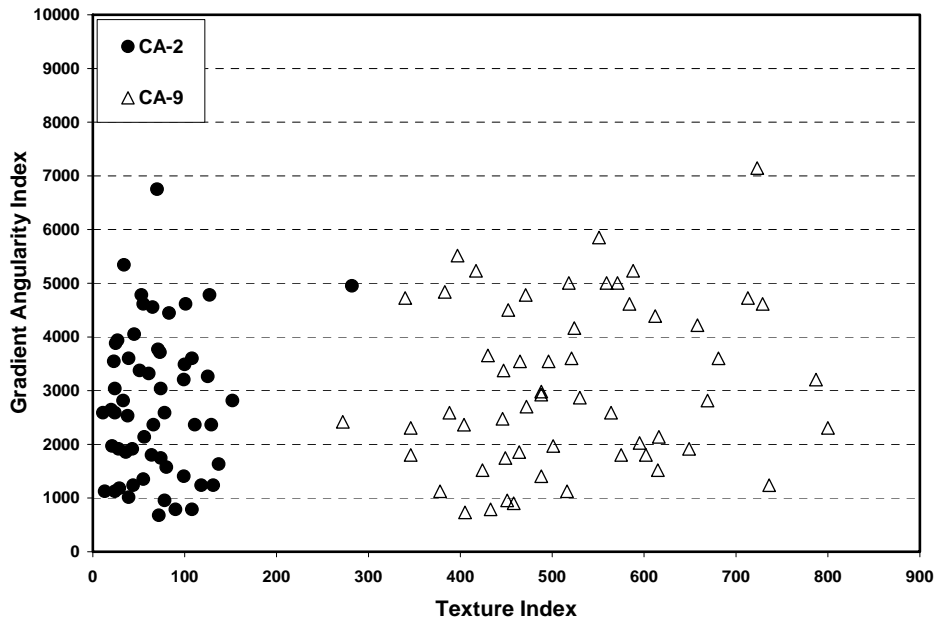
gray-scale images) of fine aggregates. This finding led to simplifying the AIMS design since angularity measured on black and white images is deemed sufficient to characterize fine aggregates. This is an easier task than capturing the surface texture of fine aggregates rapidly and accurately using a computer-automated system. In case of coarse aggregates, it was found that there is a distinct difference between angularity and texture, and these two properties have different effects on performance (Fletcher et al. 2003). This point is further illustrated in Fig. 6.5(a), which shows the average texture and corresponding angularity for each of the coarse aggregate samples. As can be seen, aggregates could have high angularity but low texture, and vice versa. This is even true for individual particles, as shown in Fig. 6.5(b). Particles from aggregates CA-2 and CA-9 had comparable angularity values but there was a significant difference in texture.

Fig. 6.6 shows the cumulative distribution of texture in the coarse aggregate samples. It is evident that the texture of these aggregate samples was spread over a wide range. In fact, none of the other shape properties had such a wide range. Texture also had higher variability than angularity within an aggregate sample (see Fig. 6.3(a) versus Fig. 6.3(b)).

Unfortunately, a direct measure of texture has not been implemented in the past, which might have caused discarding some aggregate sources that exhibit reasonable texture levels. Aggregate selection and mix design should be based on the evaluation of both the angularity and texture of coarse aggregates. Both of these characteristics contribute to friction among aggregates, which is an important mix property that contributes to the resistance to permanent deformation. Proper performance can be achieved by determining the acceptable limits of angularity and texture.



(a) Average Texture and Angularity of Coarse Aggregates



(b) Texture and Angularity of Coarse Aggregate Particles

Fig. 6.5. Variations in Texture and Angularity Properties in Coarse Aggregates

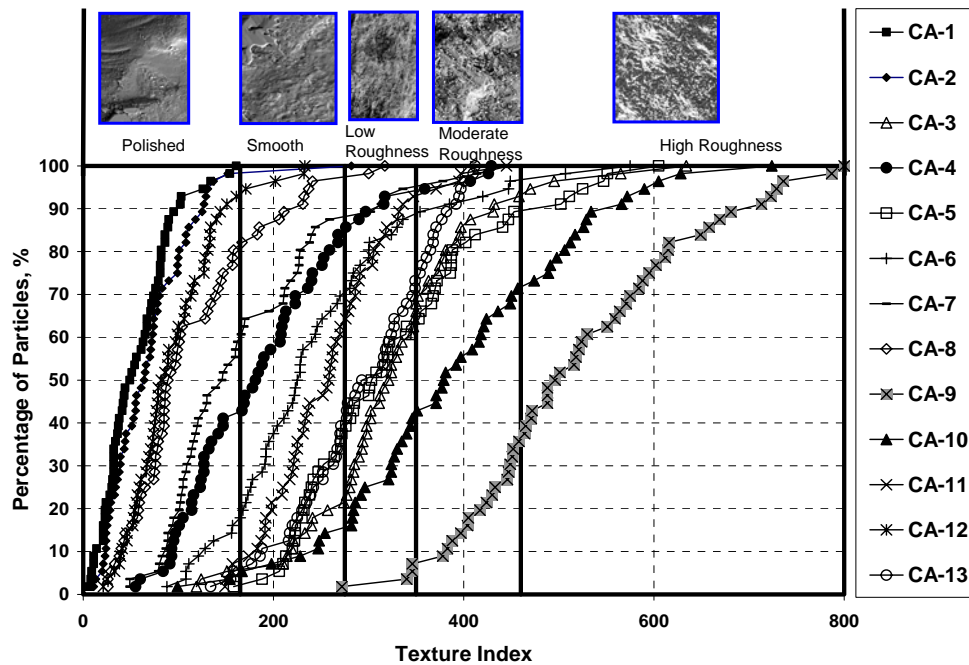


Fig. 6.6. Texture Index for Different Coarse Aggregate Types

Effect of Crushing and Size on Shape Properties

The developed methodology can be used to examine the influence of crushing on shape. Two types of crushed and uncrushed aggregates were used in this study. The first was river gravel (CA-1 and CA-2), and the second was glacial gravel (CA-7 and CA-8). CA-1 and CA-8 were uncrushed, while CA-2 and CA-7 were crushed. The results in Figs. 6.3(a) and 6.3(b) show that crushing the gravel did not improve texture, while it did significantly increase their angularity.

Texture measurements were conducted on different sizes of the same aggregate type in order to investigate the influence of aggregate size on texture. Examples of results are shown in Fig. 6.7. Aggregate size did not have a noticeable influence on texture. On the other hand, it was found that aggregate angularity changed as a function of aggregate size.

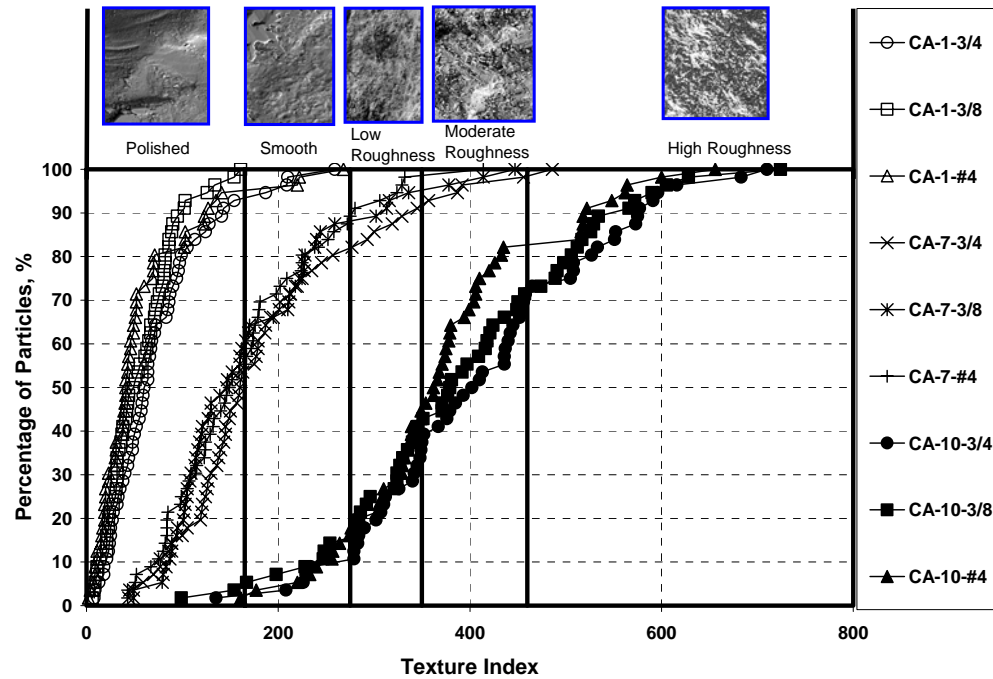


Fig. 6.7. Examples of the Effect of Coarse Aggregate Size on Texture

The analysis methods were also able to capture the influence of crushing on form or proportions of particle dimensions. The effect of aggregate size on sphericity varied from one aggregate to another. For example, the sphericity of CA-2 was higher than that for CA-1, indicating that aggregate crushing made the particles more equi-dimensional. On the contrary, crushing the glacial gravel made CA-7 to have less sphericity than CA-8.

Crushing the natural sand FA-1 to become FA-2 increased angularity, as depicted in Fig. 6.4a. FA-1 is an example of high quality natural sand that had angularity comparable to or even better than some manufactured sands. For example, FA-1 had higher angularity than FA-6, which is crushed limestone.

Shown in Fig. 6.8 is an example of the effect of size on fine aggregate angularity. Angularity increased as particle size decreased due to crushing. The form analysis of fine aggregates showed that crushing and aggregate size had very slight effect on the resulting values of the form index. The form index tended to become larger (more elongated) as particles got smaller.

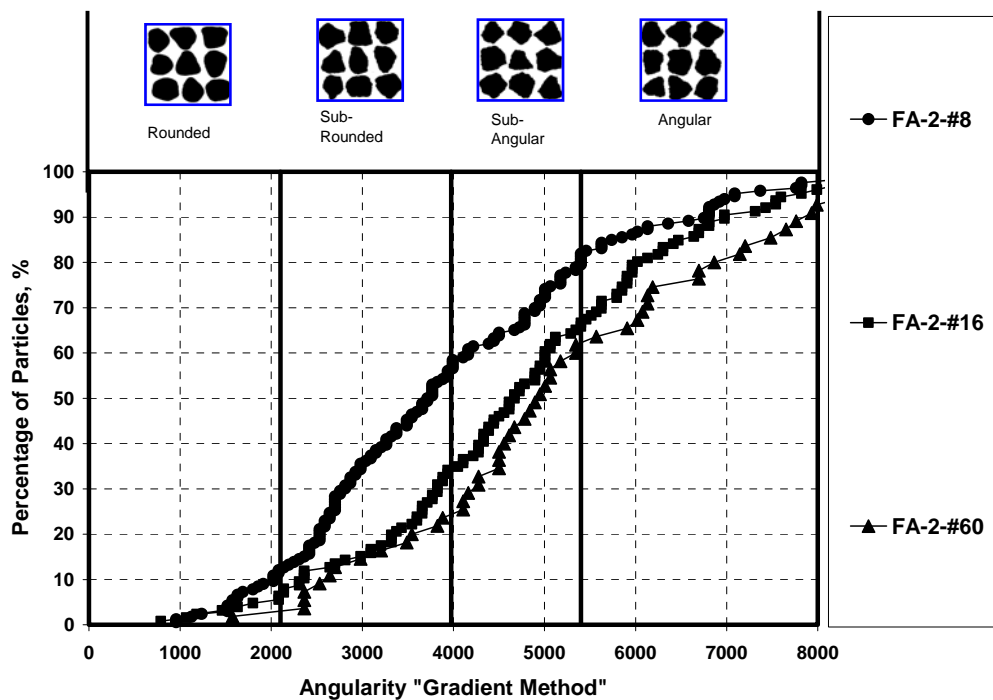


Fig. 6.8. Example of the Effect of Fine Aggregate Size on Angularity

Identifying Flat, Elongated, or Flat and Elongated Particles

The sphericity value gives a very good indication of the proportions of particle dimensions. However, one cannot determine whether an aggregate has flat, elongated, or flat and elongated particles using the sphericity alone. To this end, the chart shown in

Fig. 6.9 is included in the AIMS software to distinguish among flat, elongated, and flat and elongated particles. Superimposed on this chart are the 3:1 and 5:1 limits for the longest to shortest dimension ratio. The use of this chart is illustrated here with the aid of the results from CA-2 and CA-4. Both aggregates CA-2 and CA-4 pass the 5:1 Superpave requirement (both had less than 10% particles with dimensional ratio of 5:1), but they had distinct distributions in terms of flat and elongated particles.

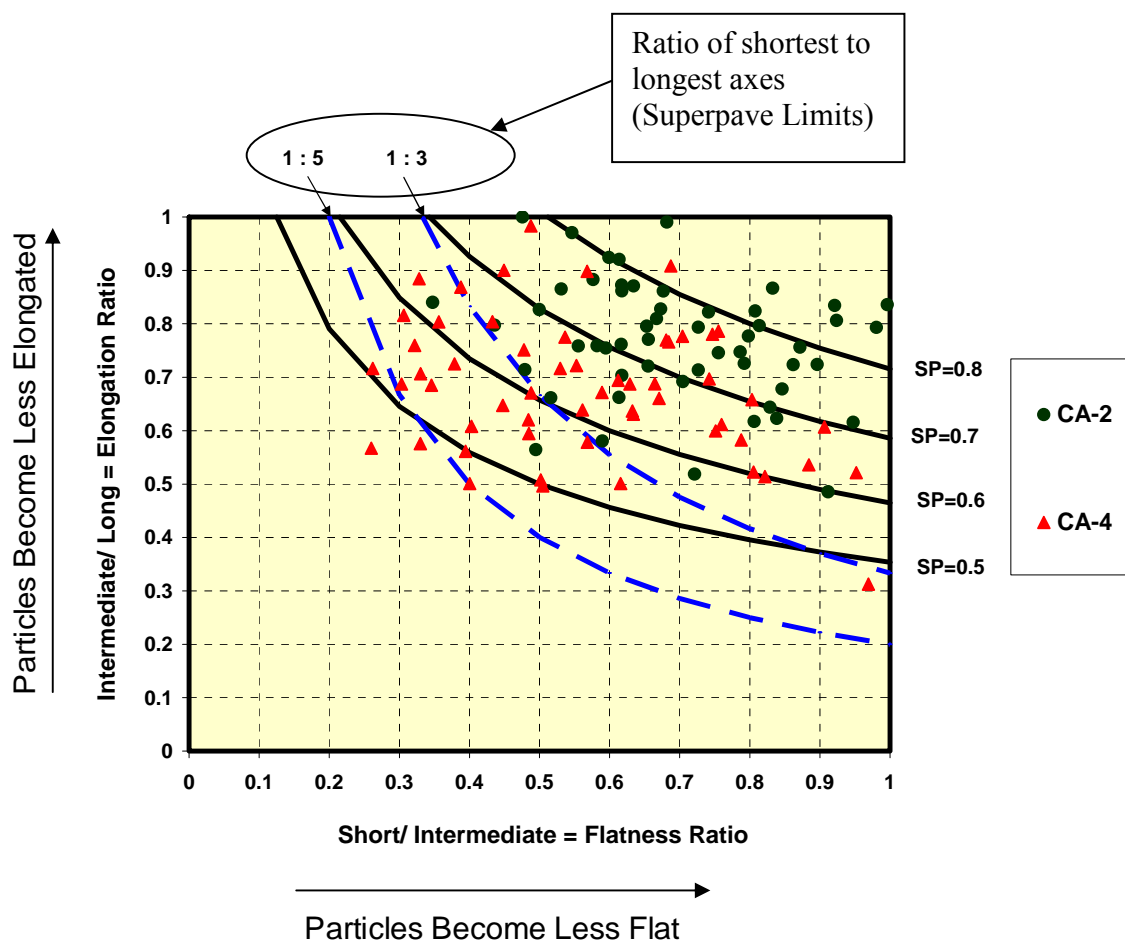


Fig. 6.9. Chart for Identifying Flat, Elongated, or Flat and Elongated Aggregates

The analysis in Fig. 6.9 reveals valuable information about the distribution that would not have been obtained if aggregates were classified based on the ratio of 5:1 only. Such details are needed to understand the influence of shape characteristics on asphalt mix performance. It is believed that some of the discrepancies in the literature regarding the influence of shape on performance are attributed to the lack of such details and relying on indirect methods of measuring average indices to describe shape.

SUMMARY

In this chapter, the third objective (develop a methodology for the classification of aggregates based on the distribution of their shape characteristics measured using the improved version of AIMS) was achieved. Cluster analysis was used to set new limits for aggregate shape classes. The developed classification methodology is based on direct measurements of form (three dimensions), angularity, and texture. It unifies the methods used to measure the shape characteristics of fine and coarse aggregates. The analysis methods are simple and the results have physical meanings that can be interpreted easily. The limits for the different shape groups were found to be similar for the different aggregate sizes. This finding simplified the methodology, as one set of limits are needed irrespective of aggregate sizes.

The classification results are presented in terms of the distribution of shape properties within an aggregate sample. This feature gives the methodology the capabilities to (1) explore the influence of different processes such as crushing and blending on aggregate shape, (2) conduct quality control activities to detect changes in the distribution of any of the shape characteristics, (3) relate the distribution of different shape characteristics to performance, and (4) develop specifications based on the distribution of aggregate shape characteristics rather than average indices.

CHAPTER VII

SUMMARY, CONCLUSIONS, IMPLEMENTATION, AND RECOMMENDATIONS

SUMMARY AND CONCLUSIONS

The comprehensive literature review conducted as part of this study revealed that the shape properties of coarse and fine aggregates used in hot-mix asphalt, hydraulic cement concrete, and unbound base and subbase layers are very important to the performance of the pavement system in which they are used in. Aggregate shape can be decomposed to three independent characteristics: form, angularity, and texture. Current methods used in practice for measuring these characteristics have several limitations; they are laborious, subjective, lack direct relation with performance parameters, and limited in their ability to separate the influence of angularity from that of texture. A number of research studies have shown that aggregates that exhibit high texture do not necessarily have high angularity, especially in coarse aggregates. Consequently, it is important to develop methods that are able to quantify each of the aggregate characteristics rather than a manifestation of their interactions.

The first objective of this study was achieved through the development of an improved version of the Aggregate Imaging System (AIMS). Several improvements were made in the design of the hardware and software components of AIMS to enhance the operational characteristics of the system, reduce human involvement and errors, and enhance the automation of the test procedure.

One of the important improvements made to AIMS was the development of a standard lighting scale. Lighting is an important factor influencing the quality of an image and analysis results of texture extracted from it. Therefore, a lighting scale based on a parameter measured on the captured images rather than the specifics of the lighting hardware components was developed. The mean of the gray-scale histogram was used as scale parameter, and a range of values was specified so that images can be captured with minimum influence of color variation on the results.

Visualization capabilities were added to the control software to allow the user to specify both the aggregate size and shape characteristics being analyzed and to determine whether an image is captured within the correct lighting scale or not. In AIMS, images for the analysis of angularity and texture are captured based on specified criteria for resolution and magnification in order to significantly reduce the influence of particle size on the shape characterization results.

The second objective was achieved by evaluating the improved version of AIMS along with other test methods used for measuring aggregate shape properties. The evaluation was conducted based on accuracy, repeatability, reproducibility, cost, ease of use, ease of interpretation of the results, readiness of the test for implementation, and portability. Thirteen different coarse aggregate types and five different fine aggregate types were used in this evaluation.

Analyses of repeatability and reproducibility results were conducted under the guidelines of ASTM standards E177, C802, and C670. Accuracy of the analysis methods used in the imaging systems was assessed by analyzing some particle projections that have been used by geologists for visual evaluation of particles' shape. Also, all analysis methods were used to analyze images of aggregate particles in order to identify the ability of these methods to accurately rank aggregates and capture unique characteristics of aggregates. The analysis results revealed that some of the available analysis methods are influenced by both angularity and form changes and, consequently, are not suitable to distinguish between these two characteristics. Also, some of the analysis methods are not capable of distinguishing between changes in texture and angularity. The following analysis methods are recommended:

- Texture: Wavelet analysis of gray images of particle surface (Implemented in AIMS software),
- Angularity: The gradient method (implemented in AIMS software) and the changes in the slope of a particle outline.
- Two-dimensional form: Aspect ratio.
- Three-dimensional form: Sphericity or the proportions of the three particle

dimensions.

Accuracy of test methods was assessed through statistical analysis of the correlations between the results from test methods with measurements of shape using a digital caliper and visual rankings of surface irregularity and texture by experienced individuals. AIMS results were ranked at or very close to the top for all shape characteristics.

The Analytical Hierarchy Process (AHP) was implemented in a program to rank the test methods. AHP is a process of developing a numerical score to rank test methods based on how each of these methods meets certain criteria of desirable characteristics. AHP requires the user to enter numeric values that indicate the relative importance of the different characteristics and numeric values that indicate how the methods compare against each other for each of the characteristics. The measurements of repeatability, reproducibility, and accuracy were used to obtain the input for the AHP. In addition, information about cost and operational characteristics, which was collected using a survey of vendors, researchers, and operators who have dealt with the test methods, was also used as input for the AHP.

AHP was found to be a powerful and flexible tool to rank test methods. It provides flexibility to examine the influence of changes in the importance of the characteristics on the ranking of test methods. It also provides a great deal of information on the relationship between test methods and desirable characteristics. The AHP rankings clearly demonstrated the advantage of AIMS over other test methods as a comprehensive methodology for measuring the shape characteristics of both coarse and fine aggregates.

The third objective in this study was to develop a methodology for the classification of aggregates based on the distribution of their shape characteristics measured using the improved version of AIMS. Cluster analysis was used to set new limits for aggregate shape classes. The developed classification methodology is based on direct measurements of form (three dimensions), angularity, and texture. It unifies the methods used to measure the shape characteristics of fine and coarse aggregates. The analysis methods are simple, and the results have physical meanings that can be interpreted easily. The limits for the different

shape groups were found to be similar for the different aggregate sizes. This finding simplified the methodology, as one set of limits are needed irrespective of aggregate sizes.

The classification results are presented in terms of the distribution of shape properties within an aggregate sample. This feature gives the methodology the capabilities to (1) explore the influence of different processes such as crushing and blending on aggregate shape, (2) conduct quality control activities to detect changes in the distribution of any of the shape characteristics, (3) relate the distribution of different shape characteristics to performance, and (4) develop specifications based on the distribution of aggregate shape characteristics rather than average indices.

In summary, the comparative analysis and the intensive evaluation conducted in this study highlighted the advantages of AIMS in measuring aggregate shape properties:

- Captures images and analyzes the shape of a wide range of aggregate sizes (coarse and fine) and types, which covers those used in asphalt mixes, hydraulic cement concrete, and unbound aggregate layers of pavements.
- Measures all three aggregate shape properties (form, angularity, and texture) for all aggregate types and for different aggregate sizes.
- Performs two- and three-dimensional analysis as needed.
- Captures images of aggregates at specified resolutions in order to minimize the influence of particle size on shape results.
- Uses image analysis techniques that are based on sound scientific concepts.
- Presents each of the shape characteristics by a cumulative distribution function rather than an average value, therefore, the system is able to better represent the influence of blending of different sources on aggregate characteristics.
- Provides rapid, computer automated, accurate, practical, and user-friendly operation.
- Works in central and field laboratories.

IMPLEMENTATION

This study provides the pavement community with a practical, reliable, and accurate method for rapidly measuring aggregate characteristics. AIMS is based on sound scientific concepts, is practical, and yields results that are easy to interpret and implement in specifications. AIMS will be useful for the industry, highway agencies, and researchers in Quality Control (QC), Quality Assurance (QA), and problem diagnosis to advance the fundamental understanding of aggregates and their effects on performance of pavement structures. In addition, AIMS will help the industry to understand its own product and set criteria for providing better product to ensure the quality of aggregates in pavements and significantly improve their performance, which will lead to considerable cost savings in the construction and rehabilitation of pavements. AIMS can be implemented in the following aspects of pavement engineering:

- Measuring aggregate shape properties before and after subjecting aggregates to skid forces. The change in aggregate shape properties, especially texture, can be used as an indication of aggregate resistance to polishing.
- Developing a method to quantify the resistance of aggregates to abrasion. The changes in aggregate shape characteristics after subjecting it to abrasion forces such as those in the Micro-Deval test can be used to assess resistance to abrasion.
- Monitoring QA and QC of aggregate properties during production. to ensure good quality of aggregates in pavements. The use of AIMS in QC and QA will lead to considerable cost savings in the construction and rehabilitation of pavements.
- Evaluating different crushing methods. AIMS can be used to evaluate different crushing procedures by measuring aggregate shape properties resulting from each method. This evaluation will be very helpful for aggregate industry to know which of the crushing methods would produce aggregate with the most desirable shape characteristics.

- Unifying the methods used to measure all of the three shape characteristics of fine and coarse aggregates and representing each of the shape characteristics by a cumulative distribution. This feature facilitates developing specifications for aggregate shape. Consequently, pavement performance models can be developed relating shape properties to performance measures.
- Conducting different research studies related to hot-mix asphalt, hydraulic cement concrete, and unbound aggregate layers. In hot-mix asphalt pavements, AIMS can be used to study the relationship between the bond of asphalt and aggregates and shape characteristics. AIMS can also be used to develop performance-based aggregate shape classification considering the fact that aggregate shape properties for both coarse and fine aggregates affect permanent deformation, fatigue cracking, and frictional resistance of HMA pavements. In hydraulic cement concrete pavements AIMS can be used to study the effect of aggregate shape properties on workability, compactibility, and aggregate-paste bond. In unbound layers, AIMS can be utilized to explore the effect of aggregate shape properties on the resilient modulus, permeability, and compactibility.

RECOMMENDATIONS

The main recommendation of this study is to move forward in adopting AIMS as a test for aggregate shape properties. It is recommended that future studies should be performed to relate the distribution of different aggregate shape characteristics to performance of different types of pavements. This is essential in order to develop new specifications for aggregate shape based on the relationship to performance of various pavement layers.

In this study, the rankings of test methods were conducted based on the average value of shape property measurements. This approach was followed since some of the available systems provide average values only. It is recommended that more statistical analysis should be conducted that considers the distribution of shape properties within a sample.

The repeatability and reproducibility analysis of AIMS was conducted using only

one unit. It is highly recommended that ruggedness of AIMS be further analyzed using multiple units and in a number of research laboratories.

REFERENCES

- Ahlich, R. C. (1995). "Influence of aggregate gradation and particle shape/texture on permanent deformation of hot-mix asphalt pavement." Ph.D. Dissertation., Auburn University. Auburn, AL.
- Al-rousan, T., Masad, E., Myers, L., and Speigelman, C. (2005). "A new methodology for shape classification of aggregates used in asphalt mixes." *Transportation Research Record*, Transportation Research Board, National Research Council, Washington, D.C. (submitted).
- American Association of State Highway and Transportation Officials AASHTO. (1988). *Standard specifications for transportation materials and methods of sampling and testing*, 19th Edition, Washington, D.C.
- American Society of Testing and Materials ASTM. (2000). *Annual Book of ASTM Standards (03-04)*, West Conshohocken, PA.
- American Society of Testing and Materials ASTM. (2002). "Standard practice for preparing precision and bias statements for test methods for construction materials." *ASTM C670, Annual Book of ASTM Standards*, 4(2), West Conshohocken, PA.
- American Society of Testing and Materials ASTM (2002). "Standard practice for conducting an inter laboratory test program to determine the precision of test methods for construction materials." *ASTM C802, Annual Book of ASTM Standards*, 4(2), West Conshohocken, PA
- American Society of Testing and Materials ASTM. (2002). "Standard Practice for use of terms precision and bias in ASTM test methods." *ASTM E 177, Annual Book of ASTM Standards*, 4(2), West Conshohocken, PA.
- Barksdale, R. D., and Itani, S. Y. (1994). "Influence of aggregate shape on base behavior." *Transportation Research Record 1227*, Transportation Research Board, National Research Council, Washington, D.C., 171-182.
- Barksdale, R. D., Kemp, M. A., Sheffield, W. J., and Hubbard. J. L. (1991).

- “Measurement of aggregate shape, surface, roughness.” *Transportation Research Record 1301*, Transportation Research Board, National Research Council, Washington, D.C., 107-116.
- Barksdale, R. D., Pollard C. O., Siegel, T., and Moeller, S. (1992). “Evaluation of the effect of aggregate on rutting and fatigue of asphalt.” Technical Report FHWA-AG-92-8812. Georgia Department of Transportation, Atlanta, GA.
- Barrett, P. J. (1980). “The shape of rock particles, a critical review.” *Sedimentology*, 27, 291–303.
- Bathina M. (2004). “Analysis of the Quality of the Aggregate Imaging System (AIMS) measurements.” Master’s Thesis, Dept. of Civil Engineering, Texas A&M University, College Station, TX, in progress.
- Benson, F. J. (1970). “Effects of aggregate size, shape, and surface texture on the properties of bituminous mixtures, a literature survey.” *Highway Research Board 109*, Transportation Research Board, National Research Council, Washington, D.C., 12–22.
- Blum, H. (1967). “A transformation for extracting new descriptors of shape.” *Models for the Perception of Speech and Visual Form*, W. Wathen-Dunn, ed., M.I.T. Press, Cambridge, MA, 362-380.
- Brown, E. R., McRea, J. L., and Crawley A. B. (1989). “Effect of aggregates on performance of bituminous concrete.” *American Society for Testing and Materials ASTM STP*, 1016, 34-63.
- Browne, C., Rauch F. A., Haas T. C., and Kim H. (2001). “Comparison tests of automated equipment for analyzing aggregate gradation.” *Proceedings of the 9th Annual Symposium of the International Center for Aggregates Research (ICAR)*, Austin, TX.
- Brzezicki, J. M., and Kasperkiewicz, J. (1999). “Automatic image analysis in evaluation of aggregate shape.” *ASCE Journal of Computing in Civil Engineering (Special Issue on Image Processing)*, 13(2), 123–130.
- Button, J. W., Perdomo, D., and Lytton, R. L. (1990). “Influence of aggregate on rutting

- in asphalt concrete pavements.” *Transportation Research Record 1259*, Transportation Research Board, National Research Council, Washington D.C., 141-152.
- Calabi, L., and Hartnett, W. E. (1968). “Shape recognition, particle fires, convex deficiencies and skeletons.” *American Math Monthly*, 75, 335-342.
- Campen W. H., and Smith, J. R. (1948). “A Study of the role of angular aggregate in the development of stability in bituminous mixtures.” *Association of Asphalt Paving Technologists Proceedings*, 17, 114-143.
- Chandan, C., Sivakumar, K., Fletcher, T., and Masad, E. (2004). “Geometry analysis of aggregate particles using imaging techniques.” *Journal of Computing in Civil Engineering*, ASCE, 18 (1), 75-82.
- Chowdhury A., and Button, J. W. (2001). “Fine aggregate angularity: Conventional and unconventional approach, aggregate contribution to hot-mix asphalt HMA performance.” *American Society for Testing and Materials ASTM, Special Technical Publication*, 1412, 144-159.
- Chowdhury, A., Button, J. W., Kohale, V., and Jahn, D. (2001). “Evaluation of superpave fine aggregate angularity specification.” *International Center for Aggregates Research ICAR Report 201-1*, Texas Transportation Institute, Texas A&M University, College Station, TX.
- Ehrlich, R., Kennedy, S. K., Crabtree, S. J., and Cannon, R. L. (1984). “Petrographic image analysis. I. analysis of reservoir pore complexes.” *Journal of Sedimentary Petrology*, 54, 1365-1378.
- Field, F. (1958). “Effect of percent crushed variation in coarse aggregates of bituminous mixes.” *Association of Asphalt Paving Technologists Proceedings*, 27, 294-322.
- Fletcher, T. (2002). “Aggregate imaging system for characterizing fine and coarse aggregate shape.” Master’s Thesis, Dept. of Civil and Environmental Engineering, Washington State University, Pullman, WA.
- Fletcher, T., Chandan, C., Masad, E., and Sivakumar, K. (2002). “Measurement of aggregate texture and its influence on HMA permanent deformation.” *Journal of*

- Testing and Evaluation, American Society for Testing and Materials, ASTM*, 30 (6), 524-531.
- Fletcher, T., Chandan, C., Masad, E., and Sivakumar, K. (2003). "Aggregate Imaging System (AIMS) for characterizing the shape of fine and coarse aggregates." *Transportation Research Record 1832*, Transportation Research Board, National Research Council, Washington, D.C., 67-77.
- Folliard, K. J. (1999). "Aggregate tests related to performance of Portland cement concrete pavements." *National Cooperative Highway Research Program Project 4-20B*, Phase 1 Interim Report, Austin, TX.
- Forster, S. W. (1981). "Aggregate microtexture: Profile measurement and related frictional levels." *Report Federal Highway Administration FHWA/RD-81/107*. FHWA, U.S. Department of Transportation, Washington, D.C.
- Foster, C. R. (1970). "Dominant effect of fine aggregate on strength of dense-graded asphalt mixes." *Highway Research Board Special Report 109*. Transportation Research Board, National Research Council, Washington, D.C., 1-3.
- Fowler, D. W., Zollinger, D. G., Carrasquillo, R. L., and Constantino, C. A. (1996). *Aggregate Tests Related to Performance of Portland Cement Concrete*, Phase 1 Unpublished Interim Report, National Cooperative Highway Research Program (NCHRP) Project 4-20, Lincoln, NE.
- Herrin, M., and Goetz, W. H. (1954). "Effect of aggregate shape on stability of bituminous mixes." *Highway Research Board Proceedings*, Washington D.C., 293-308.
- Hough, P. (1962). "Methods and means for recognizing complex patterns." *U.S. Patent Number 3,069,654*.
- Hryciw, R. D., and Raschke, S. A. (1996). "Development of a computer vision technique for in-situ soil characterization." *Transportation Research Record 1526*, Transportation Research Board, National Research council, Washington, D.C., 86-97.
- Indiana University - Purdue University Fort Wayne IPFW Geosciences Website,

- (www.geosci.ipfw.edu).
- Ishai, I., and Gellber, H. (1982). "Effect of geometric irregularity of aggregates on the properties and behavior of asphalt concrete." *Association of Asphalt Paving Technologists*, 51, 494-521.
- Ishai, I., and Tons, E. (1977). "Concept and test methods for a unified characterization of the geometric irregularity of aggregate particles." *Journal of Testing and Evaluation*, 5(1), 3-15.
- Jahn, D. (2000). "Evaluation of aggregate particle shapes through multiple ratio analysis." *Proceedings of the 8th Annual Symposium of the International Center for Aggregate Research (ICAR)*, Denver, CO.
- Janoo, V. C. (1998). "Quantification of shape, angularity, and surface texture of base course materials." *U.S. Army Corps of Engineers Special Report 98-1*, Cold Regions Research & Engineering Laboratory, Hanover, NH.
- Janoo, V. C., and Korhonen, C. (1999). "Performance testing of hot-mix asphalt aggregates." *U.S. Army Corps of Engineers Special Report 99-20*, Cold Regions Research & Engineering Laboratory, Hanover, NH.
- Johnson, R. A. and Wichern, D. W. (2002). *Applied Multivariate Statistical Analysis*. Prentice Hall, Englewood Cliffs, NJ.
- Kalcheff, I. V. (1968). "Bituminous concrete properties with large-sized aggregates of different particle shape." *Highway Research Board Special Report 109*, Transportation Research Board, National Research Council, Washington D.C., 27-32.
- Kalcheff, I. V., and Tunnicliff, D. G. (1982). "Effect of crushed stone size and shape on properties of asphalt concrete." *Journal of Association of Asphalt Paving Technologists*, 51, 453-470.
- Kandhal, P. S., and Parker, F. Jr. (1998). "Aggregate tests related to asphalt concrete performance in pavements." *National Cooperative Highway Research Program Report 405*, Transportation Research Board, National Research Council, Washington, D.C.

- Kandhal P.S., and Wenger M.E. (1973). "Effect of crushed gravel coarse aggregate on properties of bituminous concrete." *Pennsylvania Department of Transportation. Research Report, 70-82*, Harrisburg, PA.
- Kandhal, P. S., Motter, J. B., and Khatri, M. A. (1991). "Evaluation of particle shape and texture: manufactured versus natural sands." *Transportation Research Record 1301*, Transportation Research Board, National Research Council, Washington D.C., 48-67.
- Kim, H., Haas, C., Rauch, A., and Browne, C. (2001). "A prototype laser scanner for characterizing size and shape properties in aggregates." *Proceedings of the 9th Annual Symposium of the International Center for Aggregate Research (ICAR)*, Austin, TX.
- Kim, H., Haas, C. T., Rauch, A. F., and Browne, C. (2002). "Wavelet-based 3D descriptors of aggregate particles." *Transportation Research Record 1787*, Transportation Research Board, National Research Council, Washington, D.C., 109-116.
- Kosmatka, S. H., Kerkhoff, B., and Panarese, W. C. (2002). *Design and control of concrete mixtures*, 14th edition, Portland Cement Association, Skokie, IL.
- Kuo, C., and Freeman, R. B. (2000). "Imaging indices for quantification of shape, angularity, and surface texture of aggregates." *Transportation Research Record 1721*, Transportation Research Board, National Research Council, Washington D.C., 57-65.
- Kuo, C. Y., Frost, J. D., Lai, J. S., and Wang, L. B. (1996). "Three-dimensional image analysis of aggregate particle from orthogonal projections." *Transportation Research Record 1526*, Transportation Research Board, National Research Council, Washington, D.C., 98-103.
- Krumbein, W. C. (1941). "Measurement and geological significance of shape and roundness of sedimentary particles." *Journal of Sedimentary Petrology*, 11(2), 64-72.
- Lee, J. C., Changlin, P., and White, T. (1999a). "Review of fine aggregate angularity

- requirements in superpave.” *Journal of the Association of Asphalt Paving Technologists*, 68, 305-318.
- Lee, J. C., White, D. T., and West, R. T. (1999b). “Effect of fine aggregate angularity on asphalt mixture performance.” *Federal Highway Administration, Indiana Dept. of Transportation, Joint Transportation Research program FHWA/INDOT/JTRP-98/20*, Final Report, West Lafayette, IN.
- Lefebure, J. (1957) “Recent investigations of design of asphalt paving mixtures.” *Association of Asphalt Paving Technologists Proceedings*, 26, 321-394.
- Li, L., Chan, P., Zollinger, D. G., and Lytton, R. L. (1993). “Quantitative analysis of aggregate shape based on fractals.” *ACI Materials Journal*, 90 (4), 357-365.
- Li, M. C., and Kett, I. (1967). “Influence of coarse aggregate shape on the strength of asphalt concrete mixtures.” *Highway Research Record 178*, Transportation Research Board, National Research Council, Washington, D. C., 93-106.
- Maerz, N. H. (2004). “Technical and computational aspects of the measurement of aggregate shape by digital image analysis.” *Journal of Computing in Civil Engineering*, 18(1), 10–18.
- Maerz, N. H., and Lusher, M. (2001). “Measurement of flat and elongation of coarse aggregate using digital image processing.” *Transportation Research Board Proceedings, 80th Annual Meeting*, Washington D.C., Paper No. 01-0177.
- Maerz, N. H., and Zhou, W. (2001). “Flat and elongated: advances using digital image analysis.” *Proceedings of the 9th Annual Symposium of the International Center for Aggregates Research (ICAR)*, Austin, TX.
- Maerz, N., Palangio, H., and Franklin, J.A. (1996). “WipFrag image based granulometry system.” *Proceedings of the FRAGBLAST 5*, Workshop on Measurement of Blast Fragmentation, Montreal, Quebec, Canada, 91-99.
- Mallat, Stephane G. (1989). “A Theory for multiresolution signal decomposition: The wavelet representation.” *IEEE Transactions on Pattern Analysis and Machine Intelligence*, 11, 674-693.
- Mandelbrot, B. B. (1984). *The Fractal Geometry of Nature*, W. H. Freeman, San

Francisco, CA.

- Masad, E. (2001). "Review of imaging techniques for characterizing the shape of aggregates used in asphalt mixes." *Proceedings of the 9th Annual Symposium of the International Center for Aggregate Research (ICAR)*, Austin, TX.
- Masad, E. (2003). "The development of a computer controlled image analysis system for measuring aggregate shape properties." *National Cooperative Highway Research Program NCHRP-IDEA Project 77 Final Report*, Transportation Research Board, National Research Council, Washington, D.C.
- Masad, E., and Button, J. (2000). "Unified imaging approach for measuring aggregate angularity and texture." *Journal of Computer-Aided Civil and Infrastructure Engineering*, 15(4), 273-280.
- Masad, E., Button, J., and Papagiannakis, T. (2000). "Fine aggregate angularity: automated image analysis approach." *Transportation Research Record 1721*, Transportation Research Board, National Research Council, Washington D.C., 66-72.
- Masad, E. A., Muhunthan, B., Shashidhar, N., and Harman, T. (1999b). "Effect of Compaction Procedure on the Aggregate Structure in Asphalt Concrete." *Transportation Research Record 1681*, Transportation Research Board, National Research Council, Washington, D.C., 179-184.
- Masad, E., Muhunthan, B., Shashidhar, N., and Harman T. (1999a). "Internal structure characterization of asphalt concrete using image analysis." *ASCE Journal of Computing in Civil Engineering (Special Issue on Image Processing)*, 13(2), 88 - 95.
- Masad, E., Olcott, D., White, T., and Tashman, L. (2001). "Correlation of fine aggregate imaging shape indices with asphalt mixture performance." *Transportation Research Record 1757*. Transportation Research Board, National Research Council, Washington, D.C., 148-156.
- Meininger, R. C. (1998). "Aggregate test related to performance of portland cement concrete pavement." *National Cooperative Highway Research Program Project 4-*

- 20A Final Report*. Transportation Research Board, National Research Council, Washington, D.C.
- Mindness, S., and Young, J. F. (1981). *Concrete*, Prentice Hall Inc., Englewood Cliffs, NJ.
- Monismith, C. L. (1970). "Influence of shape, size, and surface texture on the stiffness and fatigue response of asphalt mixtures." *Highway Research Board 109 Special Report*, Transportation Research Board, National Research Council, Washington, D.C., 4-11.
- Morrison, D. (2004). *Multivariate Statistical Methods*. Brooks/Cole Thomson Learning, Stamford, CT.
- National Instruments Website (www.ni.com).
- Park, D., Chowdhury, A., and Button, J. W. (2001). "Effects of aggregate gradation and angularity on VMA and rutting resistance." *International Center for Aggregate Research (ICAR), Report 201-3F*, Texas Transportation Institute, Texas A&M University, College Station, TX.
- Powers, M. C. (1953). "A new roundness scale for sedimentary particles." *Journal of Sedimentary Petrology*, 23(2), 117-119.
- Rao, C. (2001). "Development of 3-D image analysis techniques to determine shape and size properties of coarse aggregate." Ph.D. Dissertation, Dept. of Civil Engineering, University of Illinois at Urbana-Champaign, Urbana, IL.
- Rao, C., and Tutumluer, E. (2000) "A new image analysis approach for determination of volume of aggregates." *Transportation Research Record 1721*, Transportation Research Board, National Research Council, Washington, D.C., 73-80.
- Rao, C., Tutumluer, E., and Kim, I. T. (2002). "Quantification of coarse aggregate angularity based on image analysis." *Transportation Research Record 1787*, Transportation Research Board, National Research Council, Washington, D.C., 117-124.
- Rao, C., Tutumluer E., and Stefanski, J. A. (2001). "Coarse aggregate shape and size properties using a new image analyzer." *ASTM Journal of Testing and Evaluation*,

- JTEVA, 29(5), 79-89.
- Riley, N. A. (1941). "Projection sphericity." *Journal of Sedimentary Petrology*, 11 (2), 94-97.
- Rittenhouse, G. (1943). "A visual method of estimating two dimensional sphericity." *Journal of Sedimentary Petrology*, 13(2), 79-81.
- Rosenfeld, A., and Kak, A. C. (1976). *Digital Picture Processing*, Academic Press, New York, NY.
- Russ, J. C. (1998). *The Image Processing Handbook*, CRC Press LLC, Boca Raton, FL.
- Saaty, T. L. (1980). *The Analytic Hierarchy Process: Planning, Priority Setting, Resource Allocation*, McGraw-Hill Inc., New York, NY.
- Saeed, A., Hall, J., and Barker, W. (2001). "Performance-related tests of aggregates for use in unbound pavement layers." *National Cooperative Highway Research Program Report 453*, Transportation Research Board, National Research Council, Washington, D.C.
- Sanders, C. A., and Dukatz, E. L. (1992). "Evaluation of percent fracture of hot-mix asphalt gravels in Indiana." *Effect of Aggregate and Mineral Filler on Asphalt Mixture Performance*, R. C. Meininger, ed., American Society for Testing and Materials, STP 1147. Philadelphia, PA.
- Stephens, J. E., and Sinha, K. C. (1978). "Effect of aggregate shape on bituminous mix characteristics." *American Association of Paving Technologists Proceedings*, 47, 434-456
- Thales-Optem Zoom 160 Brochure,
(www.thales-optem.com/pdf/Zoom160Brochure.pdf).
- Tons, E., and Goetz, W. H. (1968). "Packing volume concepts for aggregates." *Highway Research Record* 236, Transportation Research Board, National Research Council, Washington D.C., 79-96.
- Tutumluer, E., and Thompson, M. R. (1997). "Granular base moduli for mechanistic pavement design." *ASCE Airfield Pavement Conference Proceedings*, Seattle, WA, 33-47.

- Tutumluer, E., Rao, C., and Stefanski, J. (2000). "Video image analysis of aggregates." *Final Project Report, FHWA-IL-UI-278, Civil Engineering Studies UILU-ENG-2000-2015*, University of Illinois Urbana-Champaign, Urbana, IL.
- Tyler, W. S. (2001). "*Particle size and shape analyzers (CPA)*." Product Brochure, Mentor, OH.
- Wadell, H. (1932). "Volume, shape, and roundness of rock particles." *Journal of Geology*, 40, 443-451.
- Wadell, H. (1935). "Volume, shape, and roundness of quartz particles." *Journal of Geology*, 43, 450-480.
- Wang, L. B., and Lai, J. S. (1998). "Quantify specific surface area of aggregates using an imaging technique." *Transportation Research Board 77th Annual Meeting*, Washington, D.C.
- Wang, L. D., Park, J., and Mohammad, L. (2003). "Quantification of morphology characteristics of aggregate from profile images." *Transportation Research Board 82nd Annual Meeting*, Washington, D.C.
- Wedding, P. A., and Gaynor, R. D. (1961). "The effect of using crushed gravel as the coarse and fine aggregate in dense-graded bituminous mixtures." *Association of Asphalt Paving Technologists Proceedings*, 30, 469-492
- Weingart, R. L., and Prowell, B. D. (1999). "Specification development using the VDG-40 Videograder for shape classification of aggregates." *Proceedings of the 7th Annual Symposium of the International Center for Aggregate Research (ICAR)*, University of Texas, Austin, TX.
- Wilson, J. D., and Klotz, L. D. (1996). "Quantitative analysis of aggregates based on hough transform." *Transportation Research Record 1530*, Transportation Research Board, National Research Council, Washington D.C., 111-115.
- Wilson, J. D., Klotz, L. D., and Nagaraj, C. (1997). "Automated measurement of aggregate indices of shape." *Particulate Science and Technology*, 15, 13-35.
- Winford, J. M. (1991). "Evaluation of fine aggregate particle shape and texture and its effect on permanent deformation of asphalt paving mixtures." Ph.D. Dissertation,

Dept. of Civil Engineering, Auburn University, Auburn, AL.

- Yandell, W. O. (1970). "A new theory of hysteretic friction." *Waer*, 17, 229- 244.
- Yeggoni, M., Button, J. W., and Zollinger, D. G. (1994). "Influence of coarse aggregate shape and surface texture on rutting of hot-mix concrete." *Texas Transportation Institute Report 1244-6*, Texas A&M University, College Station, TX.
- Yeggoni, M., Button, J.W., and Zollinger, D.G. (1996). "Fractals of aggregates correlated with creep in asphalt concrete." *Journal of Transportation Engineering (ASCE)*, 122 (1), 22-28.
- Young, I. T., Peverini, R. L., Verbeek, P. W., and Van Otterloo, P. J. (1981). "A new implementation for the binary and minkowski operators." *Computer Graphics and Image Processing*, 17(3), 189-210.

VITA

Taleb Mustafa Al Rousan was born in Irbid, Jordan on 11/16/1971. He was awarded, in 2/1994, the degree of Bachelor of Science in Civil Engineering from Jordan University of Science and Technology (JUST) with a specialization in transportation and materials. After graduation, he worked for 1.5 years in a local consultant company supervising the construction of a highway.

He started his graduate studies at JUST in 9/1995. He served as a part-time teaching assistant from 9/1995 to 1/1998. His research thesis title was “*Analysis of Urban Trips with Perceived Risks in Amman.*” He published a paper on his master work with the title “*The Impact of Perceived Risk on Urban Commuters Route Choice*” in the *Road and Transportation Research Journal*, Vol. 7, No. 4, 1998. He was awarded a Master of Science degree in Civil Engineering with specialization in transportation in 2/1998. From 10/1998 to 1/2001, he worked in Saudi Arabia in a well-known consulting company in the region “Dar Alhandasah—Sha’er & Partners” supervising the construction of an expressway project (150 km long, more than \$200 million cost).

In 1/2001, Taleb was awarded a scholarship from The Hashemite University in Jordan to pursue his Ph.D. program in Civil Engineering in the United States. While pursuing his Ph.D. at Texas A&M University, he worked as part-time research assistant at the Texas Transportation Institute for the period from 1/2003 till 12/2004. Taleb was awarded his Ph.D. degree in Civil Engineering in 12/2004.

Taleb has published as first author and co-author. Most important of these works is the NCHRP 4-30A Final Report “*Test Methods for Characterizing Aggregate Shape, Texture, and Angularity*” 2004. Taleb will serve as a faculty member in the civil engineering department at the Hashemite University in Jordan. **Address: Department of Civil Engineering / The Hashemite University/ P.O. Box 150459/ Zarqa, 13115/ Jordan. Tel.: 962-5-3826600 ext. 4465/ Fax: 962-5-3826613. e-mail: trousanm@yahoo.com.**